

**Development and application of antimicrobial
peptides based on sC18 to fight antibiotic resistance
and bacterial adhesion**

Inaugural-Dissertation

zur

Erlangung des Doktorgrades
der Mathematisch-Naturwissenschaftlichen Fakultät
der Universität zu Köln

vorgelegt von

Marco Gerry Drexelius

Aus Köln

Köln, 2022

Gutachter:

Prof. Dr. Ines Neundorf

Prof. Dr. Ulrich Baumann

Disputation:

Köln, 02.12.2022

Die im Rahmen der vorliegenden Arbeit durchgeführten Experimente und Untersuchungen wurden im Zeitraum von Februar 2019 bis September 2022 am Institut für Biochemie der Universität zu Köln unter der Anleitung von Frau Prof. Dr. Ines Neundorf durchgeführt.

Abstract

Bacteria remain one of the most concerning medical threats to humanity, causing millions of deaths each year. Even after almost a century of antibiotic development, further research is required to combat the growing number of bacterial resistances to common antibiotics and the formation of biofilms on medical equipment. In the last decades, antimicrobial peptides have emerged as promising candidates to offer a solution to both problems owing to their ability to lyse the bacterial membranes selectively, without harming host tissues.

In this work, the antimicrobial activity of the recently developed cell-penetrating peptide **sC18** (GLRKRLRKFRNKIKEK) should be increased by modulating its amino acid sequence. Overall, three approaches were used to design novel antimicrobial peptides and these were tested for antibiotic activity against a range of bacteria.

At first, specific substitutions with phenylalanine and fluorinated phenylalanine were utilized to modify the physicochemical properties and develop peptides with high antimicrobial activity combined with selectivity towards mammalian cells. These peptides were further investigated for their proteolytic stability and membrane disruptive mechanism. Furthermore, new sets of antimicrobial peptides were designed using a rational approach introducing cationic and hydrophobic amino acid substitutions to enhance their overall antibacterial activity without haemolytic side effects. With these peptides the influence of peptide length and the specific substitution positions were investigated. Based on the most promising variant, chimeric peptides were designed and immobilized onto solid titanium surfaces to prevent the adhesion of bacteria and further biofilm formation.

Zusammenfassung

Bakterien sind nach wie vor eine der besorgniserregendsten medizinischen Bedrohungen für die Menschheit und verursachen jedes Jahr Millionen von Todesfällen. Auch nach fast einem Jahrhundert der Entwicklung von Antibiotika ist weitere Forschung erforderlich, um die wachsende Zahl bakterieller Resistenzen gegen gängige Antibiotika und die Bildung von Biofilmen auf medizinischen Geräten zu bekämpfen. In den letzten Jahrzehnten haben sich antimikrobielle Peptide aufgrund ihrer Fähigkeit Bakterienmembranen selektiv zu lysieren, ohne das Wirtsgewebe zu schädigen, als vielversprechende Kandidaten herausgestellt, um eine Lösung für beide Probleme anzubieten.

In dieser Arbeit sollte die antimikrobielle Aktivität des zellpenetrierenden Peptids **sC18** (GLRKRLRKFRNKIKEK) durch Modulation seiner Aminosäuresequenz gesteigert werden. Insgesamt wurden drei Ansätze verfolgt, um neuartige antimikrobielle Peptide zu entwerfen und diese wurden auf ihre antibiotische Aktivität gegen eine Reihe von Bakterien getestet.

Zunächst wurden spezifische Substitutionen mit Phenylalanin und fluoriertem Phenylalanin genutzt, um die physikalisch-chemischen Eigenschaften zu modifizieren und Peptide mit hoher antimikrobieller Aktivität, kombiniert mit Selektivität gegenüber eukaryotischen Zellen, zu entwickeln. Diese Peptide wurden weiter auf ihre proteolytische Stabilität und ihren Wirkungsmechanismus untersucht. Darüber hinaus wurden neue antimikrobielle Peptide unter Verwendung eines rationalen Ansatzes entwickelt, bei dem kationische und hydrophobe Aminosäuresubstitutionen eingeführt wurden, um ihre antibakterielle Gesamtaktivität ohne hämolytische Nebenwirkungen zu verstärken. Bei diesen Peptiden wurde der Einfluss der Peptidlänge und der spezifischen Substitutionspositionen untersucht. Basierend auf der vielversprechendsten antimikrobiellen Variante wurden chimäre Peptide entworfen und auf Titanoberflächen immobilisiert, um die Anhaftung von Bakterien und die weitere Bildung von Biofilmen zu verhindern.

Table of content

1.	Introduction	1
1.1.	Bacterial Infections and Biofilms	1
1.2.	Antibiotics and Resistances	5
1.3.	Antimicrobial peptides	8
1.4.	Immobilization of Peptides	13
1.5.	Preliminary work	17
2.	Aims of the thesis	21
3.	Materials	23
3.1.	Equipment	23
3.2.	Buffers, Media, and solutions	24
3.3.	Bacterial strains	25
3.4.	Cell lines	26
3.5.	Peptide sequences	26
4.	Methods	28
4.1.	Solid phase peptide synthesis	28
4.2.	Biological experiments	31
4.3.	Titanium surface assays	36
5.	Hydrophobic substitutions optimize antimicrobial activity and selectivity	38
5.1.	Synthesis and physicochemical evaluation	39
5.2.	Antibacterial experiments	42
5.3.	Peptide stability	45
5.4.	Haemolytic activity and cytotoxic profiles in mammalian cells	49
5.5.	Membrane disruption mechanism	54
5.6.	Conclusion	56
6.	R,L variants of different sC18-based peptides	58
6.1.	First RL-sC18 variants – influence of peptide length	59
6.2.	Second RL-sC18 variants – influence of the specific substitution	64
6.3.	Conclusion	70
7.	Surface immobilization of antibacterial chimeric peptides	71
7.1.	Polydopamine immobilization of AMPs	71
7.2.	Synthesis and physicochemical evaluation of chimeric peptides	73
7.3.	Antimicrobial activity of chimeric peptides in solution	77
7.4.	Immobilized chimeric peptides	85
7.5.	Conclusion	88
8.	Thesis Conclusion and Outlook	89

9.	References	91
10.	Attachments	104
10.1.	List of abbreviations	104
10.2.	List of amino acids	106
10.3.	Register of figures	107
10.4.	Register of tables	111
10.5.	Register of Supplementary	113
10.6.	Peptide Analysis Spectra	115
10.7.	Preliminary antibacterial data	121
10.8.	Dose response curves of chimeric peptides	124
10.9.	Fluorescence microscopy of chimeric peptides	125
10.10.	XPS elemental analysis spectra	128
11.	Danksagung	129
12.	Eidesstattliche Erklärung	131
13.	Lebenslauf	133

1. Introduction

1.1. Bacterial Infections and Biofilms

The existence of bacteria was discovered almost 350 years ago with the invention of microscopy by Antoni van Leeuwenhoek^[1]. Still, bacterial infections contribute to millions of human deaths, making them one of the most prominent causes for human illness, next to viruses and cancer. The subgroup of bacteria containing antimicrobial resistances (AMR) alone are estimated to be accountable for almost 5 million deaths in 2019, making them primary targets for medical research.^[2]

Bacteria are part of the group of prokaryotic cells, which are distinct from the more complex eukaryotic cells (**Figure 1**). Prokaryotes do not contain a nucleus as a separated organelle and therefore the DNA is distributed throughout the cytosol. Overall, the interior of eukaryotic cells is described as more complex, containing diversified organelles^[3]. According to the endosymbiotic theory, organelles such as mitochondria have developed from symbiotic relationships between early eukarya and pre-mitochondrial bacteria.^[4] Furthermore, the outer membranes of both cell types can be distinguished by the distribution of phospholipids across the outer layer of the plasma membrane. In general, the membranes of bacteria are enriched with anionic lipoteichoic acid, phosphatidylglycerol and cardiolipin as well as zwitterionic phosphatidylethanolamine^[5,6]. In contrast, the outer layer of eukaryotic membranes mainly consists of zwitterionic phosphatidylcholine and phosphatidylethanolamine, as well as sphingomyelin and cholesterol^[6,7]. Some cell types, like many cancerous cells, display a high amount of negatively charged phospholipids in their outer membrane leaflet, making their surface more akin to bacterial cells^[8].

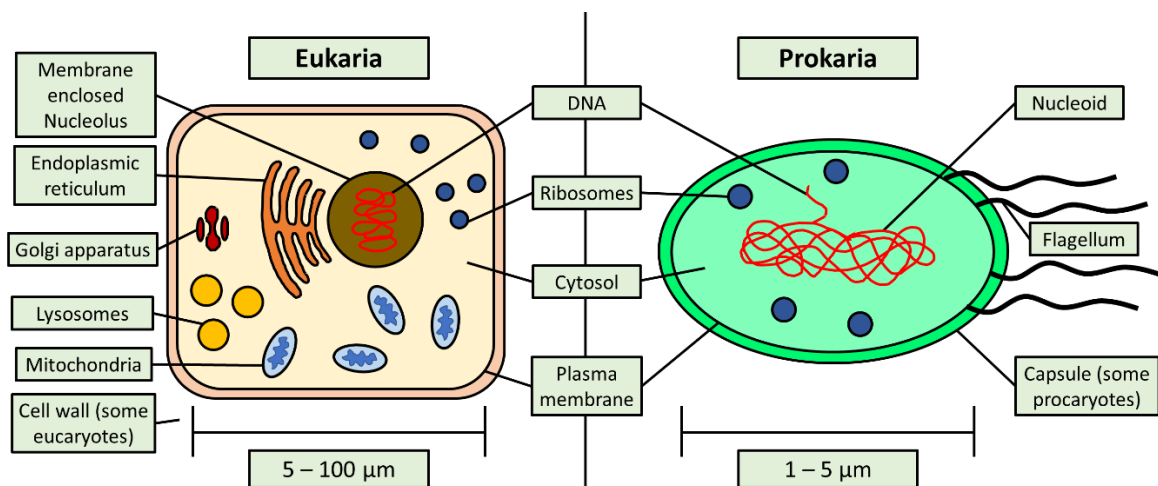


Figure 1: Differences in eukaryotic and prokaryotic cell structures.^[3]

Bacteria can further be classified by multiple parameters but one of the most prominent ways to classify them is based on their outer membranes: gram-positive and gram-negative bacteria (**Figure 2**). This classification was developed by Hans Christian Gram, who used a staining technique that specifically dyed monoderm plasmamembranes with Crystal violet, while diderm membranes remained unstained^[9].

Gram-positive bacteria consist of a cytoplasmic membrane, which is separated by a thin periplasmic layer from a thick protective layer of partly cross-linked peptidoglycans, topped by teichoic or lipoteichoic acids^[9]. Examples for gram-positive bacteria are *Bacillus subtilis*, *Corynebacterium glutamicum* and *Micrococcus luteus* as well as the highly pathogenic strain *Staphylococcus aureus* that causes a variety of clinical infections^[10].

Gram-negative bacteria have a similar composition, but with an additional lipid bilayer surrounding the peptidoglycan layer, which is thinner than in gram-positive cells in contrast to the periplasm^[9]. Examples for gram-negative bacteria are *Escherichia coli*, *Salmonella typhimurium* and *Pseudomonas fluorescens* as well as the highly pathogenic *Pseudomonas aeruginosa* attributed to several healthcare associated infections^[11] and endocarditis^[12].

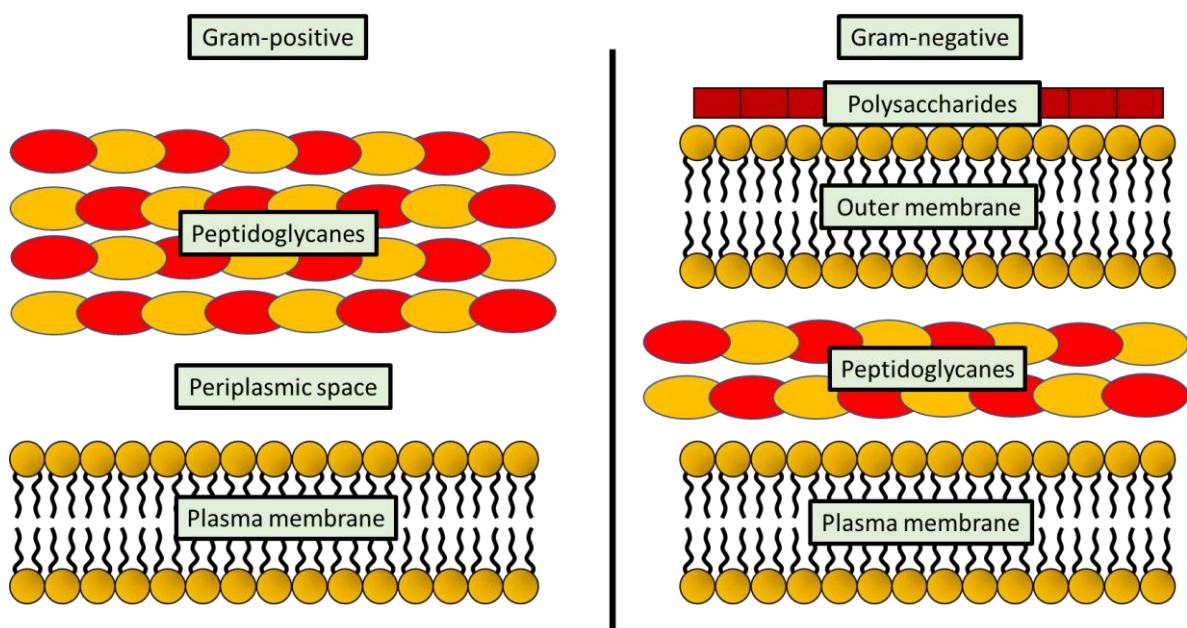


Figure 2: Composition of membranes and other types of bilayers in gram-positive and gram-negative bacterial surfaces.

Even though most bacterial strains fall under these two categories, there are also pathogens with more unusual cellular surfaces. For example, *Mycobacterium phlei* belongs to the group of so-called acid-fast bacteria. These are distinct from other bacteria in their ability to resist acid and ethanol based decolorization techniques in laboratory staining. This is attributed to the high concentration of mycolic acid in their cell wall^[13].

In contrast to planktonic prokarya, eukarya often form multicellular organisms of differentiated cell types, like animals, plants, fungi or protists. Within these organisms, many prokaryotic bacteria have developed symbiotic relations in the microbiome, for example in the digestive tract. This offers tremendous impact on health to the host organism they live in^[1]. But the interaction of bacteria with higher organisms is not always favourable. The best example are infections caused by invasive bacteria. Those infections can lead to inflammations, which destroy the surrounding tissue and can terminate the host which the bacteria have infected. Most organisms have therefore developed natural host defence systems, including immune cells, antibodies and enzymes, to fight against pathogens^[14].

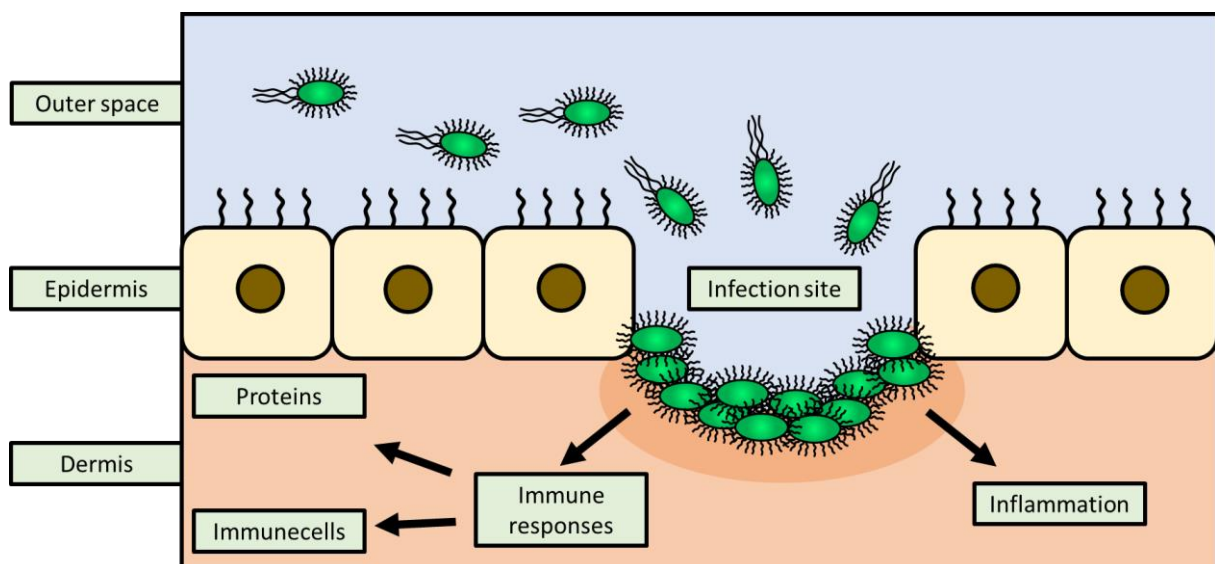


Figure 3: Schematic bacterial infection in mammalian tissue leading to inflammation and immune responses from proteins (enzymes and peptides) as well as direct immune cell and antibody involvement.

In order to infect an organism, the pathogenic bacteria need to invade it, which can naturally happen through ingestion, inhalation, or open wounds, depending on the type of bacteria^[14]. Recently, another problem has arisen which can cause severe bacterial infections and has evolved into a prominent medical challenge: the formation of biofilms on medical devices^[15].

Bacteria can accumulate onto surfaces and form colonies, a process called biofouling. The biofilm makes bacteria more resistant to environmental factors as well as antibiotics, as bacteria within this biofilm can exchange nutrients and signals with each other^[16]. This process is a severe problem in the use of medical devices and can lead to implant-associated wound infections. Indeed, device-associated infections are a main part of all healthcare-associated infections that affect millions of people annually and are attributed to thousands of deaths^[17,18]. Biofouling is especially described as complication when dental implants are used, causing the infectious disease of peri-implantitis^[19-21]. Besides implants, other types of medical devices being often affected include contact lenses^[22] or catheters^[23]. Each year the number of implants grows, with currently 500.000 implants being inserted per year worldwide^[24]. This causes biofouling to be a general threat to human health that needs to be addressed with appropriate medical and antibacterial treatment.

1.2. Antibiotics and Resistances

To fight the threat of bacterial infections, humanity has developed antibiotics, which are various chemical compounds that can effectively kill bacterial cells.

Antibiotics have unknowingly been used by humanity since a long time. For instance, in ancient civilizations special herbs, honey and even mouldy bread were used three thousand years ago to inhibit the spreading of infections in wounds^[25], even if it was not known how these natural medicals worked^[26]. However, more modern research on antibiotics started with the discovery of Salvarsan, also known as Arsphenamine, by Paul Ehrlich in 1907^[27] followed with Penicillin by Alexander Fleming in 1928^[28]. These were the first substances discovered to directly reduce bacterial infections. The application of antibiotics greatly decreased the mortality rate of bacterial infections, which in pre-antibiotic times caused more than half of human deaths^[29]. Since then, various types of antibiotics were developed^[26] and found use in diverse fields like human or veterinarian medicine^[30] and agriculture^[31].

Antibiotics consist of a wide range of very diverse compounds, that can each on their own express detrimental effects on bacterial viability. In general, the activity of antibiotics can be distinguished between bactericidal compounds that directly kill the microorganisms and bacteriostatic compounds which inhibit the proliferation of bacteria^[32]. In both cases, the antibiotics commonly affect intracellular targets and inhibit essential metabolic steps, for example DNA replication or protein synthesis^[33]. Decades of research have produced several classes of closely related molecules with antimicrobial activity against either specific pathogens or a broad range of bacterial targets^[33,34]. Though antibiotics had a remarkable impact on medicine, over the later years, the number of novel antibiotic drugs has steadily declined^[29,35], with fewer new classes developed^[36].

Table 1: *List of common antibiotics, their antibiotic class and mechanism to affect bacterial viability*^[36,37].

Class	Antibiotic	Mechanism
β -Lactams	Penicillin Ampicillin Ceftriaxon	Cell wall synthesis inhibition
Sulfonamides	Sulfadazine	Growth rate reduction
Aminoglycosides	Kanamycin Streptomycin Gentamycin	Protein synthesis inhibition
Tetracyclines	Tetracycline Doxycycline	Protein synthesis inhibition
Chloramphenicol	Chloramphenicol	Protein synthesis inhibition
Macrolides	Azithromycin Erythromycin	Protein synthesis inhibition
Glycopeptides	Vancomycin	Cell wall synthesis inhibition
Ansamycins	Geldanamycin Rifamycin	RNA synthesis inhibition
Quinolone	Ciprofloxacin	DNA replication interference
Streptogramins	Pristinamycin	Protein synthesis inhibition
Oxazolidinones	Linezolid Cycloserine	Protein synthesis inhibition

Although many antibiotics were developed in the last century, there is still the need to discover new antibiotics to overcome the growing problem of antibiotic resistance. As most antibiotic substances inhibit specific enzymes of the bacterial metabolism, simple mutations in those enzymes may directly lead to loss of functionality of many drugs^[38,39]. This ability of most bacteria to adapt to antibiotics has become a frequent

problem and is very much promoted by their overuse^[40,41]. For example, excessive treatment with antibiotics is reported in veterinary medicine, namely the keeping of industrial chicken as human food source^[42]. The consumption of poultry meat containing antibiotics has led to the development of antimicrobial-resistances in bacteria infecting humans. These strains of pathogens usually spread exponentially, slowly overtaking the population of antibiotic-susceptible bacteria and even facilitate the mutation of other cells through horizontal gene transfer^[43,44].

Of the almost 5 million annual deaths that attributed to bacteria with antimicrobial resistances, more than 1.2 million are further evaluated to be directly caused by those resistances.^[2] One group of dangerous multi-resistant bacteria are the so called ESKAPE pathogens. They are a group of seven bacterial species, that are known for their broad range of resistances. As such these pathogens pose a common threat in medical environments like hospitals.^[45-47] These pathogens are the following: *Enterococcus faecium*, *Staphylococcus aureus*, *Klebsiella pneumoniae*, *Acinetobacter baumannii*, *Pseudomonas aeruginosa* and *Enterobacteria*. Another widely spread multi-resistant species is the special variant of methicillin resistant *Staphylococcus aureus* (MRSA) that is known as a major cause of healthcare-associated infections and has further caused approximately 100.000 deaths in 2019^[2].

Based on all these negative effects, there is an ongoing need to search for new antibiotics, preferably with alternative activity mechanisms and effective against a wide range of pathogens.

1.3. Antimicrobial peptides

A novel class of antibiotics that has come into focus in recent years are the antimicrobial peptides (AMPs)^[48]. AMPs are a subclass of so-called membrane active peptides. These are naturally occurring or synthetically developed peptides, which operate in important processes like antimicrobial defence mechanisms and cargo-delivery across membranes^[6]. Two of the most prominent subclasses of membrane active peptides are cell-penetrating peptides (CPPs) and antimicrobial peptides. These two groups are similar in structure, yet they greatly differ in their activity towards different biological membranes^[6].

Cell-penetrating peptides can translocate across cellular membranes and thus enter the cytosol. The peptide sequences can be either classified as hydrophobic, cationic, or amphipathic. CPPs are commonly used to transport cargo-molecules through membranes. These cargos can range from small organic molecules and inorganic nanoparticles^[49] to proteins^[50] or RNA^[51]. The CPP hereby enables the translocation of substances across cell membranes, that cannot cross this barrier by themselves. The mechanisms of how CPPs translocate into the cell varies between peptides but can be classified into two categories, dependent on the specific interactions of the peptide with the membrane components: endocytotic pathways^[52] and direct translocation^[6,53,54].

Antimicrobial peptides are prominent parts of the innate immune system of most organisms. In general, AMPs combine a broad spectrum of antimicrobial activity with minor cytotoxicity against mammalian cells^[55]. Further distinctions of AMPs can be made between peptides that affect intracellular targets^[56,57] and membrane permeabilizing peptides^[58]. Peptides targeting intracellular processes are known to affect protein synthesis, nucleic acid synthesis, enzymatic activities, and cell wall synthesis^[57]. In the case of outer membrane permeabilization, bacteria are mostly killed through transmembral pore formation resulting in membrane lysis^[6]. Some AMPs also show potent antiviral^[59], antifungal^[60] and even anti-parasitic^[61] activity, making them versatile compounds in antibiotic research. Furthermore, some antimicrobial peptides have even been reported to act as anti-cancerous peptides (ACPs)^[62–64], mostly attributed to the similarities in membrane composition of cancerous and bacterial cells^[6].

AMPs share many similarities to cell-penetrating peptides amphipathic structure and the way they attach to cellular membranes and interact with them^[6]. In general, many

membrane-active peptides can combine several functionalities, depending on factors like concentration and cell type. Many studies have developed AMPs derived from CPP sequences by fine tuning the physicochemical properties of the peptide sequence^[54].

1.3.1. Structural properties and mechanism of AMPs

AMPs are a highly diverse group, but most have three general structural properties in common. These are a considerable number of cationic as well as hydrophobic amino acids and often a distinct secondary structure, which forms when AMPs approach the lipid membrane^[65]. Moreover, most AMPs facilitate a mechanism of action, which is usually not easily resisted by bacteria: they display high membrane-activity and lyse the bacterial outer membrane by membrane disruption^[66].

It is assumed that the cationic amino acids arginine and lysine are important for the initial interaction of the peptides with the negatively charged head groups of phospholipids of the bacterial membrane. Furthermore, this cationic part of the peptides sequence might also lead to selectivity between bacterial and the more neutrally charged eukaryotic cells, that has been reported for many AMPs^[58,67]. On the other side, hydrophobic amino acids like aliphatic isoleucine or aromatic phenylalanine are often abundant within the AMP sequence. These amino acids may support the interaction with the lipid core of the membrane bilayer. As the interaction with polar solvents is less energetically favourable than the interaction with other nonpolar substances, a direct interaction between the hydrophobic peptide sidechains and the lipid chains is favoured regarding thermodynamics. This avoidance of hydrogen bond formation is one of the most important driving forces that locate the peptide within the lipid bilayer and potentially let it diffuse through the bacterial membrane, enabling it to reach the cytosol. The last of the three general properties of antimicrobial peptides is the formation of well-defined secondary structures. Most antimicrobial peptides form helical structures^[68] but also beta-sheets^[69] hairpin-structures^[70] and extended AMPs are known^[71,72]. In many cases the secondary structure supports the partition within a hydrophobic and a hydrophilic part. As the antimicrobial activity is dependent on both types of amino acids, the formation of such a rigid amphipathic structure is for most peptides crucial to their respective activity.

AMPs act by permeabilizing the membrane and inducing bacterial lysis by different pore-formation mechanisms^[6]. The three most described pore formation models are

the barrel-stave model, the toroidal pore model, and the carpet model, dependent on the specific interactions with the lipids and the orientation of the AMP in the membrane^[57,73,74] (**Figure 4**).

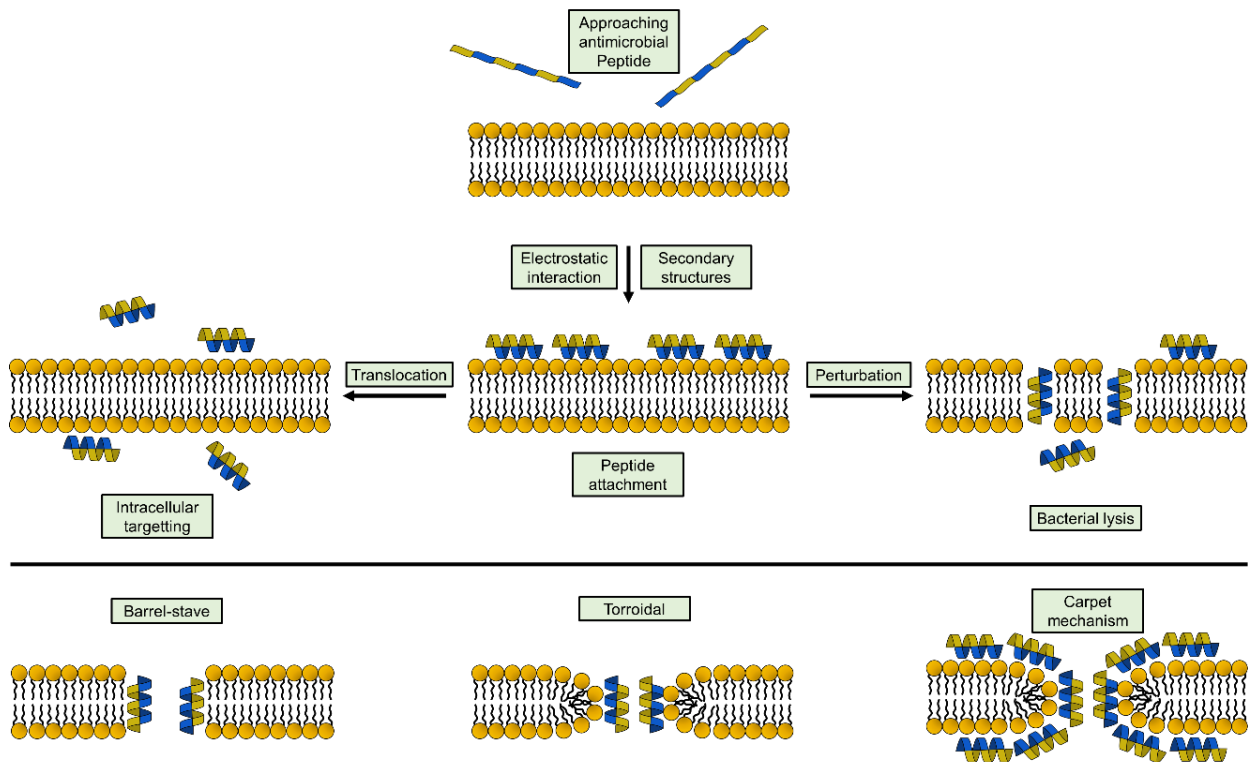


Figure 4: Mechanism of antimicrobial peptides. Top: Attachment of approaching antimicrobial peptides onto bacterial membrane by electrostatic interaction. Peptide coiling through interaction with membrane and either translocation to reach intracellular targets or perturbing the membrane to reach bacterial lysis. Bottom: The three main mechanisms of bacterial membrane perturbation by antimicrobial peptides through pore formation with the barrel-stave, toroidal or carpet mechanism^[57,73,74].

This non-specific method of antibacterial activity makes it difficult for bacteria to adapt resistances, which further highlights the importance of AMPs as promising new antibiotic candidates. Notably, this mechanism of action is completely different to most of the mechanisms used by conventional antibiotics. Still, it is possible for bacteria to develop resistances by changing their membrane compositions and their ionic cell wall potential to be less susceptible targets for peptide attachment^[6]. For these reasons, antimicrobial peptides are believed to offer a potent new variant of antibiotic

compounds, which might be able to combat the growing threat of multiresistant pathogens.

1.3.2. Sources of AMPS

Antimicrobial peptides can be found in most organisms like animals, where they are prevalent weapons of innate and adaptive immune systems^[75,76]. Their potent antibacterial, antiviral^[59], and antifungal^[60] activities make them a versatile first line in many host defence systems. Prokaryotic cells are also known to synthesize AMPs as defensive mechanism that are known to be highly effective against other types of microorganisms^[57]. Many AMPs are synthesized as part of a bigger protein, which is then secreted out of the cell. Upon cleavage of the protein by specific proteases, sometimes even from the pathogen itself, the antimicrobial sequence is separated from the parental protein and can affect other cells.

In nature AMPs are not only utilized in protecting animals from infections, but can also act as venoms secreted by animals to induce paralysis and aid in the digestion of prey^[75]. Prominent examples are the venoms of frogs and toads^[77–80], snakes^[81–83], spiders^[84–86], scorpions^[87–89], and bees^[90–93]. Among the most well-known AMPs derived from animals are Magainins isolated from African clawed frog^[80], Melittin from bee venom^[91,92] and the family of cathelicidins, like human **LL37** or rabbit **CAP18** derived peptide **C18**, from their respective innate immune systems^[94].

Table 2: *Prominent antimicrobial peptides derived from natural sources.*

Peptide	Origin	Sequence
LL-37	Human	LLGDFFRKSKEKIGKEFKRIVQRIKDFLRNLPRTES
Magainin 2	Frog	GIGKFLHSAKKFGKAFVGEIMNS
Melittin	Bee	GIGAVLKVLTTGLPALISWIKRKRQQ
C18	Rabbit	GLRKRLRKFRNKIKEKLLKI

Research on antimicrobial peptides has often emanated from natural peptides which can be further modified to increase their potential membrane activity. These

modifications have been utilized to decrease the peptide's inherent cytotoxicity towards mammalian cells or to enhance their proteolytic stability^[95].

The development of solid phase peptide synthesis (SPPS) by Dr. Robert Bruce Merrifield^[96] (1921 - 2006) has revolutionized the versatility of laboratory peptide synthesis and awarded him the Nobel price of chemistry in 1984^[97,98]. It has opened a whole new world of synthetic possibilities, as it has offered scientists the possibility to create novel peptide sequences^[99] with simple procedures and high purity on a solid support with an efficient protection group strategy. This process has further been adapted to automated SPPS using synthesis robots which can synthesize numerous peptides in parallel.^[100]

With modern synthesis methods the set of natural occurring peptides has been increased by rational designing new sequences. Foremost this was achieved through strategic substitutions in specific positions of the peptide sequence to fine tune its physicochemical properties or by fusing different sequences together to combine activities into a bifunctional peptide^[101]. Furthermore, additional compounds were easily attached to peptides like markers for fluorescent^[102] or radioactive^[103] detection. In a similar manner, unnatural amino acids were introduced as new building blocks to increase the scope of synthetic potential. One major challenge in the development of antimicrobial peptide drugs is the susceptibility of AMPs to proteolytic digestion^[103]. With the incorporation of D-amino acids or methylated amino acids, the affinity to proteolysis could be prohibited^[103,104]. One particular modification assessed in AMPs is fluorination, as it increases hydrophobicity with minimal steric alterations^[105]. As the correlation between hydrophobicity and antimicrobial activity in AMPs is well known, this modification offers great potential in further developing potent antibiotic candidates. Especially fluorinated phenylalanines have been reported in this regard.^[105,106]

1.4. Immobilization of Peptides

As previously discussed, the use of medical devices comes with a certain risk of biofouling that leads to implant-associated bacterial wound infections.^[23] These biofilms pose a severe threat for all surgical or otherwise invasive medical processes, as they can impact not only prosthetic implants, but all kinds of medical devices. To protect patients from implant associated infections, medical and material sciences have developed efficient strategies to prevent biofouling on medical relevant material.^[107,108] Hereby, it is also crucial to find biocompatible, non-toxic as well as non-cancerogenic suitable materials, to minimize complications associated with the protection strategy itself.^[109]

One promising strategy that was developed during the last years is to apply antimicrobial surface coatings on medical devices to prevent bacterial colonization on the material-tissue interface that would cause severe inflammations^[110] and thus decrease the overall success of the medical process.^[111,112] Many types of such coatings have been developed relying on distinct antimicrobial strategies applied to the surface, ranging from depositing metals that exhibit antimicrobial properties like silver^[113,114], or to directly immobilize small organic antibiotic drugs.^[115] The recent success of antimicrobial peptides as antibiotic compounds has also peaked interest in their application for antibiotic surface coating.^[112] Especially, their membrane disruption mechanism and selectivity towards different cell types have brought them into focus as biocompatible coating agents with efficient antibiofouling activity^[16,116]. For example, AMPs have been already reported to actively increase biocompatibility and promote osteointegration, which further decreases the potential of implant failures^[117-119].

Based on the aforementioned reasons, AMPs are promising candidates for antimicrobial surface coatings. During the last decade, research has focused on establishing efficient and safe immobilization techniques. Peptide immobilization on (metal) surfaces can be roughly subdivided into three main routes, namely the direct attachment of peptides, often facilitated by the introduction of specific anchor groups (primary coating), binding of peptides after surface modifications, most frequent via a chemical layer of linkers (secondary coating), or the application of matrixes for peptide intercalation and later release strategies (tertiary coating)^[120].

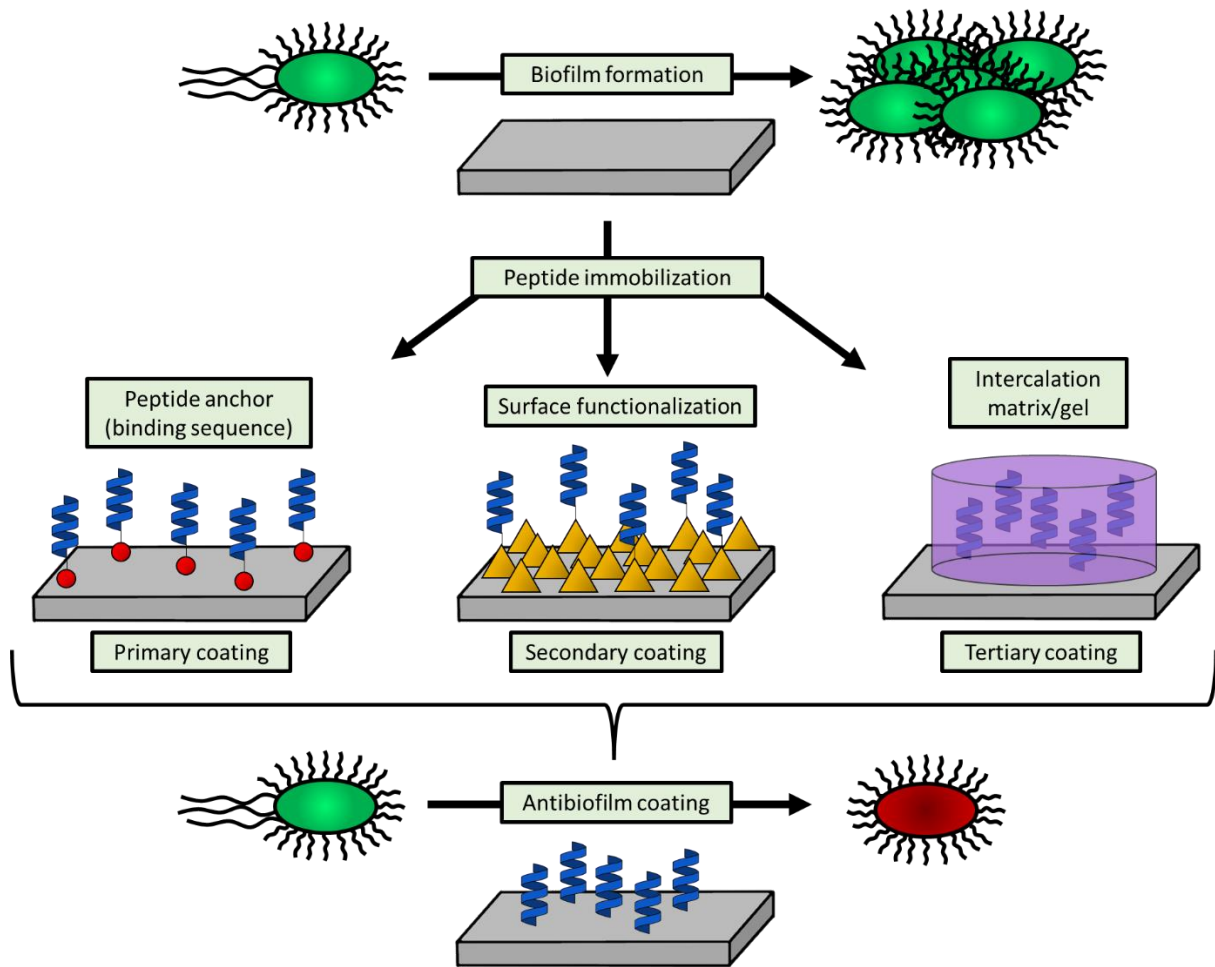


Figure 5: The three main strategies of antimicrobial surface coatings to prevent biofilm formation.^[120]

1.4.1. Primary coating

This first immobilization strategy utilizes distinct types of linker molecules that are combined with the AMPs and function as an anchor. They can bind to the material surface and thus, support the attachment of the AMP.^[120] Often, these groups are introduced via flexible spacer molecules, which grant the AMP enough spatial freedom and do not interfere with AMP function. The most common linkers in this regard are multi-glycine motives, as they do not influence the adjacent peptide sequence, but are relative flexible.^[121] However, also more rigid linkers were included and demonstrated favourable effects to the overall activity of chimeric peptides^[122].

Many anchors comprise small organic molecules for example L-3,4-Dihydroxyphenylalanin (DOPA) that has been often used to attach peptides onto titanium surfaces^[123]. Moreover, peptides came into focus which show surface binding

properties.^[124] These surface binding peptides^[125] can be specific to some kind of surface and as such different aluminium and steel binding peptides^[126], plastic and glass binding peptides^[127] or titanium binding peptides (TBP)^[128] have been classified. The usage of such binding peptides offers the possibility to use an anchor compound that does not need complex synthesis methods or produces detrimental side effects like enhanced toxicity by introducing unusual chemical composites into a host body, what increases the compatibility in medical applications. Due to this, the synthesis of a chimeric peptide bearing an antimicrobial peptide part and a surface binding sequence combined via a flexible spacer sequence, has been a favoured approach in this field^[101,122,129–131]. Especially in medical research, for example, to prevent biofilm formation on dental implants.^[24]

These binding-peptides attach to the surface by different mechanisms. For instance, one prominent example is binding via hydrogen bonds between the histidine and/or hydroxy group containing peptides and the oxidized metal surface.^[128] Other approaches including electrostatic or covalent attachment might be chosen depending on the desired material.^[132]

1.4.2. Secondary coating

Within the second strategy peptides are immobilized onto the solid support after the material was first activated by an additional linker layer before attaching the peptides.^[120] In this way, it is possible to introduce chemical functions needed for the peptide coupling.^[118]

Common linker layers are organic compounds that form polymers on the surface. Most of them are formed from multifunctional monomers, which can react with each other to form a polymeric network and still offer unreacted functional groups to attach the peptides. One prominent example is the utilization of dopamine that can form a polydopamine (PD) layer without further coupling reagents.^[133–135] This method is a simple protocol to facilitate the formation of a branched and cross-linked polymer for easy peptide coupling, that can further be enhanced with additional modifications to alternate the coating properties.^[136] Another often used layer substance is comprised by alkoxides that silanize the surface for further peptide modification. Notably, the introduction of active groups can be achieved very easily.^[137–141] Other examples of

linker layers used in recent research are inorganic calcium-phosphate^[142,143] and organic elastin-like recombinamers.^[144]

1.4.3. Tertiary coating

The last coating strategy describes the peptides loosely integrated into a surface deposited layer without covalent bonds.^[145] This strategy differs from other coating methods in that it can produce a steady release of the peptide from the coated matrix into the surroundings.^[146] It is assumed that in this way the peptides may reach further into the surrounding tissue compared to the other methods, where more or less the close vicinity is affected. Two major subcategories between these kinds of matrixes were identified: structural and applied matrixes.^[120]

The structural matrixes are themselves three dimensional nanostructures in the material. These can be pores^[117,147], nanorods^[145] or other types of specialized moulds^[148] designed in the material structure itself and filled with peptides. As the steady release of peptides might lead to cytotoxic complications, methods of sealing those nanostructures with trigger dependent release mechanisms have been investigated. This way the peptides might only be released when the environmental conditions require it, for example the reduced pH-value in an area confronted with bacterial infection.^[146]

The applied matrixes use an additional layer of permeable material, into which the peptide can be loaded and later released again. These matrixes can consist of inorganic^[149–151] or organic compounds^[152] and some are even based on proteins like collagen.^[153,154] One of the most prominent examples was the application of hydrogels as matrix materials to carry and release the AMPs.^[155] These matrixes are reminiscent of secondary coating techniques, but peptides are not covalently attached on top of these layers, instead loosely intercalated into them.

1.5. Preliminary work

In the search for new membrane active peptides, a new cell-penetrating peptide was discovered in the sequence of the protein **CAP18** found in rabbit granulocytes^[156]. The truncated version **sC18** (GLRKRLRKFRNKIKEK), a shorter version of **C18**, was found to have potent cell-penetrating activity.

In recent years, **sC18** has been modified in multiple ways to develop novel peptides with a wide array of applications. Membrane translocation of this CPP could be used to transfer inorganic compounds (e.g. carborane-clusters^[157,158] or Pt^{II}-thiosemicarbazone complexes^[159]) as peptide-conjugates into cancer cells. On the other hand, chimeric peptides were designed by fusing **sC18** with other bioactive peptides to promote wound healing (**Tylotoin**)^[160] or to target cell nuclei and subnuclear regions (**N50** and **NrTP**)^[161]. Further studies to investigate the lipid-peptide interactions have created the shorter variant **sC18*** (GLRKRLRKFRNK), which was found to have similar CPP activity^[162] with lower synthesis expense and costs.

To develop antimicrobial peptides, Dr. Andre Reinhardt has investigated new ways of modifying **sC18**^[163]. The conjugation with ionic liquids (imidazolium salts) resulted in peptides with antimicrobial activity against drug-resistant strains, but also induced haemolysis at micromolar concentrations^[164]. Further experiments to create antimicrobial peptides based on **sC18** led to a new approach of hydrophobic substitutions^[163]. Initially the sequence was investigated through a helical wheel projection (**Figure 6**) to determine the relative positions of the individual amino acids in a helical secondary structure. Based on this projection, crucial positions were assessed. The hydrophobic site in the secondary structure of **sC18** consists of 4 amino acids. Switching the positions R10 and K16 to hydrophobic amino acids were expected to enhance the antimicrobial activity by enlarging the hydrophobic site. Furthermore, the substitution of Glu15 would eliminate the only negatively charged amino acid in the larger cationic area of the peptide secondary structure, increasing the potential membrane interaction.

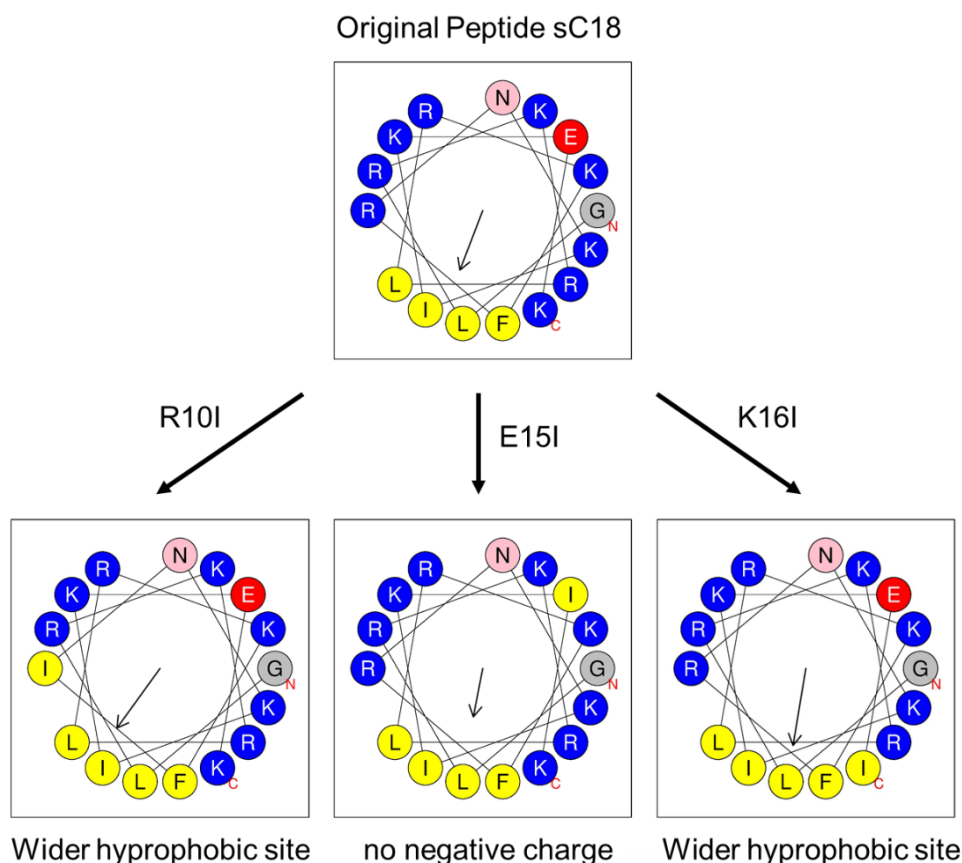


Figure 6: Helical wheel projection^[165] for prognosis of crucial substitution positions with isoleucine in **sC18** to enhance antibacterial activity by widening the hydrophobic site (R10 and K16) or removing the negative charge (E15).

The first part of these experiments was to screen a small library of 15 peptides based on **sC18** with hydrophobic isoleucine substitutions at all positions. These 15 peptides of the Ile-scan were the first generation of developed AMPs (**AMP1a-1o**). These peptides were tested in an initial screening to assess the activity against three bacterial strains of gram-positive *Bacillus subtilis* and *Micrococcus luteus*, as well as gram-negative *Pseudomonas fluorescens* (**Supplementary 7**).

With the results of the initial experiment, it was visible, that the peptides **AMP1j**, **AMP1n** and **AMP1o** with substitutions of Arg10, Glu15 and Lys16 exhibited sufficient antibacterial activity at 25 μ M against the three bacterial strains. Based on these positions, the second generation of isoleucine peptides (**AMP2a-2d**) was designed by performing double and triple substitutions on these positions. Furthermore, the third generation of AMPs was designed by mono (**AMP3a-3c**), double (**AMP3d-3f**) and triple substitutions (**AMP3g**) with the more hydrophobic amino acid phenylalanine.

With these fourteen new peptides, antimicrobial assays were performed on the seven bacterial strains of gram-positive *B. subtilis*, *C. glutamicum* and *M. luteus*, as well as *P. fluorescens*, *S. typhimurium* and *E. coli* and finally acid-fast bacterium *M. phlei* (**Supplementary 8-9**) to determine the MIC₅₀ values (**Table 3**),

To summarize the preliminary data, **sC18** showed no antimicrobial activity in the investigated concentration range below 25 µM for the seven bacterial strains, while all substitutions used in these experiments showed a significant increase in overall antibacterial activity. In comparison to the isoleucine substitution peptides, the phenylalanine peptides yielded higher antimicrobial activity with lower MIC₅₀ values. **AMP3g**, modified with three phenylalanine substitutions, was shown to be the most efficient of these fourteen peptides, with MIC₅₀ values as low as 1.5 µM for gram-positive bacteria *B. subtilis* and *C. glutamicum*. In general, no antimicrobial activity was determined for *E. coli* and the isoleucine peptides had no antimicrobial activity against the acid-fast bacterium *M. phlei*. However, both gram-positive as well as gram-negative bacteria were affected by the new antimicrobial peptides.

This makes the new peptides a promising new approach for new broad range antimicrobial compounds, that will be further investigated in subsequent studies.

Table 3: *MIC₅₀ values [μ M] for the generation two and three peptides tested against seven different bacterial strains. Incubation time was 6 h at 37°C.*

Peptide	<i>B. Subtilis</i>	<i>C. glutamicum</i>	<i>M. luteus</i>	<i>M. Phlei</i>	<i>P. fluorescens</i>	<i>S. typhimurium</i>	<i>E. Coli</i>
sC18	>25	>25	>25	>25	>25	>25	>25
AMP1j	6.9	8.2	14.2	>25	7.6	4.5	>25
AMP1n	>25	8.6	>25	>25	12.6	6.5	>25
AMP1o	5.9	5.5	18.9	>25	12.6	16.4	>25
AMP2a	3.8	4.9	6.0	>25	7.2	1.7	>25
AMP2b	2.5	5.2	1.3	>25	2.3	2.8	>25
AMP2c	3.6	7.6	5.3	>25	4.5	9.2	>25
AMP2d	2.2	5.3	10.9	>25	8.2	2.1	>25
AMP3a	18	9.7	15.0	5.8	10.1	12.1	>25
AMP3b	23.1	14.3	23.3	9.5	19.2	21.3	>25
AMP3c	18.3	10.5	21.4	10.0	12.1	18.9	>25
AMP3d	11.1	2.1	6.3	3.1	4.3	>25	>25
AMP3e	2.0	4.3	13.2	2.5	6.0	12.4	>25
AMP3f	>25	8.6	13.7	5.5	3.4	23.6	>25
AMP3g	1.5	1.5	3.8	2.0	2.2	10.7	>25

2. Aims of the thesis

The focus of this work was the development of novel antimicrobial peptides by sequence modifications of the cell-penetrating peptide **sC18**.

The first chapter of this thesis focusses on systematic substitutions with hydrophobic amino acids within the sequence of **sC18**. Based on preliminary works of Dr. Andre Reinhardt, who defined the most sufficient positions for exchanges, fluorinated phenylalanine variants were used to further improve the antimicrobial activity against a broad range of bacterial strains as well as to increase the stability against proteolytic degradation. Furthermore, the cytotoxicity profile and cell-penetrating ability were assessed as well as the mechanism of membrane interaction used by these peptides.

Within the second chapter of this thesis peptide variants of **sC18** with substitutions of arginine and leucine were investigated to optimize the amphipathic character. With two sets of novel peptides, the influence of the peptide length on the AMP activity was evaluated, as well as the specific substituted positions with focus on the differences between cationic and hydrophobic exchanges. The two sets of novel peptides were analysed to get insight into the effects on antimicrobial activity in contrast to haemolysis.

The third chapter of this thesis focusses on the development of antimicrobial peptide coatings on titanium surfaces with the most efficient antimicrobial peptide of former studies. To obtain such coatings, chimeric peptides were designed to combine surface binding and antibacterial properties within one bifunctional peptide. The activity of these fused peptides was evaluated in solution, to determine a potential effect of the fused sequences on bioactivity. Furthermore, the peptides were immobilized on small titanium plates, to assess how bacteria can attach to these coated surfaces.

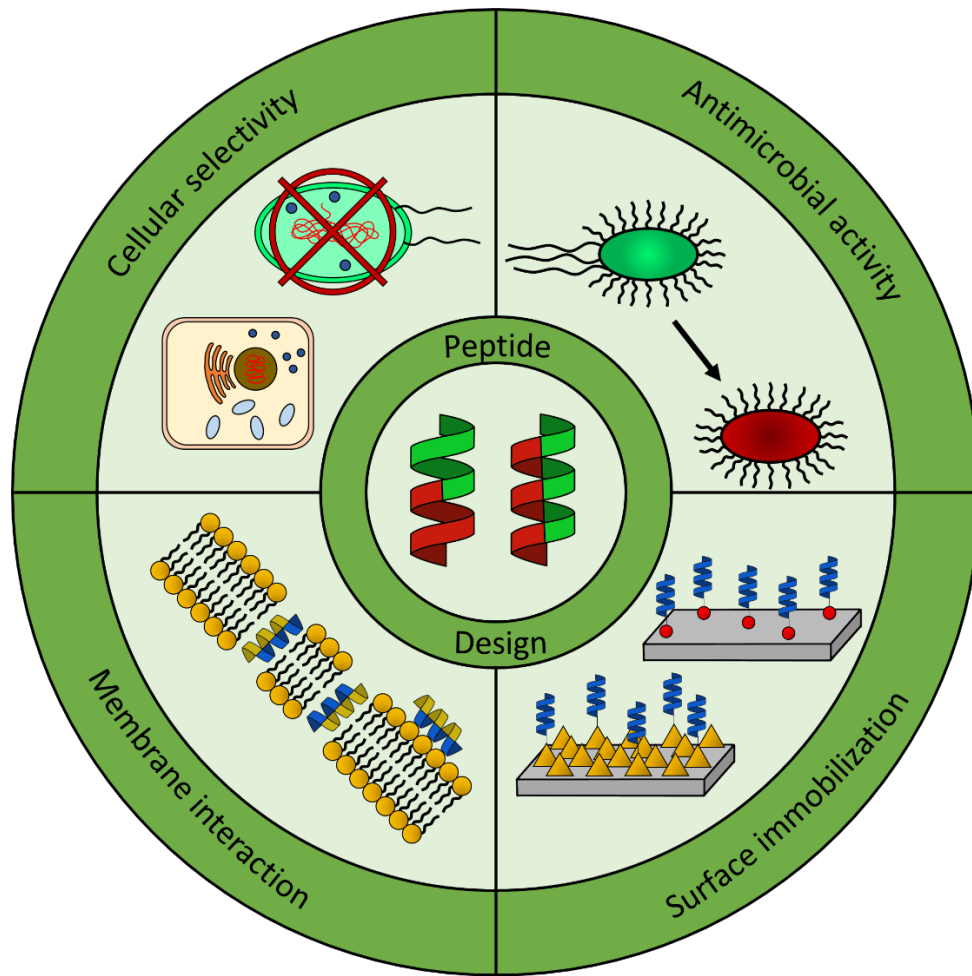


Figure 7: Versatility of activity in rationally designed peptides.

3. Materials

Chemicals, reagents, and consumables, which were used during this work, were obtained from Fluka (Taufkirchen, Germany), Merck (Darmstadt, Germany), Sarstedt (Nümbrecht, Germany), Sigma–Aldrich (Taufkirchen, Germany) and VWR (Darmstadt, Germany). N α -Fmoc protected amino acids were purchased from Iris Biotech (Marktredwitz, Germany). Protection groups for the trifunctional amino acids were Pbf (Arg), Trt (Asn, Gln, His, Cys), Boc (Trp, Lys) and tert-butyl (Asp, Glu, Ser, Thr, Tyr).

Purified red blood cells (SER-10MLRBC) were ordered from zenbio (Research Triangle Park, NC 27709, U.S.A.) via the German distributor biocat (Heidelberg).

Solid titanium foil for peptide attachment was purchased from Sigma-Aldrich as a 10x10x0.2 cm plate, that was cut into 1x1x0.2 cm pieces by the technical workshop of the Institute of Biochemistry, University of Cologne.

3.1. Equipment

Table 4: *Laboratory equipment used for the experiments in this work.*

Equipment	Model / Producer
Bacteria storage (-80 °C)	Thermo Scientific, Forma900Series
Balances	Faust, FA-210-4i Faust, FA-1500-2
CD spectrometer	Jasco Corp. J715
Centrifuges	Thermo Scientific; Multifuge X1R Thermo Scientific; PicO 17
FACS	Guava, easyCyte HT
Heating block	Eppendorf – Thermomixer compact
HPLC (preparative)	Lachrom Hitachi Autosampler L-2200, Elite Lachrom Hitachi Diode Array Detector L-2455, Teledyne ISCO Fraction Collector Foxy R1, Column: Machery-Nagel, 2,6 u, C18, 100 A, 250 x 16 mm, 4 micron
HPLC (analytic)	Hewlett Packard Series 1100, Agilent 1100 Series; Column: Machery-Nagel,

	2,6 μ , C18, 100 A, 125 x 4.6 mm Elite Lachrom Hitachi Pump L-2130, Elite
Incubator (cell culture)	Binder CO2 incubator
Incubator (bacteria)	Braun Biotech international, Certomat BS-1
Lyophilizer	Leybold Christ; Alpha 2-4 LDplus
Mass spectrometer	Thermo Scientific LTQ-XL
Microscope (Cell culture)	Motic AE31
Plate reader (96 well plates)	Tecan, Infinite F200PRO
Peptide synthesis robot	MultiSynTech Syro I
Pipettes	Eppendorf Research plus
Proteome analysis HPLC	Two-column Ultimate 3000 nano-RSLC system Reverse-phase trap column (2 cm μ PAC trapping column, PharmaFluidics) Reverse-phase analytical column (50 cm μ PAC column, PharmaFluidics)
Proteome analysis LCMS	High resolution Q-TOF mass spectrometer (Impact II, Bruker) using a nano-spray ion source (CaptiveSpray, Bruker) Bruker HyStar Software (v3.2, Bruker Daltonics).
Spectral photometer	Spectroquant Pharo300
Speed-Vac	Savant SC210A (Speedvac concentrator) Savant RVT5105 (Refrigerated vapor trap)
Sterile bench (cell culture)	Kojair Biowizard
Fluorescence microscope	Keyence BZ-X810 BZ-X filter GFP BZ-X filter TRITC
Ultrasonic bath	VWR Ultrasonic cleaner (USC300TH)
Vortex	Scientific Industries – Vortex Genie 2
Xcelvap	Horizon Technology, Xcelvap

3.2. Buffers, Media, and solutions

LCMS-solution: 10 % acetonitrile in water + 0.1 % formic acid

HPLC-solution:	10-50 % acetonitrile in water + 0.1 % trifluoroacetic acid
Phosphate-buffer (CD):	10 mM KH ₂ PO ₄ /K ₂ HPO ₄ in water (pH = 7.5)
TFE-buffer (CD):	10 mM KH ₂ PO ₄ /K ₂ HPO ₄ in water (pH = 7.5) + TFE (1:1)
Müller-Hinton broth:	2 g/L beef-infusion, 17.5 g/L peptone from casein, 1.5 g/L corn starch, pH 7.4 ± 0.2, bought from CARL ROTH
PBS-buffer:	Dulbecco's Phosphor buffered saline
Lysis buffer:	8 M urea, 5 mM EDTA, 1mM pMSF, 50 mM Tris, pH 7.5
HeLa/MCF7-medium:	RPMI-1640 (R0883) + 4 mM L-glutamine + 10 % FBS
HEK293-medium:	MEM (M2279) + 4 mM L-glutamine + 15 % FBS
FACS-medium:	DMEM (high glucose) without phenol red
Kaiser test solution 1:	Ninhydrin in ethanol (0.05 g/mL)
Kaiser test solution 2:	Phenol in ethanol (4 g/mL)
Kaiser test solution 3:	Potassium cyanide in pyridine (0.02 mM)

3.3. Bacterial strains

<i>Bacillus subtilis</i>	(ATTC 6633)
<i>Corynebacterium glutamicum</i>	(ATCC 13032)
<i>Escherichia coli</i> K12	(MG1625)
<i>Micrococcus luteus</i>	(DSM 20030)
<i>Mycobacterium phlei</i>	(DSM 48214)
<i>Pseudomonas fluorescens</i>	(DSM 50090)
<i>Salmonella typhimurium</i>	(TA100)
<i>Pseudomonas aeruginosa</i>	(PA14)
<i>Staphylococcus aureus</i>	(ATCC 29213)
MRSA	(ATCC 43300)

3.4. Cell lines

HeLa	Human cervix adenocarcinoma
MCF7	Human breast adenocarcinoma
HEK293	Human embryonic kidney cells
hRBC	Human red blood cells

3.5. Peptide sequences

Table 5: Sequences of all peptides investigated in this work.

Name	Sequence
sC18	GLRKRLRKFRNKIKEK-NH ₂
sC18*	GLRKRLRKFRNK-NH ₂
sC18ΔE / AMP4a	GLRKRLRKFRNKIKK-NH ₂
AMP3a	GLRKRLRKFFNKIKK-NH ₂
AMP3b	GLRKRLRKFRNKIFK-NH ₂
AMP3c	GLRKRLRKFRNKIKF-NH ₂
AMP3d	GLRKRLRKFFNKIFK-NH ₂
AMP3e	GLRKRLRKFFNKIKF-NH ₂
AMP3f	GLRKRLRKFRNKIFF-NH ₂
AMP3g	GLRKRLRKFFNKIKFF-NH ₂
AMP4b	GLRKRLRKFFNKIKF-NH ₂
AMP4c	GLRKRLRKFX ₁ NKIKX ₁ -NH ₂ X ₁ = 4-fluorophenylalanin
AMP4d	GLRKRLRKFX ₂ NKIKX ₂ -NH ₂ X ₂ = 3,5-bifluorophenylalanin
AMP4e	GLRKRLRKFX ₃ NKIKX ₃ -NH ₂ X ₃ = pentafluorophenylalanin
Chim1	RPRENRRERGLGGGGLRKRLRKFFNKIKF-NH ₂
Chim2	SRPNGYGGSESSGGGGLRKRLRKFFNKIKF-NH ₂
Chim3	RKLPDAPGMHTWGGGGLRKRLRKFFNKIKF-NH ₂
RL-sC18	RLRKLLRKFLRKIKRL-NH ₂
RL-sC18*	RLRKLLRKFLRK-NH ₂
RL-sC18ΔE	RLRKLLRKFLRKIKR-NH ₂
RL-1	RLRKRLRKFRNK-NH ₂

RL-2	GLRKLLRKFRNK-NH ₂
RL-3	GLRKRLRKFLNK-NH ₂
RL-4	GLRKRLRKFRRK-NH ₂
RL-1/2	RLRKLLRKFRNK-NH ₂
RL-1/3	RLRKRLRKFLNK-NH ₂
RL-1/4	RLRKRLRKFRRK-NH ₂
RL-2/3	GLRKLLRKFLNK-NH ₂
RL-2/4	GLRKLLRKFRRK-NH ₂
RL-3/4	GLRKRLRKFLRK-NH ₂
RL-1/2/3	RLRKLLRKFLNK-NH ₂
RL-1/2/4	RLRKLLRKFRRK-NH ₂
RL-1/3/4	RLRKRLRKFLRK-NH ₂
RL-2/3/4	GLRKLLRKFLRK-NH ₂
LL37	LLGDFFRKSKEKIGKEFKRIVQRIKDFLRNLVPRTES-NH ₂

4. Methods

4.1. Solid phase peptide synthesis

All peptides were synthesized using solid phase peptide synthesis (SPPS) on Rinkamide resin (loading 0.48 mmol/g, 0.015 mmol scale). The used amino acids (aa) were N-terminally Fmoc-protected and trifunctional side chains of amino acids were further orthogonally protected with acid labile protecting groups.

4.1.1. Amino acid coupling

Longer peptide sequences were synthesized using orthogonal Fmoc/tBu strategy was realized using an automated peptide synthesizer from MultiSynTech and following double coupling steps with each 8 equivalents (eq) Fmoc-aa-OH, Oxyma pure® and diisopropylcarbodiimide (DIC) for 45 minutes. Fmoc deprotection was realized with piperidine (20% in DMF) for 10 minutes. When the automated synthesis was finished, the resin was then washed with DMF, DCM, MeOH and Et₂O five times and dried under reduced pressure.

Fluorinated amino acids and 5,6-carboxyfluorescein (CF) were coupled manually. The resin was swollen in 1 mL DMF for at least 15 min. Afterwards, 2 equivalents (eq) Fmoc-protected amino acid, 2 eq N-methylmethanaminium hexafluorophosphate N-oxide (HATU) were dissolved in 300 μ L DMF and added to the resin with N,N-diisopropylethylamine (DIPEA). The reaction was shaken at room temperature for two hours. Alternatively, the coupling was repeated, using 5 eq Fmoc-protected amino acid and 5 eq Oxyma, with 5 eq DIC as coupling reagents overnight. Afterwards the resin was washed with DMF, DCM, MeOH and Et₂O five times and either air-dried under the hood or dried under reduced pressure. Manual coupling reactions were verified via a Kaiser-Test. Briefly, a few beads of dry resin were incubated with a droplet of the three Kaisertest solutions (see 3.3.) and heated for 5 min to 95 °C. Unreacted amino functions turned the resin beads blue. For Fmoc cleavage, the resin was swollen in 1 mL DMF for at least 15 min. Afterwards, the solvent was removed and 500 μ L of piperidine solution (30 % in DMF) were added to the resin and left shaking for 20 min. After removal of the reaction mixture, the deprotection was repeated. The resin was then washed with DMF, DCM, MeOH and Et₂O five times and dried under reduced pressure.

4.1.2. Peptide cleavage and purification

Peptides were removed from the resin using TFA/TIS/H₂O (95:2.5:2.5 v/v/v) for 3 h at RT under agitation. Peptides containing methionine or tryptophane were removed with a TFA/THA/EDT (90:7:3 v/v/v). Peptides were precipitated in ice-cold diethyl ether and was washed five times with ice-cold diethyl ether. The precipitate was freeze-dried.

Peptides were purified using preparative RP-HPLC (ACN in H₂O, 0.1 %TFA). Fractions were analysed by analytical RP-HPLC ESI-MS and lyophilized.

4.1.3. Peptide characterization

The synthesized peptides were analysed via reversed phase HPLC assisted electrospray ionisation mass spectrometry (RP-HPLC ESI-MS). The gradient was 10-60 % acetonitrile in water over 15 minutes with 0.1 % formic acid, using a Nucleodur column (100-5; C18ec; 4.6 x 125 mm) from Macherey-Nagel.

Determination of peptide purity was realized with analytical RP-HPLC. The gradient was 10-60 % acetonitrile in water over 15 minutes with 0.1 % trifluoroacetic acid using a Nucleodur column (100-5; C18ec; 4.6 x 125 mm) from Macherey-Nagel. Yields were calculated from mass and purity of the sample:

$$yield = purity (\%) * \frac{\left(\frac{m_{sample}}{M_{peptide}}\right)}{n_{starting}}$$

4.1.4. Circular dichroism (CD) spectroscopy

Peptide stocks were diluted in 10 mM phosphate buffer (pH 7) or 10 mM phosphate buffer (pH 7) with the addition of trifluoroethanol (TFE) (1 : 1) to a concentration of 20 μ M. Spectra were recorded from 180 to 260 nm in a 1 mm thick quartz cuvette. For specific experiments additional samples with 10, 20, 30 and 40 % TFE were prepared accordingly. Conversion of $\theta_{measured}$ in degree to the characteristic θ for the peptide was realized by using the following equation:

$$\theta = \frac{\theta_{measured}}{(10 * n_{residues} * c_{peptide} * d_{cuvette})} = \frac{deg * cm^2}{dmol}$$

R-values of spectra were calculated by division of θ at 208 and 220 nm.

4.1.5. Stability assays of peptides

4.1.5.1. Proteolytic digestion

An amount of 100 μM peptide solutions in 100 mM $(\text{NH}_4)_2\text{CO}_3$ buffer were generated and incubated with 2 μM trypsin at 37°C and shaking at 1200 rpm. At different timepoints (1, 2, 5, 10, 15, 20, 30, 60, 90, 120 minutes) 15 μl aliquots were taken, inactivated with 45 μl formic acid (10%) and stored at -18°C . After thawing for analysis, samples were diluted in LC–MS buffer (10% acetonitrile, 0.1% formic acid, 90% water) and measured by LC–MS (Agilent 1600 series and LTQ-XL, Thermo, mass spectrometer).

4.1.5.2. Medium stability

To test peptide stability in culture supernatant, a bacterial culture was centrifuged, and the supernatant was gathered. An amount of 200 μl peptide solutions of 4 \times MIC (regarding the used bacterium) was prepared in culture supernatant and incubated overnight. As control, a solution of medium only and peptide samples pre-treated with fresh growth medium were used. The next day, peptide solutions were diluted 1:3 in fresh medium and an antibacterial assay (as described in 2.4.1.2.) was performed.

4.2. Biological experiments

4.2.1. Bacterial experiments

4.2.1.1. Bacterial culture preparation

A glycerol stock of bacterial strains was spread out on antibiotics free MHB-agar plates and incubated overnight at 37 °C. Culture plates were not kept for longer than three weeks maximum, until they were discarded. One colony was picked and added to 5 mL MHB-medium for incubation at 37°C with an agitation of 180 rpm overnight. The preculture was given to 25 mL fresh MHB-medium and with the same conditions grown to an optical density at 600 nm (OD₆₀₀) of more than 0.7 arbitrary units. Only then was the bacterial culture used for further experimentations. For *S. aureus* and MRSA, cultures were grown to an OD₆₀₀ between 0.5 and 0.6 arbitrary units.

4.2.1.2. Antimicrobial activity assays

For determination of the antimicrobial potential of the peptides in solution the Iodonitrotetrazolium (INT) assay was used.

In a ninety-six well plate 10 µL of a 20-fold concentrated peptide solution, 10 µL of the bacterial culture and 180 µL MHB-medium were mixed. The resulting cultures were screened at several different peptide concentrations (as triplicates). As negative control pure water and as positive control 35% ethanol in medium were used. All samples were then incubated at 37°C for 6 h. After incubation, 10 µL of a 1 mg/mL solution of iodnitrotetrazolium-chloride in pure DMSO was added to each well. After incubation for 30 minutes at 37 °C, the absorption of formazan was measured at 560 nm using a Tecan-plate reader.

For *Staphylococcus aureus* and MRSA, a colony formation assay was performed. Bacteria culture was diluted to 2x10⁶ bacteria/mL with TG buffer. In a ninety-six well plate 50 µL bacterial solution were mixed with 50 µL serial peptide dilution in TG buffer. As living control, the bacteria were mixed exclusively with TG buffer. After two-hour incubation at 37 °C without shaking, the samples were diluted 1:40 with TG-buffer in a new 96 well plate. 50 µL of those bacterial dilution was spread out on a quarter of one TSB-agar plate each. The plates were incubated overnight at 37 °C and the colonies were counted.

The minimal inhibitory concentration (MIC) was calculated as the average of three independent experiments performed in triplicate. MIC₅₀ values were calculated from dose response curves simulated with OriginPro8.5 (Academic).

4.2.1.3. Proteome analysis

5 mL culture of *B. subtilis* were mixed with 2.75 µL peptide solution (1 mM) and incubated for 90 min at 150 rpm and 37 °C. Bacteria were centrifugated, washed with PBS, resuspended in 100 µL lysis buffer and lysed for 1 minute at 30 % amplitude. The cell debris was centrifuged (5 min, 10000 xg, 4 °C). The supernatant was added with 1 µL Dithiotreitol (1M) for 30 minutes at 37 °C and 10 µL Iodacetamide solution (0.5 M) for 30 minutes at RT and 50 mM DTT for 20 minutes in RT. 100 µg protein was bound to SP3 beads and washed with 90 % ethanol. 50 µg of the peptide sample were taken and refilled with HEPES solution (50 mM, pH 7.5). CaCl₂ solution was added to reach 5 mM final concentration and the protein was digested by 1:100 (w/w) proteomic grade Trypsin overnight (150 rpm, 37 °C). Digested proteome samples were desalted via C18 Stop and Go Extraction tips^[166].

Analysis of samples was performed on a two-column nano-HPLC setup with a gradient from 5 to 32.5 % ACN in water with 0.1 % FA for 95 min. Separated samples were introduced into a high-resolution mass spectrometer using a nano-spray ion source^[167]. Data was acquired in line-mode in a mass range from 200 to 1750 m/z at an acquisition rate of 4 Hz. The top 17 most intense ions were selected for fragmentation (2 – 20 Hz, transfer time: 100 µs, collision energy: 5.6 – 8.4 eV, radio frequency: 1500 – 1700 Vpp). Obtained mass spectrometric data was queried in a database search using MaxQuant v1.6.8.0^[168]. Resulting signals were compared to a *Bacillus subtilis* database from UniProt. Result files were analysed in Perseus v1.6.6.0^[169].

4.2.1.4. Electron microscopy

Bacteria were cultured as previously described. 270 µl aliquots were taken from each culture and mixed with 30 µl peptide solution to achieve a final concentration of 4x MIC. Samples were incubated for 90 min at 37 °C; water served as control sample. After incubation, the samples were centrifuged (5000 rpm, 10 min, 4°C) and washed twice with 100 µl PBS buffer following centrifugation. The cell pellets were fixed with

2.5% glutaraldehyde in PBS for 30 min and afterwards dehydrated with ethanol solutions of increasing concentrations (30, 50, 70, 80, 90, 99%). Cell pellets were then transferred to hexamethyldisilazane (HMDS)/ethanol (1 : 1) for 10 min followed by 100% HMDS for another 10 min as a substitute for critical point drying. Afterwards they were allowed to fall dry, mounted on sample holders and sputter coated with 12 nm gold. Samples were analysed using a FEI Quantum 250 FEG scanning electron microscopy. Measurements were performed by Dr. Frank Nitsche (University of Cologne, Department of Biology, General Ecology)

4.2.1.5. Bacterial fluorescence microscopy

In a 1.5 mL reaction vessel 100 μ L bacterial culture, 490 μ L PBS and 10 μ L 1 mM stock solution of CF-labelled peptide were incubated for 30 minutes at 37 °C, shaken at 180 rpm. As controls PBS and 70 % EtOH were used. After the incubation, the bacteria were centrifuged (4 °C, 10.000 xg, 3 min) and the supernatant was discarded, while the pellets were washed with 500 μ L PBS. To quench unwanted fluorescence, 100 μ L Tryphanblue (15 μ M with 10 mM Na-acetate in PBS) was added and afterwards the bacteria were washed twice with 500 μ L PBS. To mark dead cells, 70 μ L PBS and 30 μ L Propidium iodide were added to reach 30 μ M concentration and incubated in the dark for 15 minutes followed by washing with 500 μ L PBS. The pellet was dissolved in 100 μ L PBS and put it into a well off an ibidi for measurement.

With the Keyence fluorescence tabletop microscope BZ-X810, a 60x oil immersion lens was used for pictures of bacteria. Three different channels were pictured: Bright field (25 % Illumination, 1/300 s), Green fluorescence (Excitation: 440-470 nm, Emission: 525-550 nm, 20 % Excitation, 1/15 s) and Red fluorescence (Excitation: 525-545 nm, Emission: 605-670 nm, 20 % Excitation, 1/30 s). For better visibility, the highlight and gamma of the fluorescence pictures were increased and a composite of all three channels was generated.

4.2.2. Cellular experiments

4.2.2.1. Cellular cultivation

All cell lines were cultured as subconfluent monolayers in 10-cm petri dishes at 37 °C, in humidified atmosphere containing 5% CO₂. HeLa and MCF-7 cells were cultured in

RPMI 1640 medium supplemented with 10% FBS and 2–4 mM glutamine. HEK293 cells were cultured in MEM medium supplemented with 15% FBS and 4 mM glutamine. When reaching a confluency of ~ 80–90%, cells were splitted by using 0.5 mg·mL⁻¹ trypsin-EDTA for cell detachment. For cell culture experiments, cells were always grown to a confluency of up to 80%.

4.2.2.2. Cytotoxicity assays

HeLa (20,000), MCF-7 (15,000) or HEK293 (15,000) cells were seeded in a 96 well plate. The plate was incubated overnight for HeLa/MCF-7, or for 48 h when using HEK293 cells, at 37°C with 5% CO₂. Afterwards, cells were treated with 100 µl peptide solutions in medium. As control pure medium and 100 µl ethanol (70%) were used. These samples were incubated for 24 h at 37 °C, then cells were washed two times with PBS. An amount of 100 µl 10% resazurin solution in respective cell line suited medium were given to each well for 1 h at 37°C. The resorufin fluorescence was measured by using a microtiter plate reader (excitation: 550 nm, emission: 595 nm) to determine cellular survival.

4.2.2.3. Cellular uptake assays

For quantifying cellular uptake 100 000 HeLa or HEK293 cells, respectively, were incubated overnight in cell line suited medium at 37°C with 5% CO₂ in a 24 well plate. Afterwards, the supernatant was removed, and cells were incubated with 400 µl CF-labeled peptide solutions (5 or 10 µM) in medium without fetal bovine serum (FBS) for 30 min at 37°C. Then, cells were washed two times with 500 µl PBS, following addition of 150 µl trypsin. After 5 min incubation at 37°C, cells were resuspended in 850 µl of colorless medium with FBS. An amount of 100 µl of each solution were transferred in a 96 well plate and cellular uptake was determined with the Guava® easyCyte HTTM System (Merck) using the GRN-B (525/30) channel, counting 10 000 cells per well. Results were normalized to the uptake of **sC18**. The fluorescence spectra measured were also visualized with Kaluza analysis version 2.1 software.

4.2.2.4. Lactate dehydrogenase release assay

The CytoTox-One™ Homogeneous Membrane Integrity Assay by Promega was used for this experiment according to the manual's instructions. Briefly, cell medium was mixed with cell suspension in a dark ninety-six well plate leading to 17.000 HeLa cells in 200 µl. The plate was incubated overnight at 37°C with 5% CO₂. The next day, cells were treated with 100 µl peptide solutions. After incubation for 1 h at 37°C, the plate was equilibrated at room temperature for 20 min before lysis buffer was added to untreated samples to obtain positive controls. CytoTox-One™ reagent was added to each of the wells and the measurement of fluorescence was done using a microtiter plate reader (excitation: 560 nm, emission: 590 nm).

4.2.2.5. Haemolytic assay

Human red blood cells (hRBC) were washed in tenfold volume of PBS buffer and following centrifugation (3.000 xg, 4 °C, 5 min) four times. The cells were diluted with PBS to a concentration of 5 % (v/v) and 100 µL of this suspension were given in each well of a flat bottom 96 well plate. 50 µL peptide solutions in PBS were added to reach the desired peptide concentrations. As controls, PBS only and 1 % Triton X-100 in PBS were used. After 24 hours of incubation at 37 °C, the well plate was centrifuged (2.500 xg, 3 min) and 100 µL supernatant were transferred to another well plate. The absorption of these solutions at 560 nm was measured with a tecan plate reader to determine the haemoglobin concentration in the solution. The haemolysis was determined as percentage compared to Triton X-100.

4.3. Titanium surface assays

4.3.1. Surface immobilization of peptides (primary and secondary)

1 cm x 1 cm titanium substrates were cleaned by sonication in acetone, ethanol, and deionized water for 15 min each. The cleaned titanium substrates were transferred into a 24-well plate and sterilized under UV light for 15 min on each side.

For coating with chimeric peptides, purified titanium plates were incubated aerobically at 37 °C under constant agitation (200 rpm) with 500 µL of a 100 µM peptide solutions overnight. Controls were created with 500 µL PBS. Following the incubation with peptides, the solutions were removed from each well. The samples were washed five times with 1 mL PBS. Using sterile forceps, each titanium substrate was moved to a new 24 well plate. This preparation was performed in triplicates.

For polydopamine coating, purified titanium plates were incubated aerobically at 37 °C under constant agitation (200 rpm) with 500 µL of a 2 mg/mL solution of dopamine in TRIS-buffer overnight. The titanium plates were rinsed with PBS and incubated aerobically at 37 °C under constant agitation (200 rpm) with 500 µL of a 50 µM peptide in PBS overnight. Following the incubation with peptides, the solutions were removed from each well. The samples were washed five times with 1 mL PBS. Using sterile forceps, each titanium substrate was moved to a new 24 well plate. This preparation was performed in triplicates

4.3.2. X-ray photoelectron spectroscopy

The elemental analysis was performed with cooperation of the AG Mathur.

X-ray photoelectron spectroscopy (XPS) data were measured using a Surface Science Instruments ESAC M-Probe spectrometer with monochromatic Al K α source (200 W, 18 mA) of 1486.68 eV. Pass energy of 158.9 eV, 0.5 eV step size, 125 ms dwell time, averaged over seven scans was used for survey XPS spectra while pass energy of 55.22 eV, 0.05 eV step size, 175 ms dwell time, averaged over 25 scans was used for high-resolution XPS spectra. Charge-correction of insulating samples was performed with a flood gun (0 – 10 eV) in combination with magnetic immersion lens of extraction-electron optics. The software CasaXPS by Casa Software Ltd. was used to process the spectra.

4.3.3. Titanium binding assays

75 μL of bacterial culture (OD_{600} : 0.5) and 925 μL MH-medium are added upon the titanium plates in a 24 well plate and shaken with 75 rpm at 37 °C for six hours. As control, 75 μL bacterial solution and 925 μL ethanol (70 %) were used. After incubation, the supernatant was discarded, and the plates were washed gently with 500 mL PBS twice. Following this, the plates were added with 500 μL PBS and put into ultrasonic bath for 5 minutes. 10 μL supernatant were diluted with 990 μL PBS and 5 μL of the triplicates were each spread out on one third of an MH-agar plate. Those agar-plates are incubated overnight at 37 °C. The next day colonies were counted and thus the relative attachment of viable bacteria onto the treated titanium plates evaluated.

5. Hydrophobic substitutions optimize antimicrobial activity and selectivity

To improve the antimicrobial activity of **sC18**, the initial approach was to further develop on the hydrophobic substitutions established in the dissertation of Dr. André Reinhardt^[163]. Herein, the structure of **sC18** was tuned with hydrophobic amino acids to become more amphipathic and thus, to create novel potent antimicrobial peptides. Especially, the phenylalanine enriched peptides **AMP3a-3g** have shown potent antimicrobial activity, therefore making them a promising base for further investigation.

It is well known that the activity of membrane active peptides is often relying on the content of hydrophobic amino acids, as the side chains are utilized to interact with the lipids of the bio-membranes^[170]. To further improve hydrophobicity as well as proteolytic stability, unnatural amino acids were used within the peptide sequence. One promising candidate were fluorinated amino acids, that increase peptide hydrophobicity with minimal steric alterations^[105]. With this in mind, a novel generation of antimicrobial peptides was designed, based on substitution with fluorinated phenylalanine variants. The antimicrobial range of these novel peptide generation was determined, as well as their structure-activity relationship. As it was also well known that AMPs can commonly develop anti-cancerous activity, the selectivity of the novel peptides, as well as the phenylalanine substituted peptides **AMP3a-3g** was investigated between different types of eukaryotic cells.

The data presented in this chapter were published in the following article: "Multistep optimization of a cell-penetrating peptide towards its antimicrobial activity"^[171]. This chapter contains experiments performed by bachelor student Joshua Grabeck^[172]. It further contains data from my own master-thesis^[173], which were expanded upon in further research.

5.1. Synthesis and physicochemical evaluation

In the preliminary studies, the removal of the negatively charged Glu15 has generally improved the antimicrobial activity. Therefore, it was omitted in the next sequences. This resulted in the new 15 amino acids long peptide **AMP4a**, also known as **sC18ΔE**. With this peptide sequence substitutions at positions Arg10 and Lys15 were performed, with phenylalanine (**AMP4b**), as an analogue to **AMP3g**. To further increase the hydrophobicity of these novel peptides, different fluorinated phenylalanines were utilized in the creation of further peptides. These unnatural amino acids were used in the same double substitutions with mono- (**AMP4c**), bis- (**AMP4d**) and pentafluorinated phenylalanine (**AMP4e**) for creating the fourth generation of antimicrobial peptides.

Table 6: Sequences and physicochemical properties of the generation three and four antimicrobial peptides. Physicochemical values were calculated with the thermofisher peptide analysis tool.^[174]

Name	Sequence	MW [g/mol]	Charge	Hydro- phobicity	Hydrophobic moment
AMP3a	GLRKRLRKFFNKIKEK-NH ₂	2060.59	+8	27.52	0.639
AMP3b	GLRKRLRKFRNKIKFK-NH ₂	2087.66	+10	27.02	0.429
AMP3c	GLRKRLRKFRNKIKEF-NH ₂	2088.60	+8	27.66	0.678
AMP3d	GLEKRKRKFFNKIKFK-NH ₂	2078.65	+9	33.42	0.494
AMP3e	GLRKRLRKFFNKIKEF-NH ₂	2079.59	+7	34.59	0.728
AMP3f	GLRKRLRKFRNKIKFF-NH ₂	2106.66	+9	33.54	0.571
AMP3g	GLRKRLRKFFNKIKFF-NH ₂	2097.65	+8	38,74	0.596
AMP4a	GLRKRLRKFRNKIKK-NH ₂	1941.39	+10	20.10	0.656
AMP4b	GLRKRLRKFFNKIKF-NH ₂	1951.38	+8	35.09	0.561
AMP4c	GLRKRLRKFX ₁ NKIKX ₁ -NH ₂	1987.36	+8	36.93 ^d	/

Name	Sequence	MW [g/mol]	Charge	Hydro- phobicity	Hydrophobic moment
AMP4d	GLRKRLRKFX ₂ NKIKX ₂ -NH ₂	2023.34	+8	37.23 ^d	/
AMP4e	GLRKRLRKFX ₃ NKIKX ₃ -NH ₂	2131.28	+8	38.28 ^d	/

^aX₁: 4-fluorophenylalanine, ^bX₂: 3,5-difluorophenylalanine, ^cX₃: pentafluorophenylalanine, ^dextrapolated by correlation to HPLC retention times.

All novel peptides were obtained from solid phase peptide synthesis (SPPS) in high purities and evaluated in circular dichroism spectroscopy to assess the influence of fluorinated amino acids on the secondary structure formation.

Without the addition of trifluoroethanol (TFE) random coil formation was visible for all peptides. In hydrophobic environment, realized by addition of TFE, all peptides formed alpha helical structures (**Figure 8**). The calculated R-values for all four peptides have values around 0.9 indicating stable formation of secondary structures, with no evident influences of the fluorinated amino acids. Only **AMP4e** had slightly decreased R-value of 0.86, potentially from steric interactions of the two pentafluoro phenylalanine substitution, but only to minor degree.

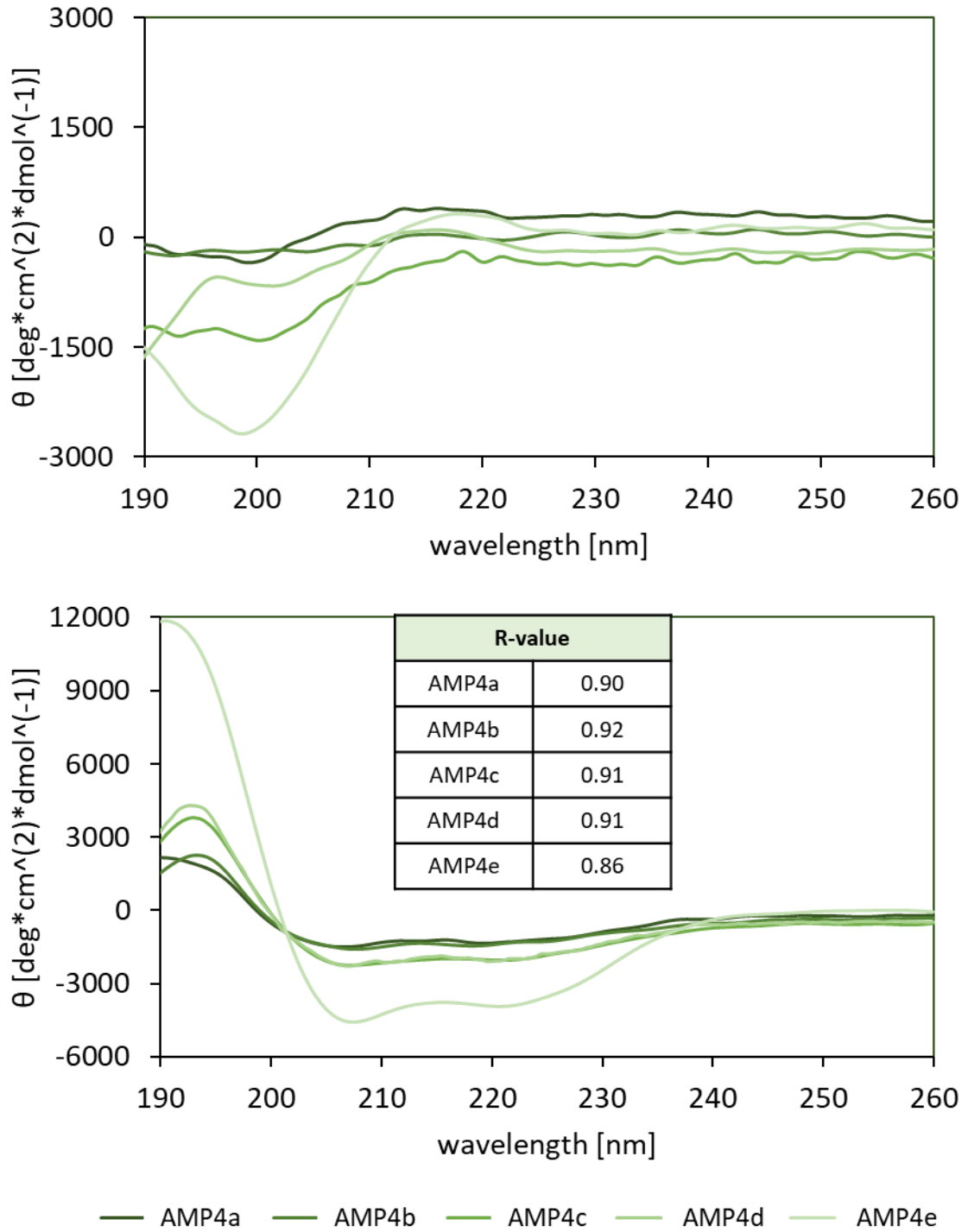


Figure 8: Circular dichroism spectroscopy of the generation four antimicrobial peptides in phosphate buffer (top) and buffer with the addition of trifluoroethanol (bottom).

5.2. Antibacterial experiments

From the results of CD-spectroscopy it was concluded that the peptides could also yield potent antimicrobial activity. The formation of alpha helices at the hydrophobic environment of the bacterial membrane is known to promote the antimicrobial activity of AMPs^[175]. For this reason, the antimicrobial assays were repeated on the seven bacterial strains, with the new peptides (**Figure 9**).

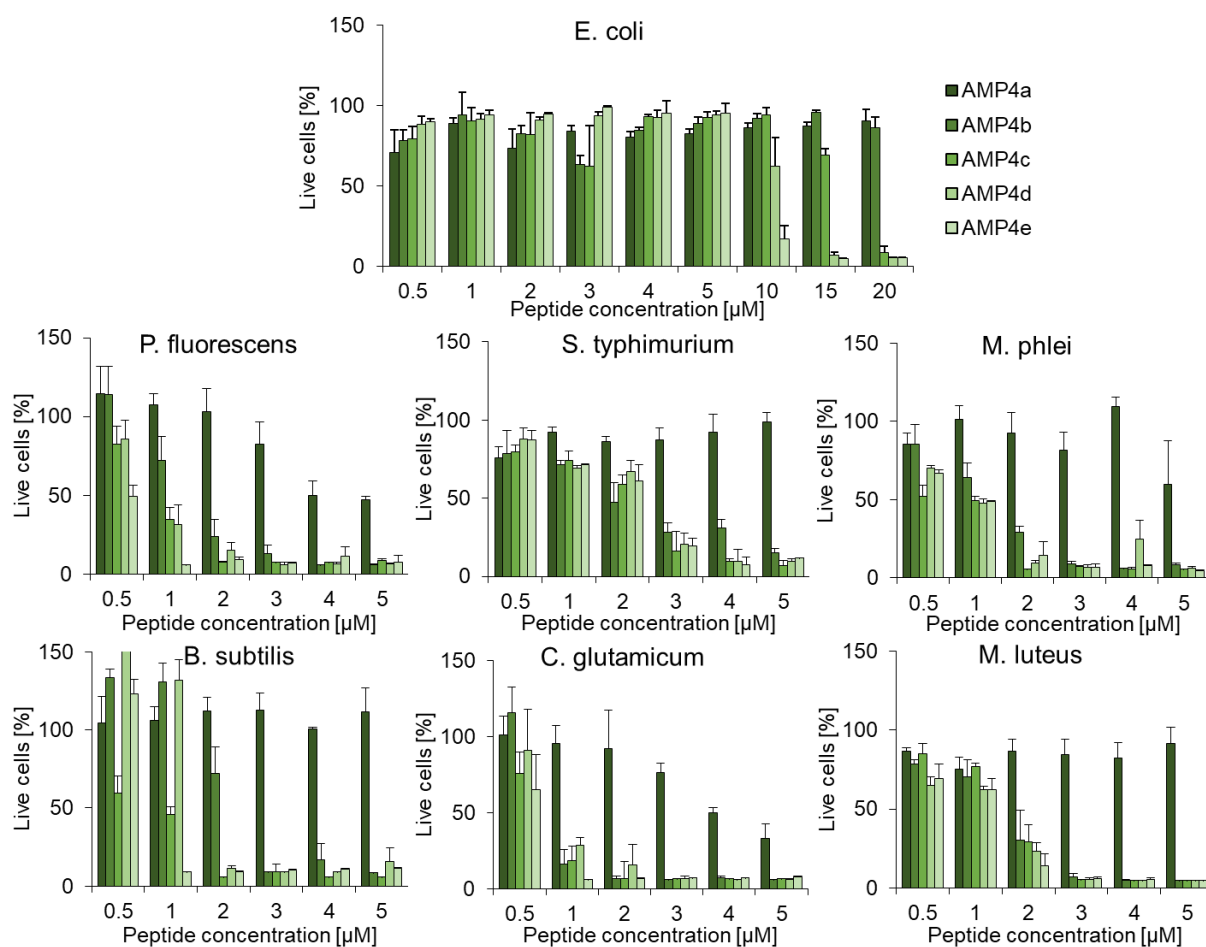


Figure 9: Screening generation four peptides for their antimicrobial activity against seven bacterial strains. Bacteria were incubated for 6 h at 37°C. Data represent the mean \pm SD of $n \geq 3$ performed in triplicate. Negative control (water) was set to 100% to calculate the relative quantity of living cells.

The fluorinated peptides were even more potent, than the peptides described in preliminary work^[163]. The results showed slightly increased antimicrobial activity of **sC18ΔE**, in comparison with **sC18**, against *C. glutamicum* and *P. fluorescens*. Nonetheless it was far less active than the other peptides in generation four. The novel

phenylalanine substituted peptide **AMP4b** had comparable activity to **AMP3g**, the most effective compound of the preliminary studies. The peptides **AMP4c–4e** featured altogether higher activities against the seven bacteria tested, also demonstrating significant impact on *M. phlei* and to less extent on *E. coli*, pointing to the high impact of the incorporated fluorinated amino acids. Interestingly, the activity of the peptides correlated with the number of fluor atoms attached to the fluorinated amino acids. Therefore, **AMP4e** exhibited the highest activity compared to the other peptides. To further evaluate the antimicrobial activity, MIC₅₀ values were calculated (**Table 7**), defined as the peptide concentration at which the bacterial growth is inhibited by 50 %.

Table 7: MIC₅₀ values [μ M] for the generation four peptides tested against seven different bacterial strains. Incubation time was 6 h at 37°C.

Peptide	<i>B. Subtilis</i>	<i>C. glutamicum</i>	<i>M. luteus</i>	<i>M. phlei</i>	<i>P. fluorescens</i>	<i>S. typhimurium</i>	<i>E. Coli</i>
AMP4a	24.4	4.8	>5.0	>5.0	6.0	>5.0	>50
AMP4b	1.9	1.4	1.2	2.0	1.8	2.8	45
AMP4c	0.8	0.9	1.2	1.0	0.8	2.7	17
AMP4d	1.6	0.7	1.0	1.0	1.1	1.2	10
AMP4e	0.5	0.6	1.0	1.0	0.4	1.0	7.5

The elimination of the negatively charged glutamate in **AMP4a** seemed to increase the antimicrobial activity and the additional enhanced hydrophobicity in **AMP4b** strengthened the formation of a secondary structure. Comparing antimicrobial activity to results of CD-spectroscopy, the novel peptides form stabilized secondary structures when in contact with hydrophobic bacterial surfaces. Moreover, the calculated hydrophobicity and hydrophobic moments fit well to the activities observed and are probably a first hint that an increase in hydrophobicity and the formation of an amphipathic helix could be linked to enhanced membrane-activity.

After performing the experiments on non-pathogenic bacterial strains, the next step was to analyse the antimicrobial activity of the most promising peptides **AMP3g**,

AMP4b and **AMP4e** on the pathogenic bacterium *Pseudomonas aeruginosa*. Together with Dr. Tom Cronenberg (Institute of Biophysics, University of Cologne) the influence of the peptide on this ESKAPE pathogen was investigated (**Figure 10**) and compared to the aminoglycoside antibiotic gentamycin.

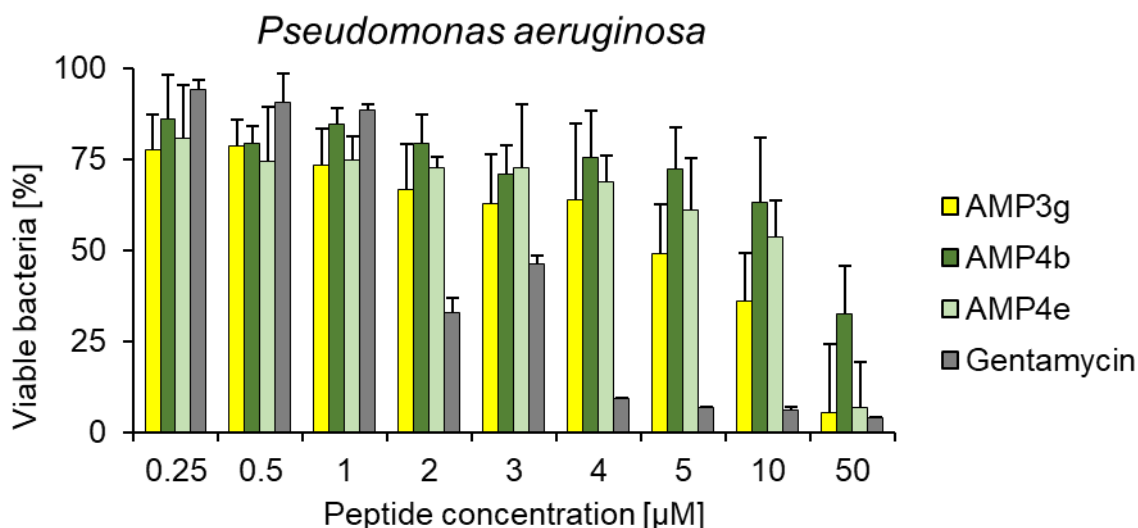


Figure 10: Antimicrobial activity of the peptides **AMP3g**, **AMP4b** and **AMP4e** against *Pseudomonas aeruginosa* in comparison to common antibiotic *Gentamycin*.

The calculated MIC₅₀ values were in the range of 9 µM for **AMP3g** and 11 µM for **AMP4e** to 19 µM for **AMP4b**. These MIC₅₀ values were higher than those measured for the other tested bacterial strains, especially looking on *Pseudomonas fluorescense*. However, *P. aeruginosa* is part of the group of ESKAPE pathogens that show increased resistance against multiple commonly used drugs, which might also inhibit the susceptibility to the new peptides. As the ESKAPE-pathogen is a well-known cause of healthcare associated infections^[11] and endocarditis^[12], the effect of new AMPs to this bacterial strain was of high interest and might contribute to the development of new drugs against this highly pathogenic species.

Overall, the strategy of using hydrophobic amino acid substitutions within the sequence of **sC18** provided novel peptides with improved antimicrobial activity against multiple types of bacteria. Especially **AMP3g**, **AMP4b** and fluorinated **AMP4c-4e**, as the most effective peptides, are of interest for further experiments.

5.3. Peptide stability

Even though AMPs are potent new candidates of antibiotic compounds, they commonly exhibit some disadvantages, like weak stability to proteolysis in physiological conditions^[176–178]. In the next set of experiments, protease and medium stability of **AMP4a-4e** were investigated.

It is known that unnatural amino acids affect the protease stability of peptides^[177], especially fluorinated amino acids^[176]. To investigate this influence in the novel AMPs containing fluorinated phenylalanine, the proteolytic stability to natural protease enzyme trypsin was investigated for the most potent variant **AMP4e**, which included the substitution with pentafluoro phenylalanine in comparison to two peptides **AMP4a** and **AMP4b** as control. After incubation at 37 °C with 1:50 (m/m) trypsin, peptide samples were taken after several time points and analysed with LC-MS (**Table 8**) to determine the identity of peptide fragments.

Table 8: *Enzymatic stability of peptides **AMP4a**, **AMP4b** and **AMP4e** after incubation with 1:50 trypsin. Cleavage-sites of peptides over time determined by LC–MS. N-terminal (A) and C-terminal (B) fragments were identified by their mass signature in ESI-MS.*

Peptide	Cleavage pattern	Time [min]	MW [g/mol]	Fragment A [g/mol]	Fragment B [g/mol]
AMP4a	GLRKR – LRKFRNKIKK	2	1941.6	628.8	1330.8
	LRKFR – NKIKK	5	1330.8	718.9	629.9
AMP4b	GLRKR – LRKFFNKIKF	2	1951.6	628.8	1340.8
	LRKFFNKIK – F	5	1340.8	1193.6	165.2
	LRK – FFNKIK	10	1193.6	415.6	796.0
	FFNK – IK	15	796.0	554.7	259.4
AMP4e	GLRKR – LRKFXNKIKX	2	2131.6	628.8	1520.8
	LRKFXNKIK – X	5	1520.8	1283.6	255.2
	LRK – FXNKIK	10	1283.6	415.6	886.0
	FXNK – IK	60	886.0	644.7	259.4

As trypsin cleaves peptides after cationic amino acids like arginine and lysine, unsurprisingly the high number of such amino acids led to multiple cleavage sites in the peptide and rapid degradation by the protease at several positions. All peptides were initially split after position Arg5 but thereafter the degradation of the peptides occurred at different major cleavage sites for the different peptides, leading to

equivalent products for **AMP4b** and **AMP4e** distinguished to the degradation of **AMP4a** already after 10 minutes. These changes in degradation can be contributed to the substitution of position Arg10 in **AMP4b** and **AMP4e** through which only **AMP4a** could be cleaved at this position. Instead, other amide bonds were cleaved for these peptides, mainly positions Lys8, Lys12 and Lys14 resulting in two major products FFNK and FXNK after an incubation time of more than 1 hour. The times in which these degradations occurred were higher for **AMP4e** when compared to the same fragmentations in **AMP4b**. Therefore, the degradation process seemed to be a bit slower because of the incorporation of the fluorinated amino acids into the sequence. Nevertheless, the fluorination of two amino acids in the 15 amino acid sequence could not prevent overall degradation of the peptide within two minutes.

To determine if those peptide fragments still retained some of the original AMP activity, some of the sequences were synthesized to be tested against *B. subtilis* and *P. fluorescens* (**Figure 11**).

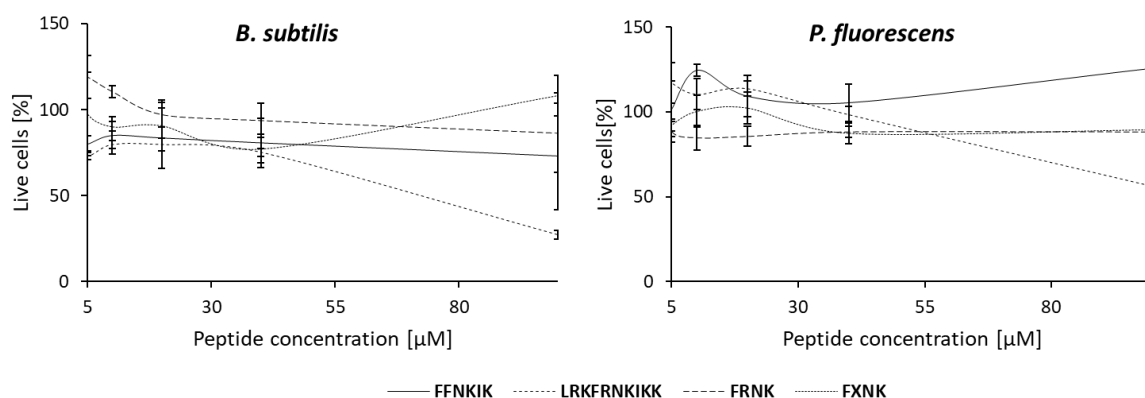


Figure 11: Antimicrobial activity (6 h, 37°C incubation) of the identified peptide fragments against *B. subtilis* and *P. fluorescens*.

None of these fragments showed antimicrobial activity when tested in a concentration range up to 50 μM. Only at higher concentration of 100 μM the longest fragment of LRKFRNKIKK resulted in visible antimicrobial effects. In conclusion the shorter fragments were not able to induce antimicrobial activity and the complete peptide sequence is needed. Therefore, the mechanism of action must be fast to avoid rapid inactivation of the peptide by proteolytic enzymes.

Together with Dr. Pitter Huesgen (Forschungszentrum Jülich), the influence of low concentrations of peptide **AMP4e** on the proteome of *B. subtilis* was analysed to see

if the bacteria would in fact express higher amounts of protease enzymes as defensive mechanism to degrade the peptides. The volcano plot of the proteomics results is presented in **Figure 12**.

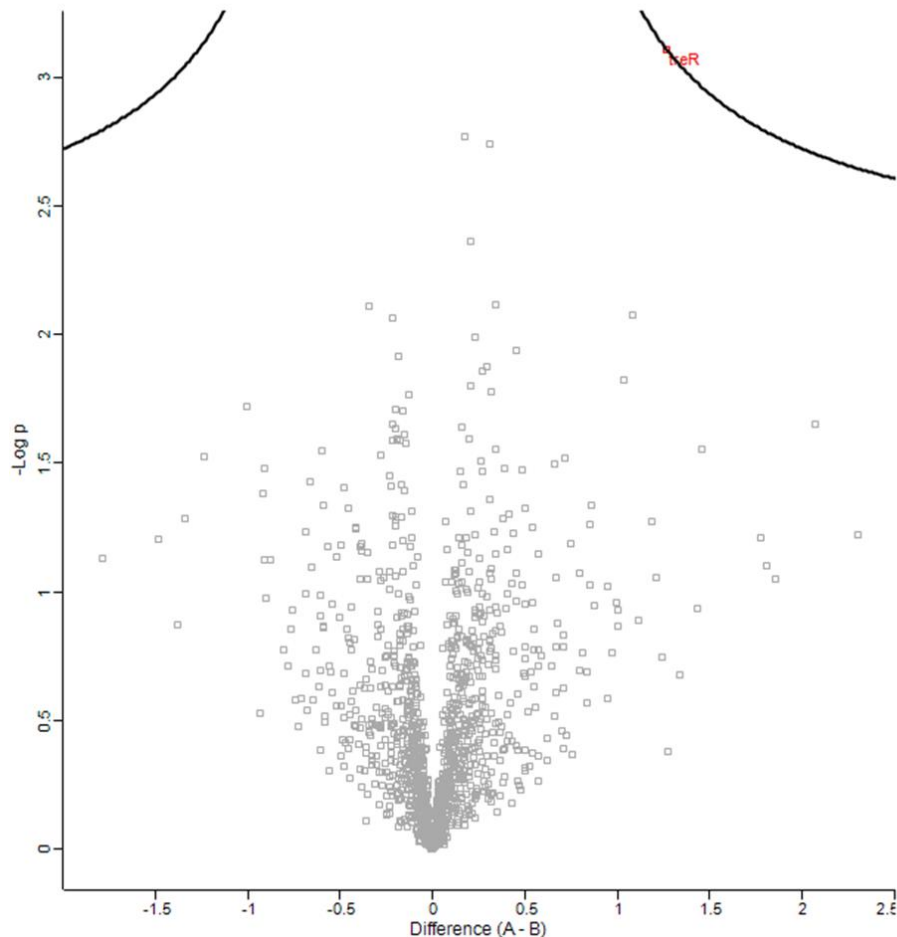


Figure 12: Proteome evaluation of *B. subtilis* treated with **AMP4e**.

No significant changes were observed for bacteria treated with **AMP4e**. There are prominent differences in protein abundance (**Figure 12**, red and blue circle) but nothing statistically significant. Only the protein trehalose operon transcriptional repressor was on the threshold of significant increase. This change might indicate a response of the bacterium in upregulating carbohydrate metabolism, especially as trehalose is known to stabilize the fluidity of membranes in response to dryness or desiccation^[179], which might indicate a stress response after peptide membrane interaction. But otherwise, no significant changes could be seen that would strengthen this hypothesis. Overall, this leads to the conclusion that the peptides kill the bacteria very fast and most probably by cell membrane lysis and not by intracellular effects.

To evaluate the stability under physiological conditions, the three peptides **sC18ΔE** and the other peptides **AMP4b**, as well as **AMP4e** were incubated in parallel with freshly prepared growth medium, as well as bacterial cell culture-conditioned supernatant. After incubation of the peptide in respective media for 18 hours, the peptides were utilized in an antimicrobial activity assay at MIC against *B. subtilis* for six hours (**Figure 13**).

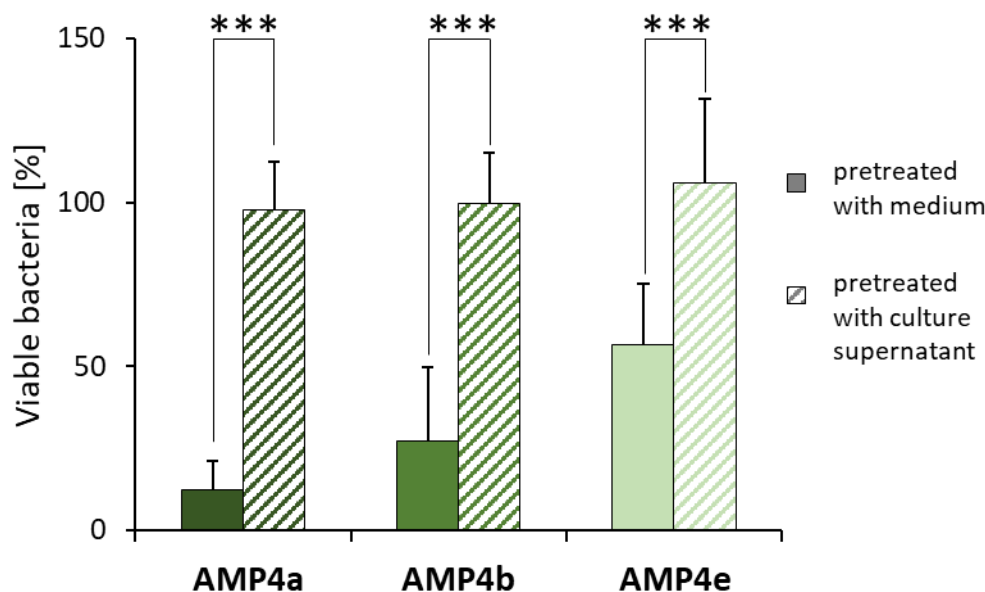


Figure 13: Antimicrobial assay (6 h, 37 °C incubation) using *B. subtilis* and **AMP4a**, **AMP4b** and **AMP4e** at minimal inhibitory concentration, with preceding 18 h treatment in fresh growth medium (full colour) or bacterial cell culture supernatant (dashed). Data represent mean \pm SD of $n \geq 3$ performed in triplicate. Statistical significance was calculated with *t*-test: ns: $P > 0.05$; ***: $P \leq 0.001$.

After pre-incubation in bacterial cell culture supernatant all peptides lost their antimicrobial activity. The samples pre-incubated in fresh growth media on the other hand retained their activity. As conclusion from those results, it might be that the microbe will secrete proteases into the surrounding environment, that have the ability to cleave the amid bonds of **sC18** based peptides, thus inhibiting the peptides bioactivity. This correlates with the former experiment on the antimicrobial activity of short fragments of degraded AMPs, which lacked in antimicrobial activity.

To conclude, the results of previously described experiments demonstrated that the peptides are susceptible to fast degradation by proteolytic enzymes like trypsin and that the shorter fragments did not exhibit significant antimicrobial activity. This degradation was delayed by incorporation of fluorinated amino acids only to a minor degree at sites where the fluorinated amino acids sterically impair proteolytic substrate binding. Peptide activity was in fact inhibited by pre-incubation with bacterial cell culture supernatant of *B. subtilis*, where they can be degraded by extracellular proteases. Nonetheless, the peptides have significant antimicrobial activity, which suggests a rapid mechanism of action.

5.4. Haemolytic activity and cytotoxic profiles in mammalian cells

A common side effect of strong antimicrobial peptides is cytotoxic behaviour^[180]. For this reason, it is crucial to investigate on cytotoxicity against eukaryotic host cells to evaluate the potential risk of applying the peptide as medical compound. As the peptides **AMP3a–3g** and **AMP4a–4e** seemed to have promising overall activities, they were utilized in experiments for haemolysis and cytotoxicity, to assess their selectivity between bacteria and eucaryotic cells.

First, the haemolytic activity was analysed by using human red blood cells (hRBC), which were incubated with the peptides for 24 hours (**Figure 14**). Strikingly, almost all peptides did not affect the erythrocytes after a full day of incubation. Only the most potent antimicrobial peptides, **AMP4d-4e**, with bi- and pentafluoro phenylalanine modification, exhibited haemolytic activities at 40 μM concentration, if only up to 15%. As shown in other studies, hydrophobicity has a crucial role in the haemolytic activity of membrane-active peptides^[181]. Only when increasing the hydrophobicity by attaching especially non-polar compounds, like pentafluoro-phenylalanine or multiple carborane clusters^[157], haemolysis occurred.

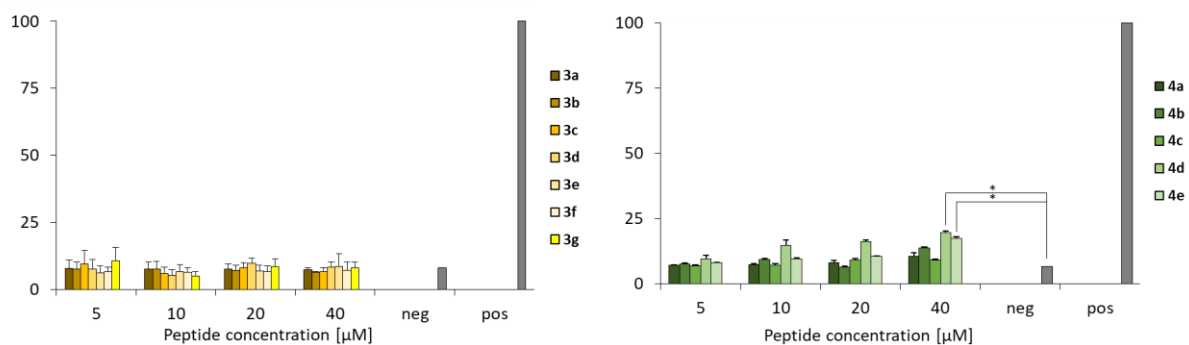


Figure 14: Haemolysis assay of the generation three and four antimicrobial peptides using human red blood cells (hRBC). The erythrocytes were incubated with peptides for 24 h at 37°C. Negative control was water and positive control 1% Triton X-100. Data represent mean \pm SD of $n \geq 3$ performed in triplicate. Statistical significance was calculated with *t*-test: *: $P \leq 0.05$.

In the next step the toxic behaviour of the new peptides against the non-cancerous cell line of human embryonic kidney cells (HEK293), was investigated. Peptides were incubated with the cells for 24 hours and cell viability was analysed through the transformation of resazurin to resofurin (**Figure 15**). Once again, the peptides had only marginal effect to the viability of HEK293 cells, comparable to the human red blood cells, with only **AMP3g** and **AMP4e** showing some toxic activity at 40 μ M concentration.

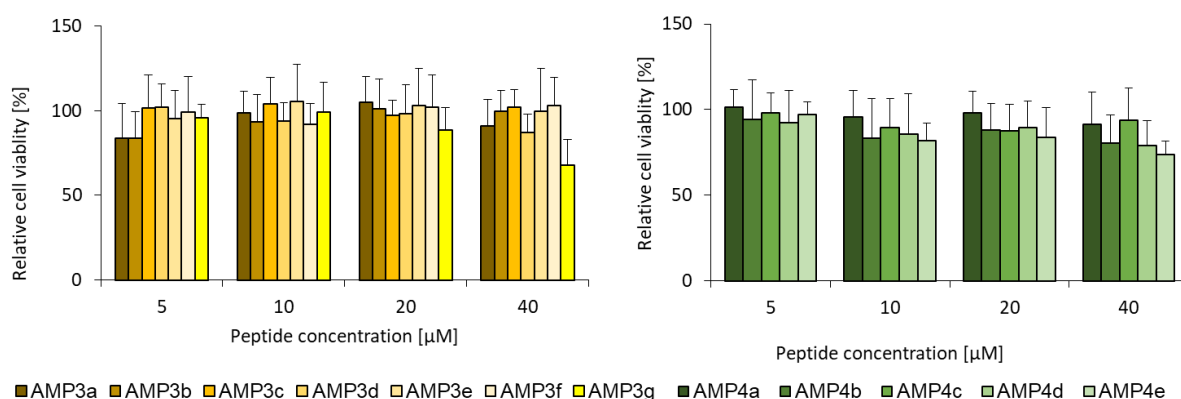


Figure 15: Cytotoxicity of the generation three and four peptides towards non-cancerous cell line HEK293 for 24 hours at 37 °C. Negative control (water) was set to 100% to calculate relative cell viability. Data represent mean \pm SD of $n \geq 3$ performed in triplicate. Statistical significance was calculated with *t*-test: *: $P \leq 0.05$; **: $P \leq 0.01$; ***: $P \leq 0.001$.

The peptides selectivity between bacterial and human non-cancerous cells was determined by calculating selectivity indices (**Table 9**). These calculations might show that all tested peptides affected HEK293 cells at least with 1.6-fold higher concentrations compared with the MIC for either *B. subtilis* or *P. fluorescens*. Interestingly, the most active peptide, **AMP4e**, displayed a selectivity index of at least ~40, offering high selectivity from bacterial to mammalian cells.

Table 9: Selectivity index calculation between bacterial and mammalian cells. Calculation (CC_{100}/MIC_{100}) was performed with the experimental values of *B. subtilis* and *P. fluorescens*, as well as CC_{100} values of HEK293 cells.

Selectivity index calculation		AMP								
		3d	3e	3f	3g	4a	4b	4c	4d	4e
MIC ₁₀₀ [μM]	<i>B. subtilis</i>	>15	>15	>20	>15	>5	>3	>2	>2	>1
	<i>P. fluorescens</i>	>25	>25	>25	>15	>5	>3	>2	>3	>1
CC ₁₀₀ [μM]	HEK293	>40	>40	>40	>40	>40	>40	>40	>40	>40
Selectivity index	HEK/BS	2.7	2.7	2	2.7	8	13.3	20	20	40
	HEK/PF	1.6	1.6	1.6	2.7	8	13.3	20	13.3	40

Cationic antimicrobial peptides are known to frequently develop anti-cancerous activity^[64], due to the similarities between bacterial and cancerous cells in distribution of negatively charged phospholipids in the outer membrane leaflet^[63]. Therefore, **AMP3a-3g** and **AMP4a-4e** were tested against different cancerous cell lines. Human cervical cancer (HeLa) and human breast cancer (MCF7) were chosen as model cell lines (**Figure 16**). In contrast to hRBC or HEK293 cells, the peptides had a significant toxic effect against the cancer cell lines. Especially **AMP3g**, as well as fluorinated peptides **AMP4c-4e**, showed high cytotoxicity starting already at 10 μM concentration. Peptides **AMP3a-3c** and **AMP4a** were almost non-toxic towards both cancerous cell lines. Interestingly, **AMP4b**, containing only natural phenylalanine substitutions similar to **AMP3g**, induced no cytotoxicity against HeLa cells but significant toxicity against MCF7 cells was observed at concentrations above 20 μM. This behaviour might indicate further selectivity between different cancerous cell lines, which could be due

to different compositions of the cell membrane and non-lipidic components like specific membrane bound proteins.

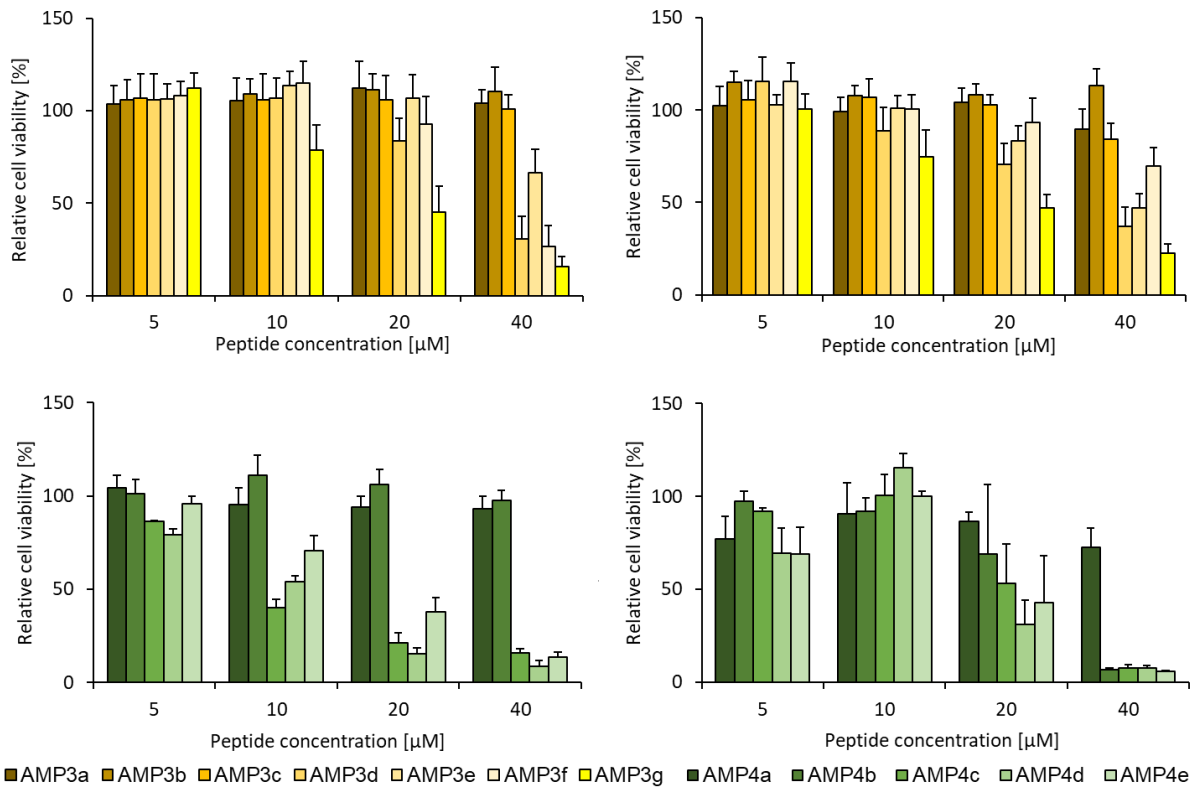


Figure 16: Cytotoxicity of the generation three and four peptides towards cancerous cell lines. (left: HeLa, right: MCF7) for 24 hours at 37 °C. Negative control (water) was set to 100% to calculate relative cell viability. Data represent mean \pm SD of $n \geq 3$ performed in triplicate. Statistical significance was calculated with *t*-test: *: $P \leq 0.05$; **: $P \leq 0.01$; ***: $P \leq 0.001$.

To further investigate the interaction of the novel peptides with different cell lines, studies of cellular uptake were performed. HeLa and HEK293 were used as models for cancerous and non-cancerous cell lines. As the novel antimicrobial peptides were developed from the sequence of the CPP **sC18**^[156], they were suspected to retain the ability to translocate in cells. For this reason, HEK293 and HeLa cells were incubated for 30 min with carboxyfluorescein (CF)-labelled peptides in non-toxic concentrations of 5 or 10 μ M, respectively, and their cellular uptake was quantified by flow cytometry (**Figure 17**).

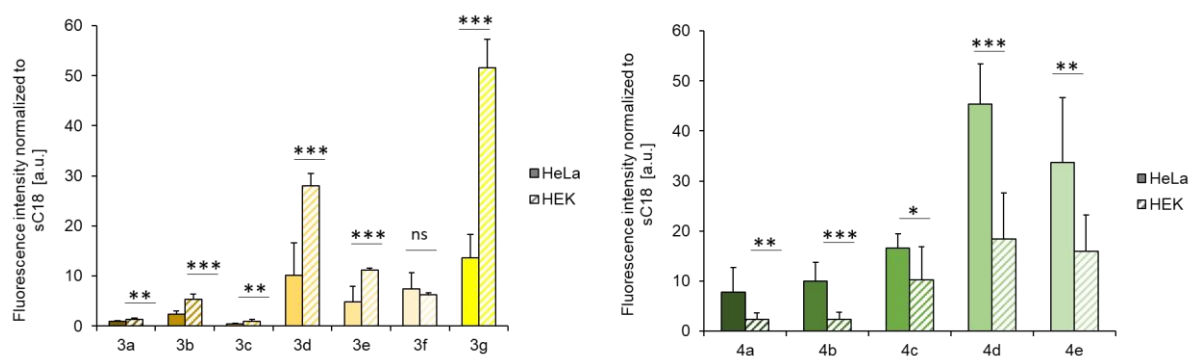


Figure 17: Cellular internalization experiment in HeLa and HEK293 cells using the third and fourth generation peptides. The sub-lethal concentrations used were 10 μM for generation three peptides and 5 μM for generation four peptides. 10.000 cells were counted, and data normalized to **sC18**, representing the mean \pm SD of $n \geq 2$ performed in triplicate. Statistical significance was calculated with t-test: ns: $P > 0.05$; *: $P \leq 0.05$; **: $P \leq 0.01$; ***: $P \leq 0.001$.

When normalized to **sC18**, all peptides, except for **AMP3a** and **AMP3c**, showed higher cellular accumulations in both cell lines than the original CPP. The uptake of peptides was quite differently between the generations. The generation three peptides (tested at 10 μM), achieved higher cellular uptake in HEK293 cells, than into HeLa cells. Here **AMP3d** and **AMP3g** showed the highest accumulation with 32- and 50-fold increased uptake values compared to **sC18**. In contrast, the uptake in HeLa cells was only moderately increased compared by nearly 5- to 14-fold. On the other hand, **AMP4a-4e** (tested at 5 μM) showed higher uptake into HeLa cells, approximately twice as much, as into HEK293. **AMP4d** displayed the highest accumulation in both cell lines, with a 45-fold and 18-fold increase in uptake, followed by **AMP4e** with a more than 24-fold and 16-fold increase compared to **sC18**. It was evident that the peptides having the highest accumulation were also the most hydrophobic ones. Therefore, a direct correlation of hydrophobicity to cellular uptake was assumed. Furthermore, the proper integration of the peptide sequences into the hydrophobic core of the lipid bilayer seemed more important for the high uptake values than the overall net charge of these peptides. As significant accumulations were obtained at concentrations without toxic effects for most peptides, especially in HEK293 cells, no correlation of uptake and cytotoxicity was possible. For this reason, the corresponding peptides should be further

investigated as cell-penetrating peptides as well as possible intracellular targeting processes in HEK293 cells and related cell lines.

Overall, the observed cytotoxicity and cellular uptake values might be the result of specific membrane interactions, most probably dependent on the different membrane compositions^[182].

5.5. Membrane disruption mechanism

From previous results, it can be concluded that the new AMPs act very fast and presumably by a membrane lysis process that is often observed for cationic AMPs. To elucidate if the mechanism of antimicrobial action relies on membrane disruption, a lactate dehydrogenase (LDH) release assay was utilized. HeLa cells were chosen as model since those were most affected after peptide treatment. Included in this experiment were **AMP3d-3g** as well as **AMP4a-4e** because they appeared to be the most active peptides.

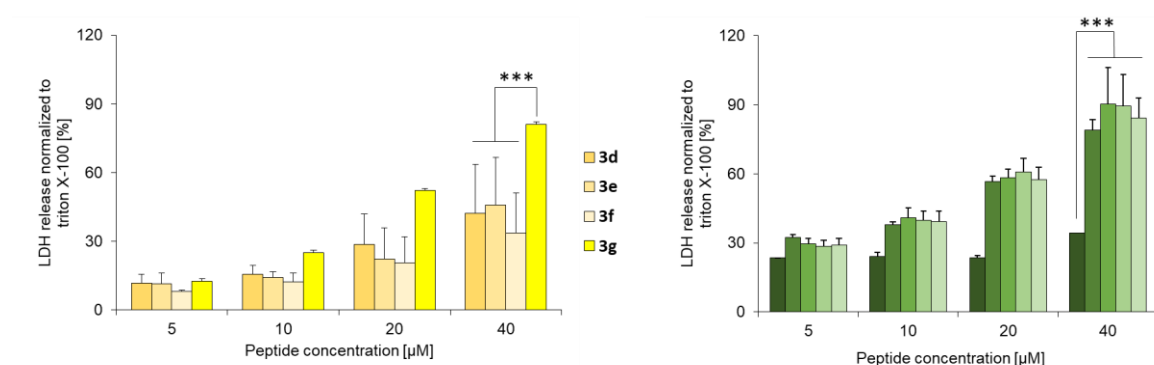


Figure 18: Lactate dehydrogenase release assay of selected peptides to investigate the membrane disruption process. Peptides were incubated with HeLa cells for 1 hour. Data represent mean \pm SD of $n \geq 2$ performed in triplicate. Statistical significance was calculated with *t*-test: ns: $P > 0.05$; ***: $P \leq 0.001$.

While increasing peptide concentrations, a high outflow of LDH after 1 h incubation was observed (Figure 18). This effect was especially prominent for **AMP3g** and **AMP4b-4e**, which all display high membrane activity, proving a lysing effect on HeLa cells. One major reason for this observation might be the electrostatic attractions to the

negatively charged cancerous outer membrane leaflet. These interactions between the positively charged AMPs and negatively charged components of cancer cell membranes play significant roles in the binding and selective disruption of cancer cell membranes^[64].

To deduce the mechanism of membrane interaction between the novel peptides and bacterial outer membranes, one additional experiment was performed with peptides **AMP3g** and **AMP4e**, as they were among the most active compounds and comprised different sequence lengths and substitutions. Scanning electron microscopy (SEM) was used to visualise alterations in the morphology of the outer bacterial membrane of *B. subtilis*, *C. glutamicum* and *P. fluorescens*. Peptides were incubated for 90 minutes with four times the MIC₅₀ and after preparation of samples, electron microscopy was performed by Dr. Frank Nitsche (Department of Biology, University of Cologne) (**Figure 19**).

As evident from **Figure 19**, a loss of structural integrity was characterized in all bacteria after peptide treatment, probably due to the disturbing effects induced by the peptides on the bacterial membranes^[183]. These same observations were made for both, gram-positive as well as gram-negative bacteria, even though they vary in setup of their cell walls. Thus, it might be that the peptides affected them in the same manner. Based on the disturbance of the bacterial surface, the novel peptides seem to gain antimicrobial activity due to lysing activity instead of intracellular targets^[56,74,184]. The depolarization and deformation processes lead to membrane disruption and finally cell lysis, which is a common mechanism for cationic antimicrobial peptides.

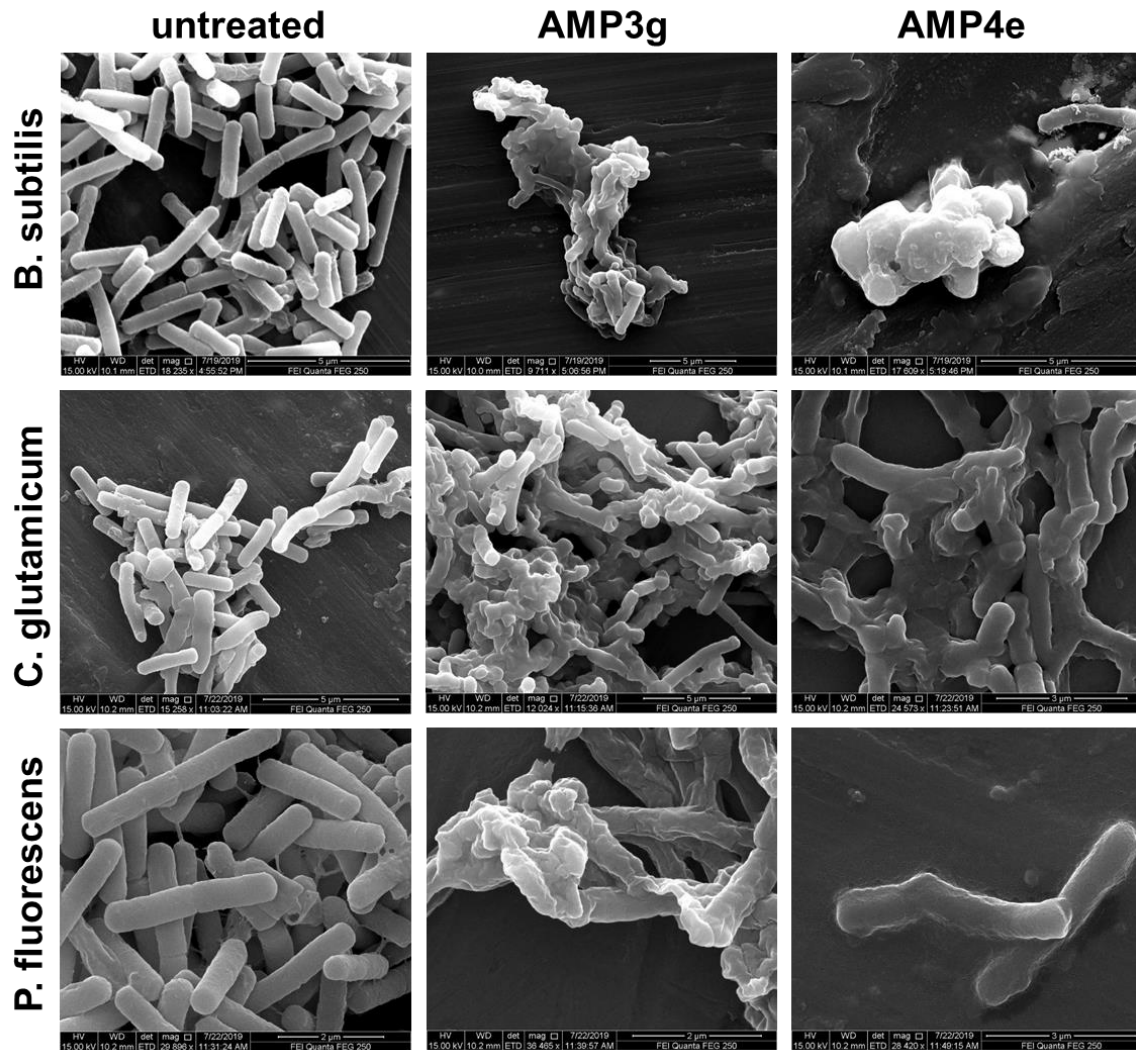


Figure 19: Characterization of morphological changes in different bacteria after peptide incubation using scanning electron microscopy. Incubation: 90 minutes at 37 °C with 4xMIC₅₀ of antimicrobial peptides or water (control).

5.6. Conclusion

The novel peptides developed so far, show greatly enhanced antimicrobial activities compared to the original cell-penetrating peptide **sC18**. Especially **AMP3g** and **AMP4b–4e** have proven as interesting candidates for further AMP development. They have demonstrated rapid activity against a broad spectrum of bacteria, most notably pathogenic *P. aeruginosa*. This was most likely caused by direct disruption of the bacterial membrane, leading to bactericidal effects. The proteolytic stability assay also showed that the novel AMPs must act very rapidly by membrane disintegration, as they were very susceptible to degradation and the resulting fragments were not as active

as the original peptides. These observations lead to the hypothesis that the novel peptides must kill the bacteria quickly before they were inactivated by bacterial proteases. This is probably supported by the fact that initial proteome studies have not revealed significant changes in protein abundances. Such fast mechanisms favour future application of the novel peptides in topical treatment strategies, such as their application as coatings of metallic surfaces minimizing the risk of device infection in prostheses or clinical devices^[112,119].

Performed experiments did not show any significantly toxic effects towards human erythrocytes or even HEK293 cells, in the case of most peptides. This indicated a promising selectivity index between bacterial and mammalian cells. The most obvious example is peptide **AMP4e** which exhibited MIC₅₀ values below 1 µM towards several bacterial strains yet showed no cytotoxicity against HEK293 cells in concentrations up to 40 µM. On the other hand, this peptide showed significant cytotoxic and even lytic activity against cancerous cell lines HeLa and MCF7. Therefore, the most interesting peptide for further research as antibacterial drug would probably be **AMP4b**, expressing significant antimicrobial activity, while still showing no cytotoxicity towards most types of human cells analysed. Additionally, the peptides **AMP3g** and **AMP4c-4e**, might be promising candidate to be evaluated as anticancer peptides (ACP), as considerable toxic effects towards cancer cells were detected. Overall, fluorinated peptides **AMP4c-4e** showed the strongest antimicrobial potential, while also expressing increased toxicity against mammalian cells. Since **AMP4d** and **AMP4e** did also translocate strongly inside cancerous cells, their application as versatile cancer-targeting transporters might be of interest.

The evident cell selectivity might originate from the different surface characteristics of the various cell types investigated. The lytic effects are proposed to originate from hydrophobicity combined with the high content of basic amino acids. These results demonstrate new insights into the sequence requirements for novel AMP development.

To summarize, the series of novel peptides have been designed as highly active antimicrobial peptides with promising selectivity between bacterial and mammalian cells, as well as also between healthy and cancerous cells. Those intriguing properties, make them interesting contribution for further research in the further application of AMPs, as well as the design of new, highly functionalized peptides.

6. R,L variants of different sC18-based peptides

To gain further insights into the physicochemical influences on the antimicrobial activity of AMPs, another approach on designing antimicrobial peptides based on **sC18** was assessed.

As already known, not only hydrophobic^[170], but also cationic amino acids are crucial to antimicrobial activity in many AMPs.^[185,186] Furthermore, the formation of two distinct sites of hydrophobic and cationic amino acids in alpha helical peptide folding has proven beneficial to antimicrobial activity in peptides. For this reason, the influence of cationic as well as hydrophobic amino acid substitutions of the sequence of **sC18** and shorter variants **sC18ΔE** and **sC18*** was investigated. Previous studies have already focussed on the cytotoxic activity of modified peptide **RL-sC18*** based on CPP **sC18*** in eukaryotic cells^[187], but the potential of this peptide as AMP has not been investigated, yet.

This chapter focusses on two factors that might have impact on peptide activity:

1. The length of the antimicrobial peptides sequence
2. The specific positions of hydrophobic and cationic substitutions

This chapter contains experiments performed by bachelor student Laura Buchwald^[188] and master students Michele Casoria^[189] and Tobias Behn.

6.1. First RL-sC18 variants – influence of peptide length

It has been shown in recent studies that an arginine/leucine substitution might be beneficial to structure the peptide **sC18*** into a nearly perfect amphipathic helix. In fact, **RL-sC18*** has been proven to have increased cytotoxicity and cellular uptake, compared to **sC18*** [187].

Based on these results, herein the aim was also to modify the longer sequences **sC18** and **sC18ΔE** in the same way, leading to **RL-sC18** and **RL-sC18ΔE** (Figure 20). The hydrophobic momentum was increased for all new R,L peptides, by reinforcing the amphipathicity in helical structures of the novel peptides.

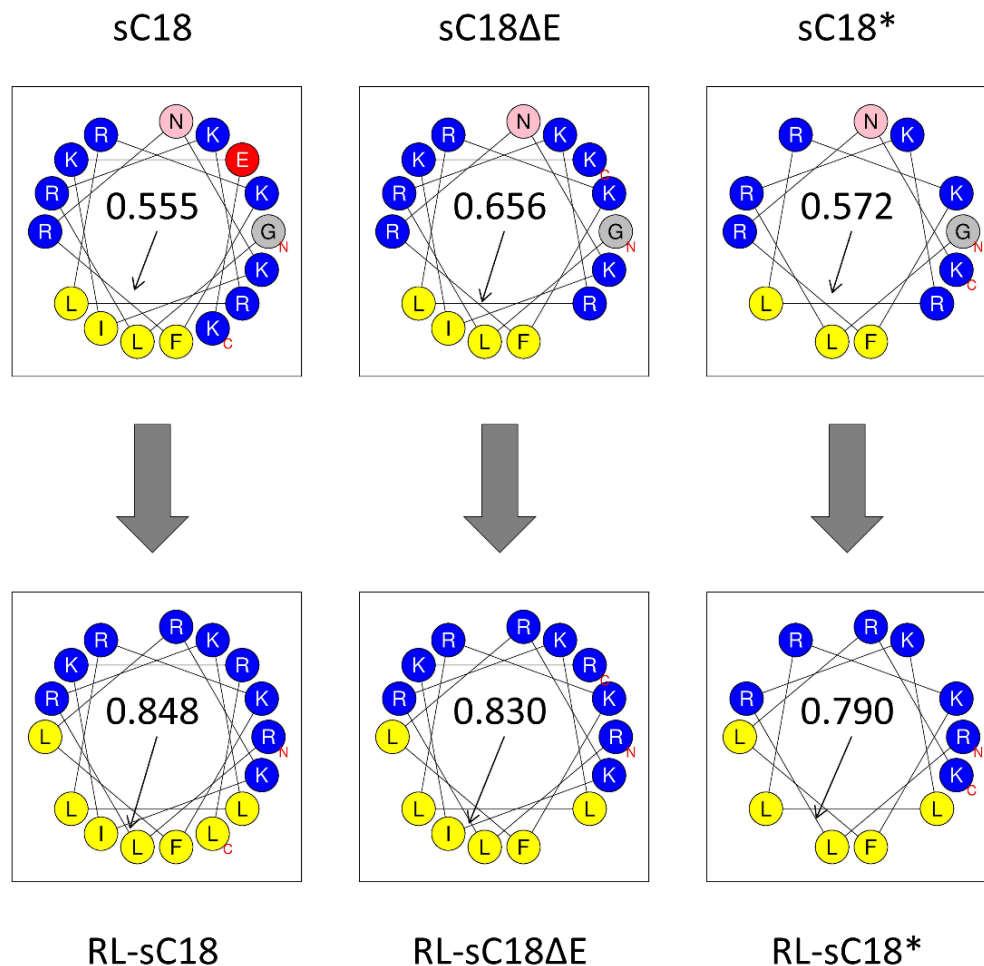


Figure 20: Helical wheel projections^[165] for peptides **sC18**, **sC18ΔE** and **sC18*** as well as **RL-sC18**, **RL-sC18ΔE** and **RL-sC18***.

Table 10: Sequences and physicochemical properties of the **RL-sC18** variants. Physicochemical values were calculated with the thermofisher peptide analysis tool^[174].

Name	Sequence	MW (g/mol)	Charge	Hydrophobicity	Theoretical pI
RL-sC18	RLRKLLRKFLRKIKRL-NH ₂	2137.8	+10	39.09	13.1
RL-sC18ΔE	RLRKLLRKFLRKIKR-NH ₂	2024.6	+10	34.83	13.1
RL-sC18*	RLRKLLRKFLRK-NH ₂	1627.1	+8	29.77	13.0

Firstly, CD spectroscopy was performed to evaluate the formation of secondary structures in different media (**Figure 21**). All peptides showed more random coil structures when in phosphate buffer solution. However, for **RL-sC18** it might be assumed that it slightly structures into an alpha helical structure, as suggested from the two characteristic minima at 208 and 222 nm^[190]. On the other side, when TFE is present, all peptides formed helical structures (**Figure 21**), as already observed for the parent peptides^[163]. Comparing the R-values of the novel peptides, a trend can be observed from most efficient folding for **RL-sC18** (0.83) that decreases correlating with the peptide's length to **RL-sC18ΔE** (0.82) and finally to the shortest version **RL-sC18*** (0.78). Thus, the length of the peptide showed a slight influence on the folding of these peptides, which might also alter the bioactivity towards bacteria or mammalian cells, what was investigated in the next experiments.

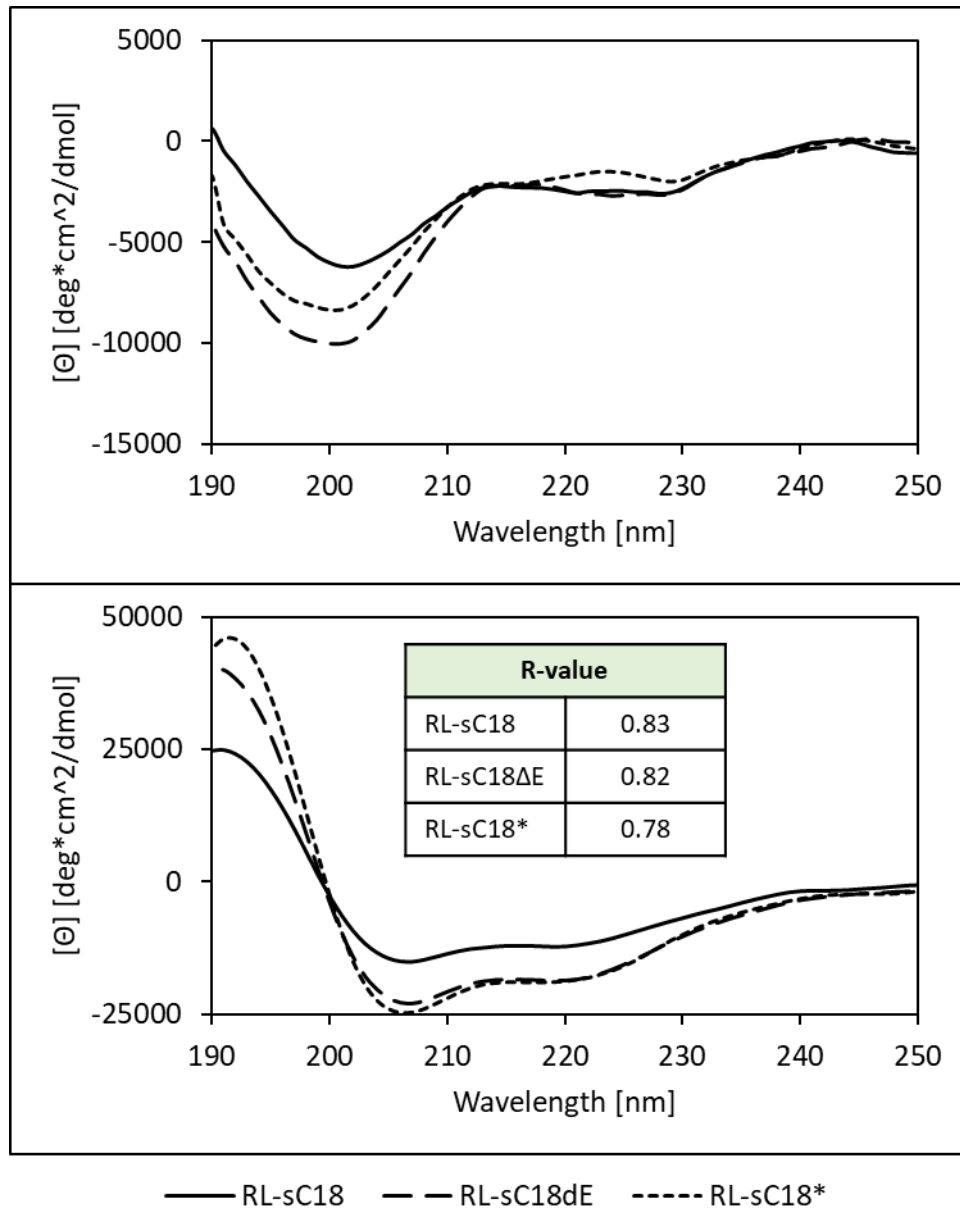


Figure 21: CD-spectroscopy of peptides *RL-sc18*, *RL-sC18ΔE* and *RL-sC18** in phosphate buffer (top) or phosphate buffer with TFE (bottom). R-values were calculated from the intensities at 208 and 222 nm.

The antimicrobial activity for these RL-variants was evaluated using seven gram-positive (*B. subtilis*, *C. glutamicum*, *M. luteus*), gram-negative (*P. fluorescens*, *S. typhimurium*, *E. coli*) and acid-fast (*M. phlei*) bacterial strains (**Figure 22**).

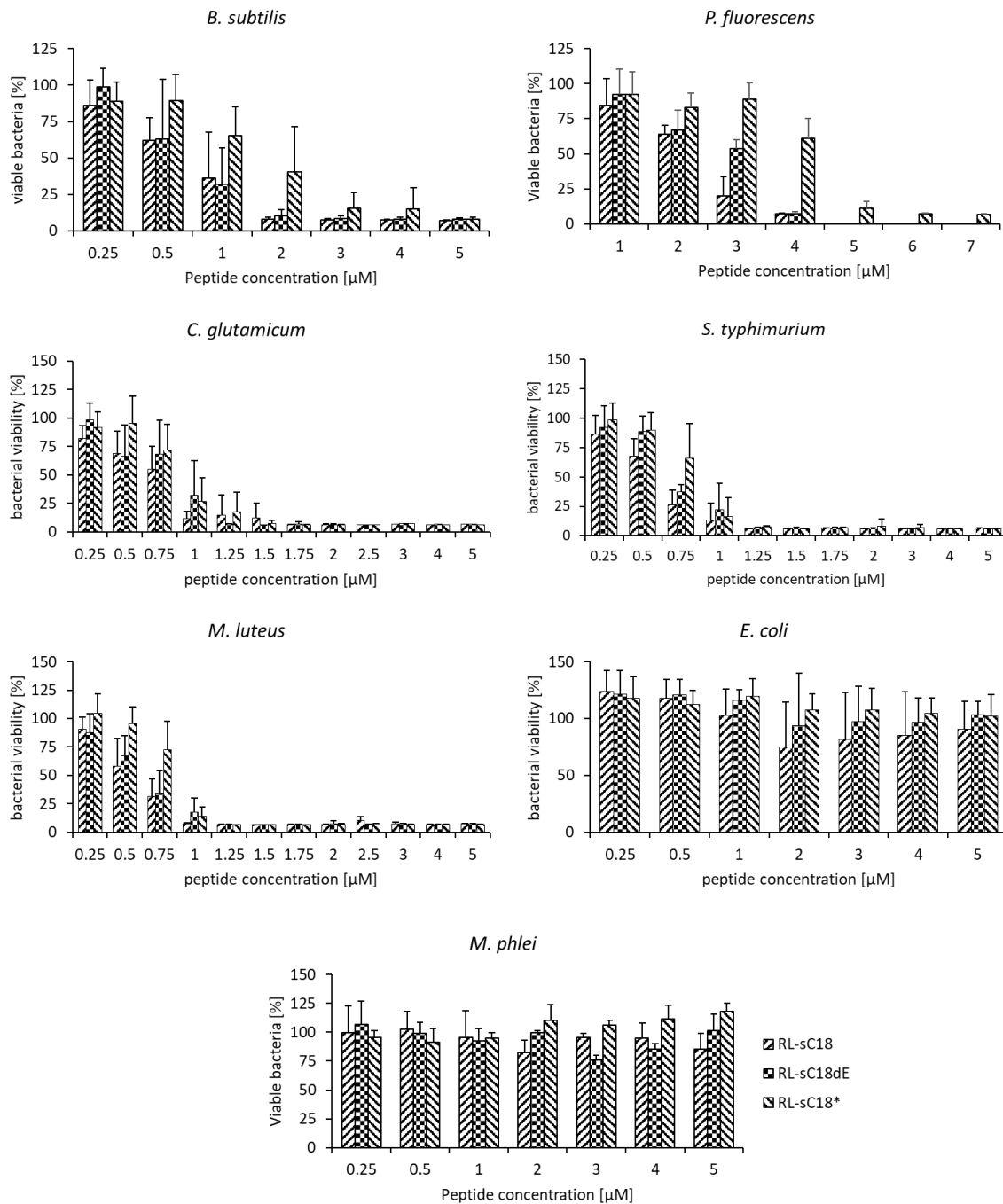


Figure 22: *Iodnitrotetrazolium chloride* assay using the **RL-sC18** variants and testing them against *B. subtilis*, *M. luteus*, *C. glutamicum*, *P. fluorescens*, *S. typhimurium*, *E. coli* and *M. phlei*, respectively.

The peptides expressed significant antimicrobial activity against most tested bacterial strains, with minimal inhibitory concentrations below 2 μM. Only *E. coli* and *M. phlei* were not affected by the peptides in the tested concentration range of up to 5 μM. These results are in line with the other **sC18**-based AMPs tested beforehand, which

showed no activity against these two strains^[163]. Also, the MIC₅₀ values were in the same range, namely between 0.5 μM and 1 μM for the other tested bacteria. **RL-sC18*** was slightly less efficient than the other two peptides for *B. subtilis*, *P. fluorescens* and *S. typhimurium*. This difference might be attributed to the shorter length of the peptide, as **RL-sC18*** is only 12 amino acids long, compared to the 15 or 16 amino acid variants. Indeed, it was recently described how AMP activity was positively influenced the longer the sequence of the peptide^[191]

Next, the interaction with eukaryotic cells, in this case human erythrocytes, was investigated to get insights into the lytic activity of the R,L-peptides and the influence of peptide length on cytotoxicity.

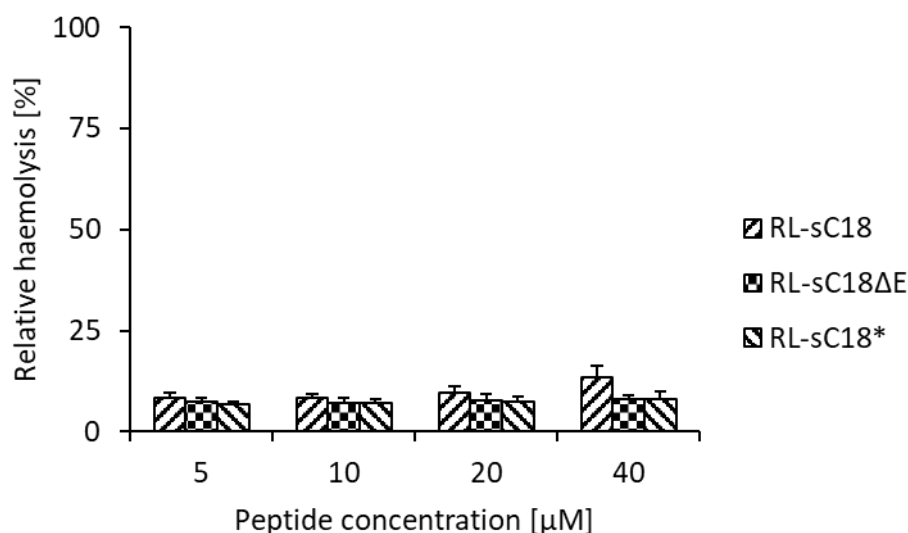


Figure 23: Haemolysis assay of the three **RL-sC18** variants, normalized to Triton X-100. Incubation: 24 hours at 37 °C.

After performing this experiment, only a slight increase in the haemolytic activity up to 13 % was observed for the longest peptide **RL-sC18**, as the other two peptides did nearly not induce any haemolysis at all. These results indicate the longer the sequence of the RL-peptides the higher the membrane activity for both prokaryotic as well as eukaryotic cells occurs. One reason for this observation might be that for instance **RL-sC18** folds probably in an easier way into a stable alpha-helical structure. This might be possible since within longer peptides more hydrogen bonds can be formed^[192,193] which have been described to enhance helical structure formation.

Table 11: Peptide sequences and physicochemical values (calculated with the thermofisher peptide analysis tool^[174]) of novel R,L-peptides.

Name	Sequence	MW (g/mol)	Charge	Hydrophobicity	Theoretical pI
RL-1	RLRKLRKFRNK-NH ₂	1671.1	+9	14.40	13.1
RL-2	GLRKLLRKFRNK-NH ₂	1528.9	+7	22.80	12.8
RL-3	GLRKLRKFLNK-NH ₂	1528.9	+7	23.11	12.8
RL-4	GLRKLRKFRRK-NH ₂	1614.0	+9	14.40	13.1
RL-1/2	RLRKLLRKFRNK-NH ₂	1628.1	+8	22.80	13.0
RL-1/3	RLRKLRKFLNK-NH ₂	1628.1	+8	23.11	13.0
RL-1/4	RLRKLRKFRRK-NH ₂	1713.2	+10	14.40	13.2
RL-2/3	GLRKLLRKFLNK-NH ₂	1485.9	+6	29.93	12.5
RL-2/4	GLRKLLRKFRRK-NH ₂	1571.0	+8	22.80	13.0
RL-3/4	GLRKLRKFLRK-NH ₂	1571.0	+8	22.89	13.0
RL-1/2/3	RLRKLLRKFLNK-NH ₂	1585.0	+7	29.98	12.8
RL-1/2/4	RLRKLLRKFRRK-NH ₂	1670.1	+9	22.80	13.1
RL-1/3/4	RLRKLRKFLRK-NH ₂	1670.1	+9	22.89	13.1
RL-2/3/4	GLRKLLRKFLRK-NH ₂	1528.0	+8	29.73	12.8

With these fourteen novel peptides in hand, antimicrobial activity assays were performed using the gram-positive bacterium *B. subtilis* and peptide concentrations ranging from 0.5 to 50 μM (**Figure 25**).

For the mono-substituted peptides it can be concluded that **RL-4** (Asn11Arg) was the most potent peptide in terms of antimicrobial activity, exhibiting a MIC value below 10 μM . In contrast, **RL-1** (Gly1Arg) showed the weakest activity since bacterial viability was still not completely inhibited at the highest concentration. Interestingly, **RL-2** (Arg5Leu) resembled in its profile more **RL-1** and was, thus, less effective than **RL-3** (Arg10Leu). However, in comparison to **sC18*** all variants, besides **RL-1**, displayed an increase in antimicrobial activity.

The double-substituted peptides shared somehow this trend in activity. Again, the weakest peptide was **RL-1/2**, combining the two substitutions with the least activity increase. Interestingly, it was peptide **RL-2/3** combining both isoleucine substitutions that exhibited the highest activity for those peptides. This might be caused by the same effects seen before, as hydrophobicity plays one major role for antimicrobial activity in peptides.

Notably, the triple substituted peptides showed all very similar activities, comparable to the double-substituted variants. Nevertheless, they seemed less active than **RL-2/3** and as such the further combination of arginine substitutions in **RL-1/2/3** and **RL-2/3/4** did not seem to further impact the antimicrobial potential more than the combined hydrophobic substitutions alone.

Overall, the highest antimicrobial effect was obtained when combining the two leucine substitutions at position Arg5 and Arg10, which increased the hydrophobic part of the peptides resulting in obvious improved antimicrobial activity compared to the substitutions of Gly1 and Asn11 with arginine.

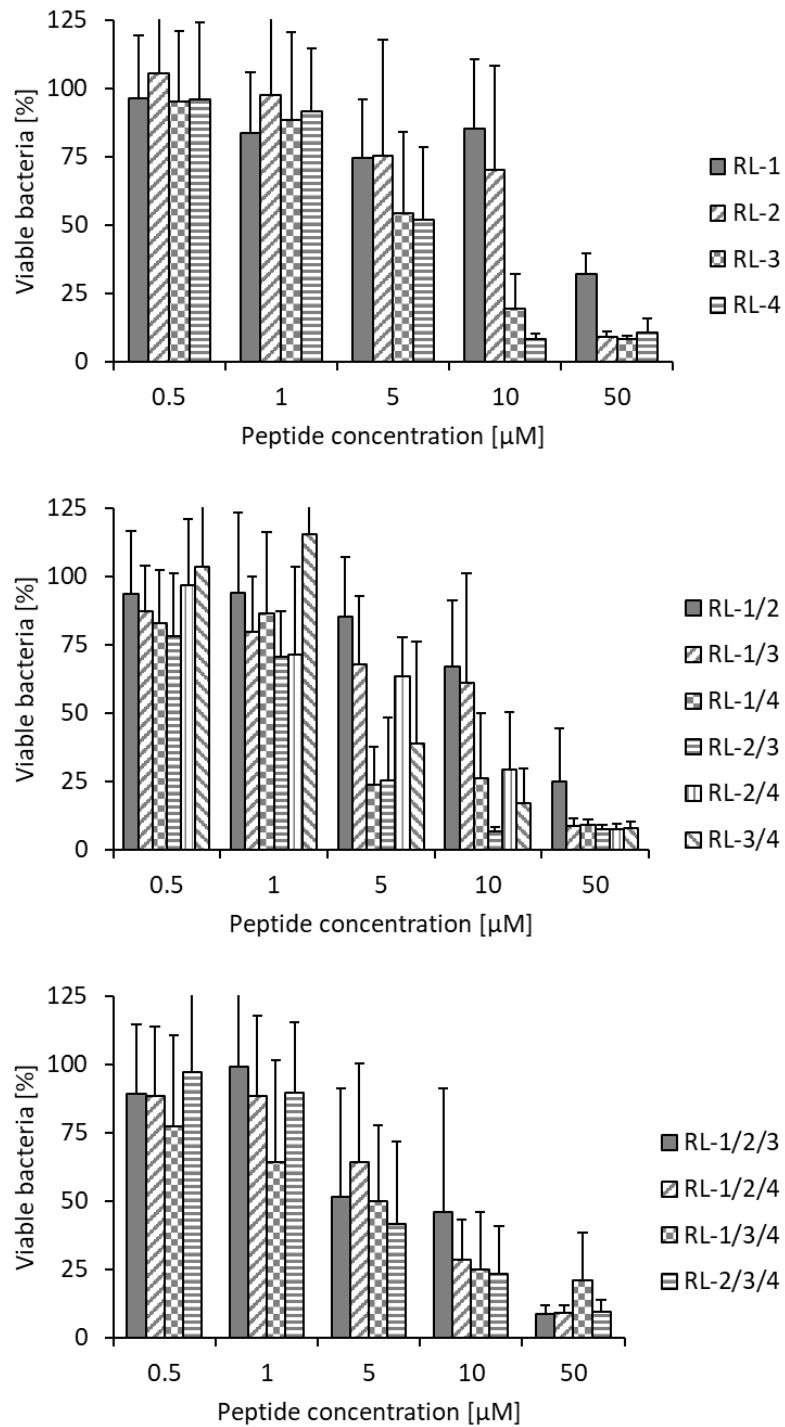


Figure 25: *Iodinitrotetrazolium chloride* assay using RL-peptides and testing them against *Bacillus subtilis*. Top: Mono-substitutions, middle: double-substitutions, Bottom: Triple-substitutions.

Based on these results, it was decided to further pursue experiments with four selected peptides. The less antimicrobial active peptide **RL-1** was chosen as well as the more potent **RL-2/3**, **RL-3/4**, and **RL-1/3/4** as examples for double and triple substitutions.

Firstly, the antimicrobial activity of these peptides was investigated using a spectrum of six gram-positive (*C. glutamicum*, *M. luteus*), gram-negative (*P. fluorescens*, *S. typhimurium*, *E. coli*) and acid-fast (*M. phlei*) bacterial strains (**Figure 26**).

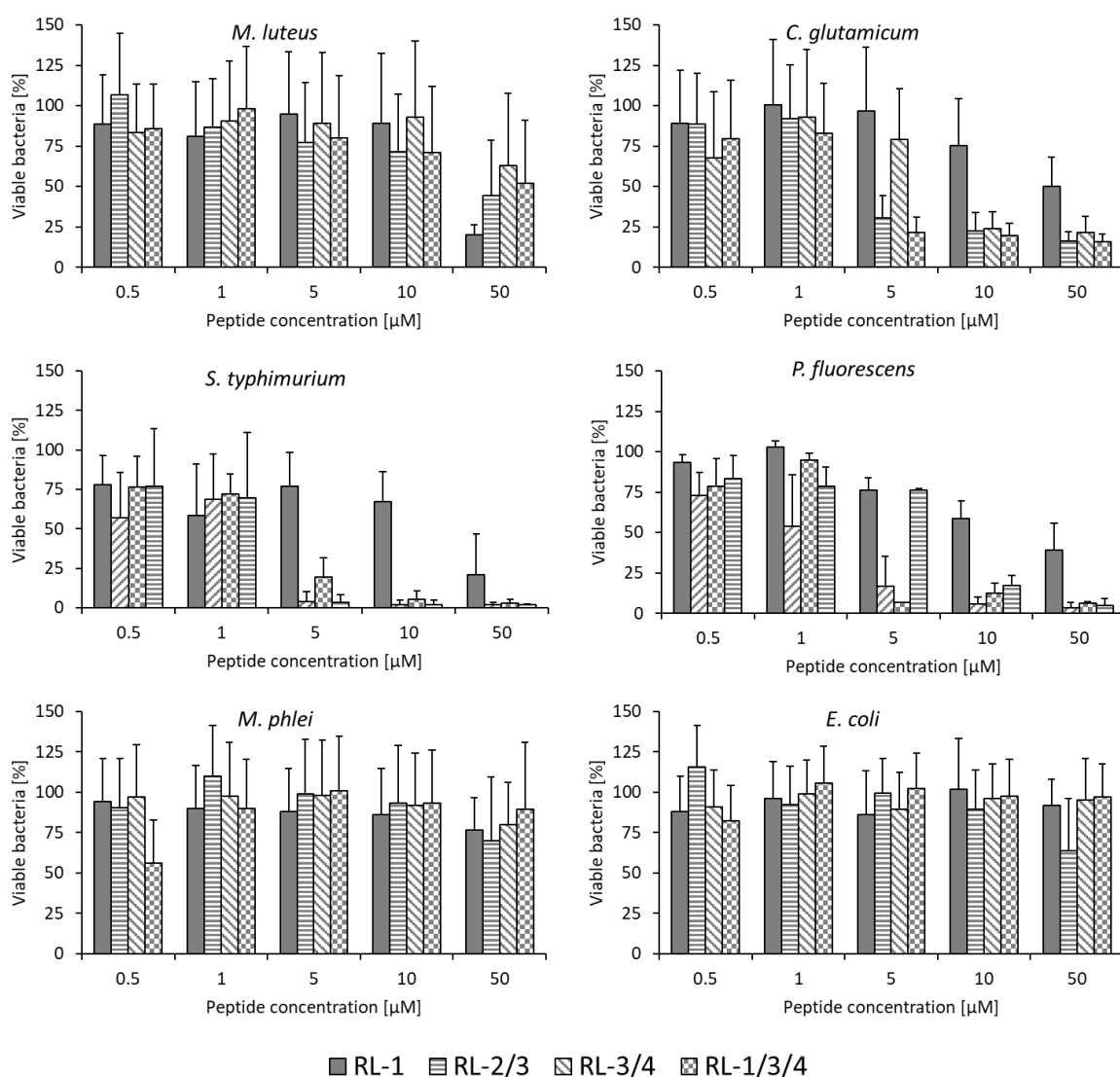


Figure 26: *Iodnitrotetrazolium chloride* assay using selected RL-peptides and testing them against *M. luteus*, *C. glutamicum*, *S. typhimurium*, *P. fluorescens*, *M. phlei* and *E. coli*.

For this selection of peptides, no significant changes were observed in the viability of *M. phlei* and *E. coli*. This result is consistent with previous results of **sC18**-derived AMPs for example **AMP2a-2d** and **AMP3a-3c** and the other **RL-sC18** variants (**Figure 26**). Overall, **RL-1** had only minor impact on the growth of most bacterial strains and has increased MIC values compared to the other peptides, except in *M. luteus*, where it was the only peptide to show slightly increased antimicrobial activity at 50 μM . **RL-3/4** had less impact on gram-positive *C. glutamicum*, *M. luteus* and gram-negative *S. typhimurium* than **RL-2/3** with two isoleucine substitutions, even though it was combining the two alternations with the highest impact of mono-substituted peptide sequences. This once again demonstrates the importance of the increased hydrophobic content in the peptide sequence relative to the enriched cationic amino acids. The trifold substituted peptide **RL-1/3/4** had similar impact on the bacterial growth as the two double-substituted peptides, indicating that the combination of both arginine-substitutions with one leucine-substitution did not further increase the membrane activity.

As last experiment, the influence of the amino acid substitutions on the haemolytic activity against hRBCs was investigated (**Figure 27**). After incubation with the selected peptides for 24 hours, no haemoglobin release was detected proving their good selectivity towards bacteria compared to erythrocytes.

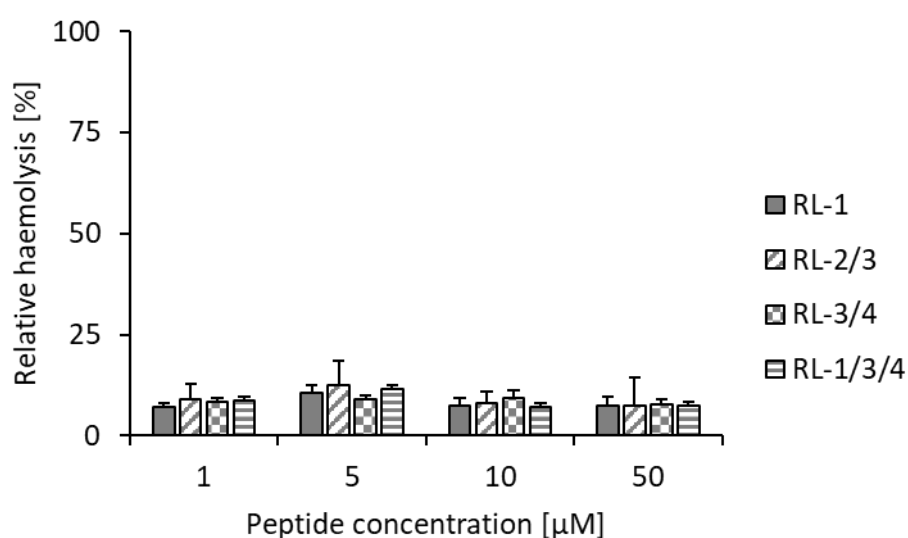


Figure 27: Haemolysis assay for the four selected RL-screen peptides, normalized to Triton X-100. Incubation: 24 hours at 37 °C.

6.3. Conclusion

Through rational design, a series of new antimicrobial peptides with specific arginine and leucine substitutions was developed. These were designed to form amphipathic alpha helical structures with two distinct faces, one consisting purely of cationic and the other of hydrophobic amino acids. In general, the length of the peptides seemed to play a crucial role in antimicrobial activity. Indeed, the 16 and 15 amino acids long peptides **RL-sC18** and **RL-sC18ΔE** had lower MIC values than the 12 amino acid short peptide **RL-sC18***. This can be attributed to better interaction with the membrane for a longer peptide, as it has more potential to interact with the full length of lipids^[191] of which the bacterial membrane is constructed. The longest peptide **RL-sC18** was also the only peptide that had an increase in haemolytic activity after incubation for 24 hours, although this increase was not high, compared to the haemolytic activity of Triton X-100 and **LL37**.

Furthermore, the different substitution sites in the sequence of **RL-sC18*** were investigated, both individually as well as in combination with each other, to compare the influences on antimicrobial activity. The substitution of the *N*-terminal glycine with arginine (**RL-1**) contributes to the lowest activity increase, whereas the two isoleucine substitutions, enlarging the hydrophobic area in helical formation (**RL-2** and **RL-3**), resulted in potent increases individually and even more significant in combination, than any combination with arginine substitution.

Overall, the peptides developed herein might be promising antimicrobial candidates, particularly owing to the finding that almost no haemolytic activity was detected. This was most likely caused by the differences in charge of the membrane that is different between bacterial and eukaryotic membranes.^[194] Further experiments need to be done to determine side-effect on other cell types, as **RL-sC18*** has already been known to induce cytotoxicity in previous studies^[187].

7. Surface immobilization of antibacterial chimeric peptides

After developing antimicrobial peptides with broad range of activity and investigating the physicochemical influences, the next step was to apply some of the new peptides as antibacterial surface coatings.

As the problem of bacterial biofilm formation is a remaining threat on medical devices, especially inorganic implants^[15,23], the development of protective antimicrobial layers on small titanium plates, is in high demand^[108]. Antimicrobial peptides immobilized with chemical linker layers and chimeric peptides fused with surface binding sequences, have been assessed in such application to prevent biofouling.

As the most efficient antimicrobial peptides of former studies, **AMP3g**, **AMP4b** and **AMP4e** were considered for this adaption in surface modification. The antimicrobial and haemolytic profile of chimeric peptides was investigated. Furthermore, the antibiofouling potency of AMPs immobilized with linker layers and surface binding sequences on small titanium plates was evaluated.

This chapter contains experiments performed by bachelor student Rebekka Arnold^[195].

7.1. Polydopamine immobilization of AMPs

The three peptides **AMP3g**, **AMP4b** and **AMP4e** were the most promising AMPs developed within this thesis and as such, their ability to prevent biofilm formation on small titanium plates, as model compound for medical equipment and prosthetic material, was examined.

To investigate the potential antibiofilm activity of the three peptides, they were immobilized on titanium plates (1cm x 1cm) by utilizing a binding layer of polydopamine in a simple two step protocol. This method is well known and consists of the formation of a polydopamine layer from dopamine monomers on freshly cleaned titanium plates^[133-135]. The polydopamine layer could be seen as a golden colour of the pure silvery metal, indicating efficient loading of the linker. This was followed by another 24 hours incubation with the peptides, which were then covalently coupled to the functional groups of the linker layer.

After this, the titanium plates were incubated with bacterial cultures of *B. subtilis* for six hours, followed by subsequent removal of adhered bacteria from the metal plate in

ultrasonic bath. The bacterial solution was spread out on agar plates, to assess the colony formation in comparison to the pure titanium control (**Figure 28**).

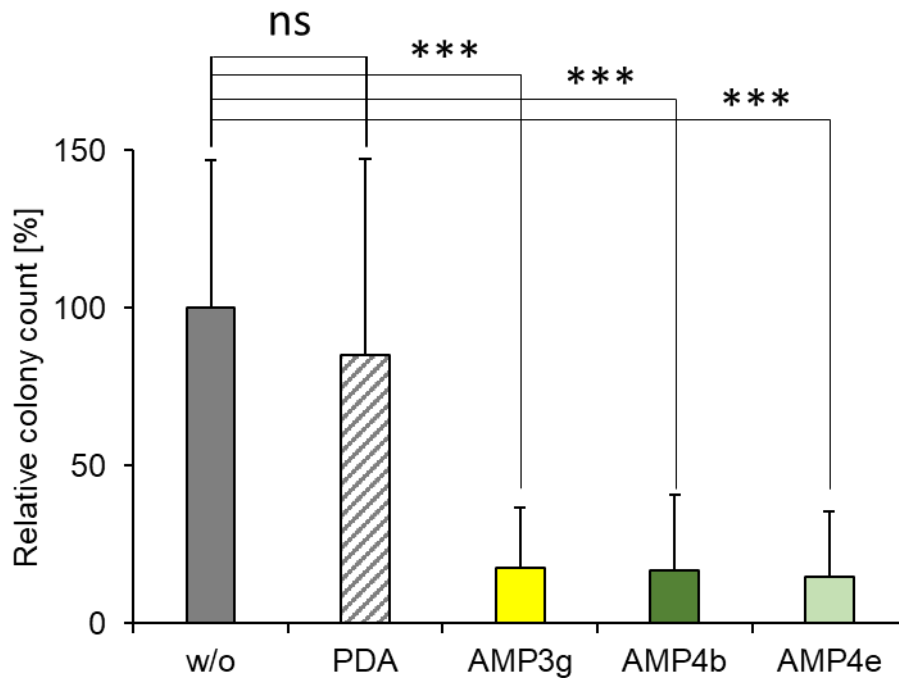


Figure 28: Efficiency of immobilized antimicrobial peptides **AMP3g**, **AMP4b** and **AMP4e** on preventing the adhesion of *B. subtilis* on titanium plates. Data represent mean \pm SD of $n \geq 3$ performed in triplicate. Statistical significance was calculated with t-test: *: $P \leq 0.05$; **: $P \leq 0.01$; ***: $P \leq 0.001$.

Significantly less formed colonies were counted when peptide treated Titanium plates were used (**Figure 28**). These results showed that the attachment of the three antimicrobial peptides each had significantly interfered on the adhesion of *B. subtilis*.

As the three AMPs had a similar effect on *Bacillus subtilis*, it was decided to use the peptide **AMP4b** for further experiments, as it has shown the least cytotoxicity against human cells, while maintaining promising antimicrobial activity.

7.2. Synthesis and physicochemical evaluation of chimeric peptides

To investigate another method of peptide immobilization, chimeric peptides were designed by fusing **AMP4b** with specific surface binding sequences that would anchor the peptide directly onto the titanium surface. [54]

For this reason, three chimeric peptides were designed, by fusing three distinct titanium binding sequences of twelve amino acids length to the *N*-terminus of **AMP4b**. A triple-glycine spacer was inserted between both parts, yielding three novel chimeric peptides **Chim1**, **Chim2** and **Chim3** (Table 12), respectively. The titanium binding peptides **TiBP1** (RPRENRRERGL) and **TiBP2** (SRPNGYGGSESS)^[101] as well as **TBP-1** (RKLPDAPGMHTW)^[130] were selected from literature.

Table 12: Peptide sequences and physicochemical properties of the three chimeric peptides and LL37, used as control in this work. Physicochemical values were calculated by Thermofisher peptide analysis tool.^[174] R-values were calculated by taking the ratio between the molar ellipticity at 220 nm and 208 nm ($R\text{-value} = [\Theta]_{220} / [\Theta]_{208}$).

Name	Sequence	MW (g/mol)	Charge	Hydrophobicity	R-value (50% TFE)
Chim1	RPRENRRERGLGGG-GLRKRLRKFFNKIKF-NH ₂	3600.2	+11	33.35	0.88
Chim2	SRPNGYGGSESSGGG-GLRKRLRKFFNKIKF-NH ₂	3301.8	+8	32.56	0.93
Chim3	RKLPDAPGMHTWGGG-GLRKRLRKFFNKIKF-NH ₂	3513.3	+9	41.29	0.89
LL37	LLGDFFRKSKEKIGKEFKRIVQRIKDFLRNLPRTES-NH ₂	4493.4	+8	47.79	0.93

All peptides were synthesized via automated Fmoc/tBu solid phase peptide synthesis with Fmoc-protected amino acids on a rinkamide resin. After cleavage from the resin with trifluoro acetic acid, the peptides were purified using reverse phase HPLC, and identified by HPLC-MS (**Supplementary 5**). The chimeric peptides were also synthesized with an *N*-terminal attached 5(6)-carboxyfluorescein as marker for fluorescence experiments. These fluorescently labelled peptides had a mass increase of 358.2 g/mol, as was indicated by their LC-MS analysis (**Supplementary 6**).

One concern with the elongation of the peptide sequence was the influence it might have on the formation of the secondary structures necessary for membrane interaction. Indeed, comparison of helical wheel projections between the AMP and the chimeric variants (**Figure 29**) showed the chimeric peptides to have less pronounced hydrophobic moments. As the binding sequence is lacking the AMP-typical distribution of hydrophobic and cationic amino acids, it could inhibit the folding stability of the overall helical structure. The triple glycine spacer was included to provide independent folding of both peptide parts and might potentially prevent such occurrences, even though the chimeras lack the overall rigid amphipathic distribution of amino acids.

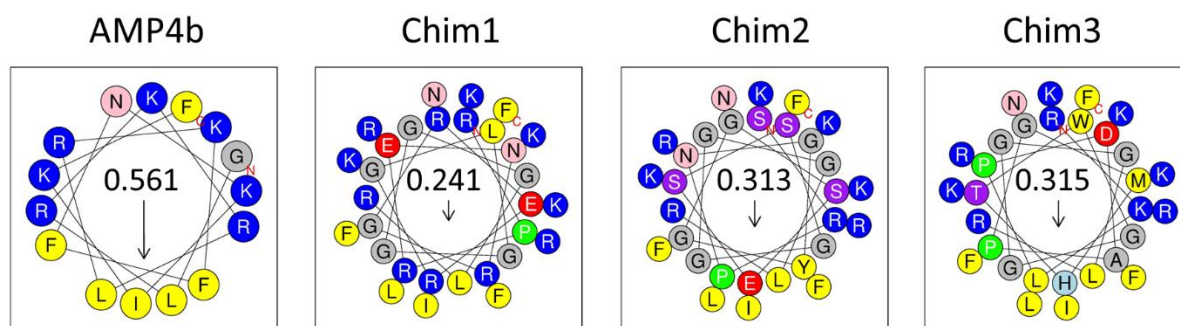


Figure 29: Helical wheel projections^[165] and hydrophobic momentum of **AMP4b** and the chimeric peptides **Chim1**, **Chim2** and **Chim3**.

To evaluate the potential of the chimeric peptides to form distinct secondary structures, circular dichroism (CD) spectroscopy was performed. As can be seen in **Figure 30**, all three peptides showed the formation of alpha helical structures when present in aqueous solution containing 50 % TFE^[196,197]. This change in structure formation was evident by the characteristic signals for alpha helices at 208 nm and 220 nm^[190]. From these, R-values were calculated as determinants for helicity^[198] and values from 0.88

to 0.93 for all three peptides were obtained (**Table 13**), indicating well established helical structures. These values were similar to the parent peptide **AMP4b** (0.92).

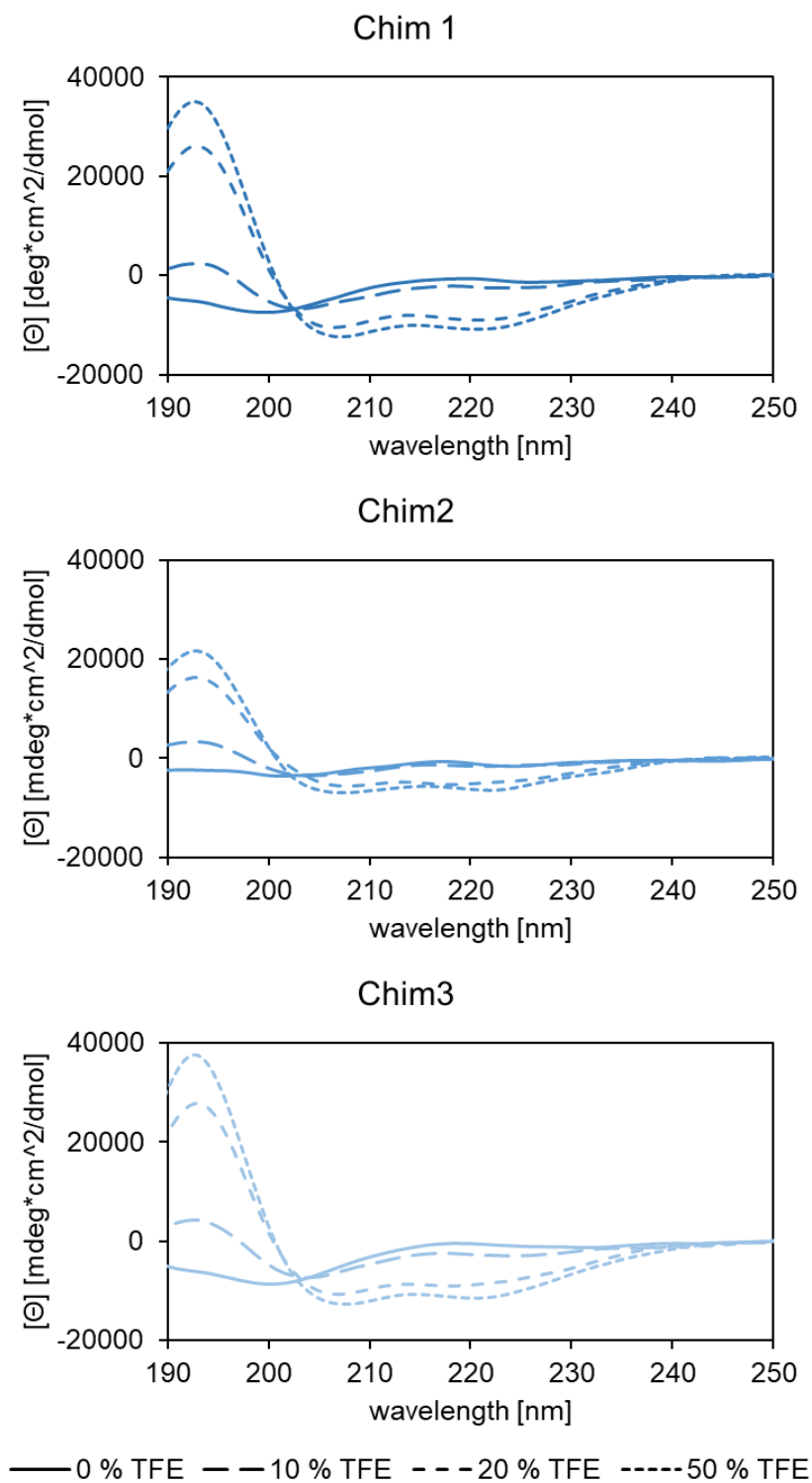


Figure 30: Circular dichroism spectroscopy of the three chimeric peptides in phosphate buffer with variable content of trifluoroethanol (TFE).

TFE titration experiments (**Figure 30**) showed alpha helical structure formation already at 20% TFE. Furthermore, the calculated R-values (**Table 13**) for this condition exceeded 0.84, indicating that the helix was already formed in this environment. Even with 10 % TFE concentration, the peptides showed initial helical structures and R-values above 0.5. No significant differences were determined between the novel chimeric peptides. **Chim3** has shown the marginally lower R-values than **Chim2** with differences not exceeding 0.07. Although the novel chimeras differentiated in hydrophobic moments, the formation of alpha helical structure was only marginally affected by the addition of the titanium binding sequence.

Table 13: Calculated R-values for the three chimeric peptides ($\Theta_{222} / \Theta_{208}$).

TFE content [%]	Chim1	Chim2	Chim3
0	0.24	0.58	0.14
10	0.51	0.54	0.50
20	0.88	0.87	0.80
50	0.88	0.93	0.89

Overall, it can be concluded that the binding sequences have no negative impact on the formation of alpha helical structures, even though a predictably less pronounced hydrophobic moment. This is important, as it has been stated that stable formation of secondary structures can be crucial for membrane interactions.^[197]

7.3. Antimicrobial activity of chimeric peptides in solution

The next step was the evaluation of antimicrobial and haemolytic activity in solution. This way, the effect of titanium binding sequences on the overall bioactivity was investigated. For this reason, a series of experiments with non-pathogenic and pathogenic bacteria, as well as human red blood cells was performed to determine the general bioactivity of these peptides.

7.3.1. Activity screen against non-pathogenic bacteria

The first step in this series of experiments was the determination of the general antibacterial spectrum against several types of non-pathogenic bacteria: gram-positive *Bacillus subtilis* as well as gram-negative *Pseudomonas fluorescense* and *Salmonella typhimurium*. These bacterial strains are examples to which the original **AMP4b** was highly effective. If the binding sequences had a negative impact to the activity of the chimeric peptide this should be visible as regulation in the antimicrobial activity.

For all new peptides, MIC values in the lower micromolar range were observed, regardless of the tested strains (**Figure 31**). Compared to the parent peptide **AMP4b** only **Chim2** seemed to exert reduced antimicrobial activity. For the other two chimeras the activity was close or equal to **AMP4b**, demonstrating that the titanium binding motives did not really impact their potency. This difference between the chimeras is especially evident in treatment of *S. typhimurium*. Here the peptide concentrations of 2 µM reduced the viability of the bacteria to the range of ethanol control when **Chim1** or **Chim3** were applied, but after treatment with **Chim2**, 20 % viability remained. Therefore, it seems that the fusion of the serine rich binding sequence of **Chim2** had in fact a regulatory effect on the antimicrobial activity of the fused AMP, even though still the minimal inhibitory concentrations is in the lower micromolar range.

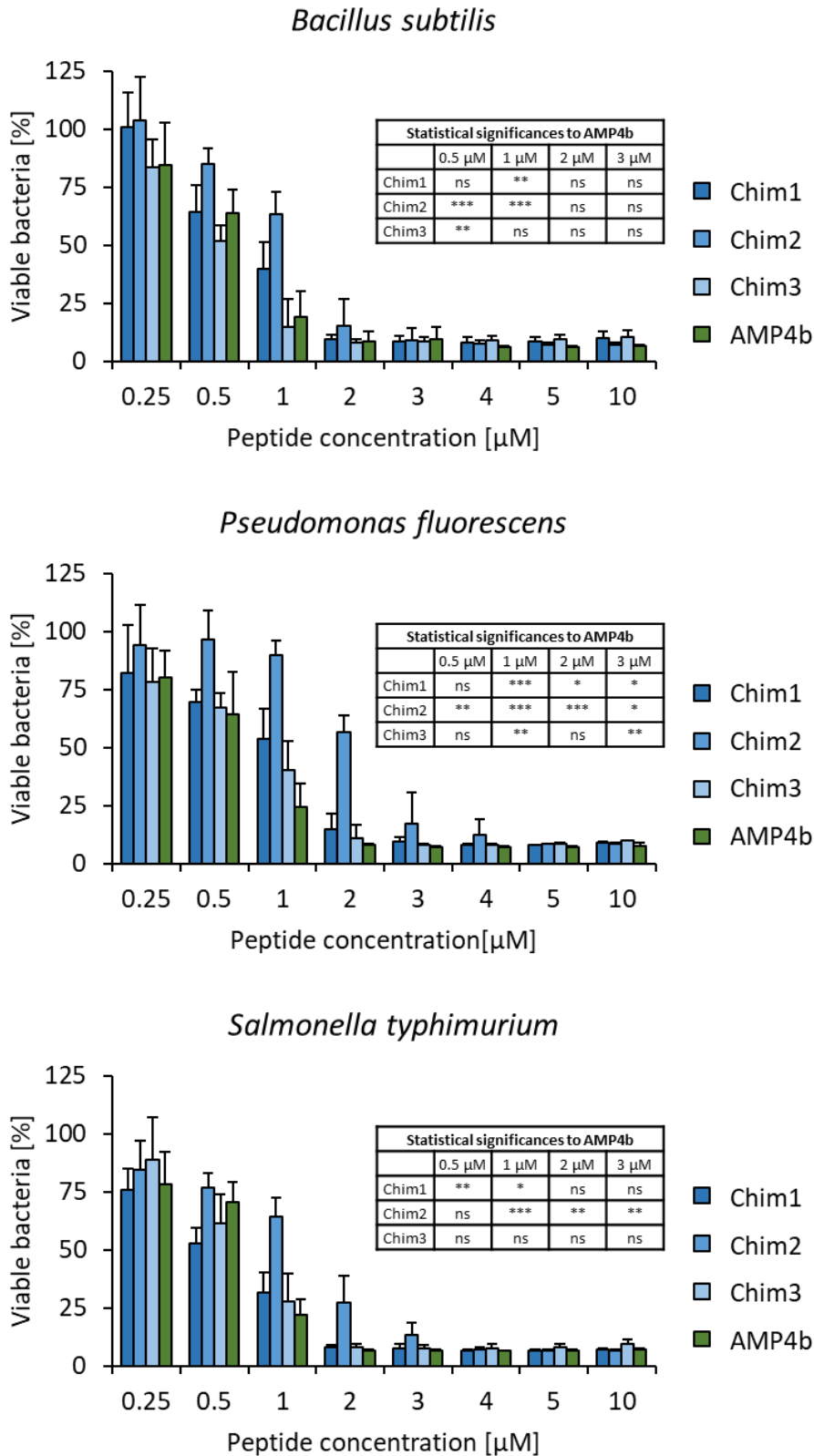


Figure 31: Antimicrobial activity assay of chimeric peptides with *B. subtilis*, *P. fluorescens* and *S. typhimurium*. Incubation for 6 h at 37°C. Data represent mean \pm SD of $n = 3$ performed in triplicate. To calculate the relative quantity of living cells, negative control (water) was set to 100%.

To further assess the antibacterial activity of the chimeras, dose-response curves were generated (**Supplementary 10**) and through a sigmoidal dose response fit the MIC₅₀ was calculated as a standardized value for peptide comparability (**Table 14**).

Table 14: MIC₅₀ values [μ M] for peptides **Chim1-3** when in presence of different bacterial strains as determined by a colorimetric iodnitrotetrazolium assay. bacteria were incubated for 6 h at 37 °C with different peptide concentrations, respectively. Standard deviations were calculated from the three separate experiments in triplicate.

MIC ₅₀ -values [μ M]	Chim1	Chim2	Chim3
<i>B. subtilis</i>	0.8 \pm 0.2	1.5 \pm 0.1	0.4 \pm 0.1
<i>P. fluorescens</i>	0.6 \pm 0.1	1.3 \pm 0.1	0.4 \pm 0.1
<i>S. typhimurium</i>	0.7 \pm 0.1	1.5 \pm 0.1	0.5 \pm 0.1

The MIC₅₀ values presented in **Table 14** show some more differences between the three chimeric peptides. Notably, **Chim2** exhibited 2-3-fold higher MIC₅₀ values and thus, lower antimicrobial activity compared to the other two peptides. All in all, **Chim3** seemed to be the most active compound, with MIC₅₀ values around 0.4 μ M, followed by **Chim1** with such values roughly around 0.7 μ M. However, for all peptides the determined MIC₅₀ values were comparable to **AMP4b** further indicating the minor influence of the surface binding sequences to the AMP activity.

7.3.2. Antimicrobial activity against *S. aureus* and MRSA

Inspired by these results, the chimeric peptides were tested against the ESKAPE pathogen *Staphylococcus aureus* and its methicillin-resistant variant (MRSA). *S. aureus* is a major human pathogen, which mostly affects the skin or soft tissue and causes a variety of clinical infections^[10]. MRSA is often present on medical devices, where it is difficult to treat with common antibiotics.^[199] Thus, an antimicrobial effect of the herein described peptides would be highly beneficial for a future treatment of these

critical pathogens. Furthermore, *S. aureus* is known for causing implant associated orthopaedic infections^[110], which further increased interest in this particular pathogen. A colony proliferation assay was performed with Denise Meinberger from AG Klatt (Institute of clinical chemistry, University of Cologne) to determine activity of **AMP4b** and the chimeric peptides against these human pathogens. The potency was assessed in comparison to the antimicrobial peptide **LL37**, which was recently investigated concerning its role in preventing *S. aureus* biofilm formation^[200,201].

The results demonstrated for all tested peptides a steady decrease in bacterial viability (**Figure 32**). Overall, the peptides were more active against *S. aureus* than MRSA, resulting in twice as high MIC₅₀ values for MRSA, than for *S. aureus*. Interestingly, **LL37** exhibited less potency compared to the novel peptides tested. **AMP4b** was also not as efficient as the chimeric peptides besides **Chim2**, while **Chim3** was particularly effective against MRSA. This further indicates an impact of the fusion with different titanium binding peptide sequences, with beneficial influence of **TiBP1** and **TBP-1** and no evident effects for **TiBP2**, which can be related to other studies in which chimeric peptides containing **TiBP1** showed lower MIC values than its **TiBP2** counterpart.^[202]

Based on the results so far, promising antibacterial activity for the newly created chimeric peptides is evident, even against drug-resistant strains. As the peptides affect the bacteria more than the control peptide **LL37**, this further pronounces their high potential in treating such specific pathogens.

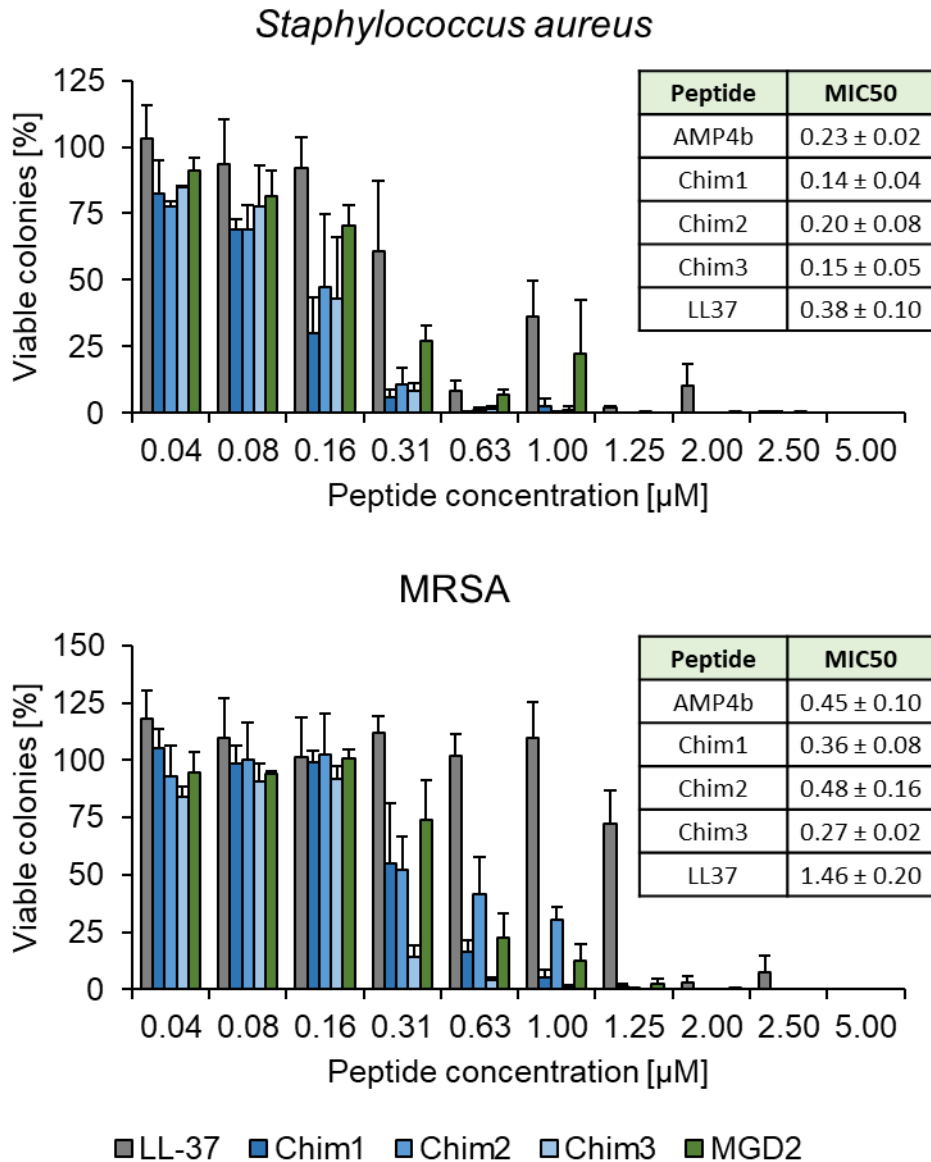


Figure 32: Antimicrobial activity assay of chimeric peptides, **AMP4b**, and control peptide LL37 using *S. aureus* and methicillin resistant *S. aureus* (MRSA). Bacteria were incubated for 6 h at 37°C. Data represent mean ± SD of $n = 1$ performed in triplicate. To calculate the relative quantity of living cells, negative control (water) was set to 100%.

7.3.3. Haemolysis of chimeric peptides

Following the activity against bacteria, the influence of the surface binding motives on the haemolytic activity of **AMP4b** was evaluated. When applied on medical surfaces, the immobilized peptides interact with various tissue cells, depending on the coated device. In many applications, they may also come into contact with blood, so hemolysis of peptide functionalization is a great concern^[203]. Therefore, hRBCs are well suited as control cells for lytic effects of the chimeras on mammalian cells.

A 24-hour experiment was utilized to assess if the novel chimeric peptides provoke haemolysis of erythrocytes. **LL37** was used as control peptide^[204].

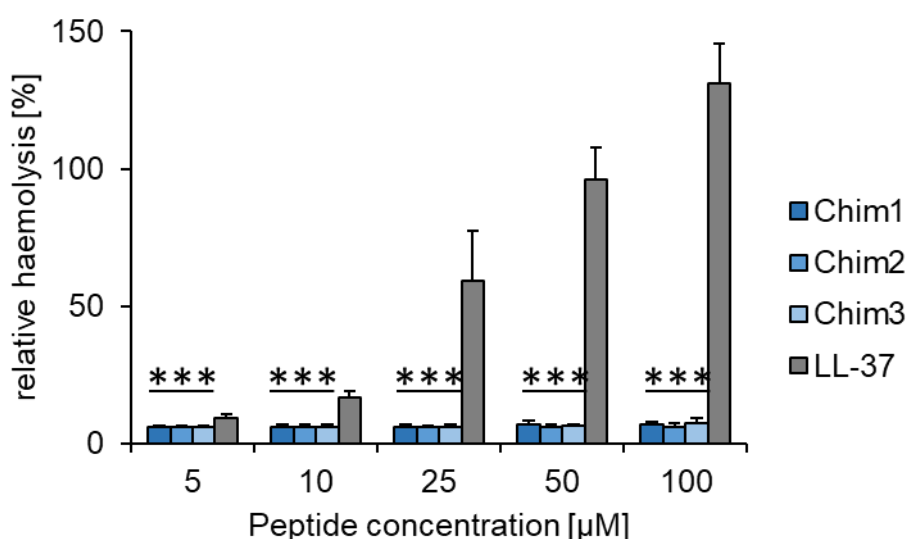


Figure 33: Haemolysis assay using the three chimeric peptides and LL37. Purified human red blood cells (hRBC) were incubated for 24 h at 37°C. Positive control 1% Triton X-100 and negative control was water. Data represents mean \pm SD of $n=3$ performed in triplicate. Statistical significance in relation to LL37 was calculated with *t*-test: ***: $P \leq 0.001$.

After treatment of hRBCs with peptide concentrations up to 100 μ M no haemolytic activity was observed. This was in line with former results for parental peptide **AMP4b** (**Figure 14**), as well as most other **sC18** based AMPs. In contrast, **LL37** exhibited significant lysis of RBCs starting already at concentrations of 5 μ M. These results are clearly distinct from toxicity assays performed using bacterial cells and might provide

a promising therapeutic window to find concentrations at which bacteria are lysed but the cells of the human body remain unaffected. Although highly charged and equipped with an amphipathic structure, the results indicate no interaction with the neutrally charged membrane of the hRBCs. Thus, it can be hypothesised that they are, therefore, less attractive compared to the more negatively charged bacterial cell walls and membranes. To get a closer look into this specificity, other types of human cells need to be addressed in the future.

7.3.4. Bacterial interaction of chimeric peptides

To assess how the novel chimeric peptides would interact with bacteria, fluorescence microscopy studies were performed using 5(6)-carboxyfluorescein (CF) labelled peptides. As a determinant for dead cells, the bacteria were also stained with propidium iodide (PI), which enters only dead cells by their leaky cellular membranes. The three bacterial lines *B. subtilis*, *P. fluorescens* and *S. typhimurium* were investigated in this experiment (**Supplementary 11-13**). After incubating the different bacteria with 10 μ M peptide solution, all cells were dead as was confirmed by the red fluorescence of the PI staining (**Supplementary 11-13**). Moreover, in the case of treatment with **AMP4b**, **Chim1** and **Chim3**, all bacteria were also unequivocally stained with peptide. This could point towards membrane interaction, probably distortion and subsequent internalization and entrapment of those peptides. Interestingly, no green fluorescence was observed after applying **Chim2** to the bacteria, even though most of the treated bacteria were dead. All external fluorescence of membrane bound and 5(6)carboxyfluorescein-labelled peptide should have been quenched at this point through the treatment with trypanblue. Therefore, it can be hypothesized that **Chim2** acts either by a completely different mechanism or is less membrane active as the other studied peptides. The latter aspect would probably fit to the toxicity data, which demonstrated less activity of **Chim2** compared to **Chim1** and **Chim3**, as well as the parental peptide **AMP4b**.

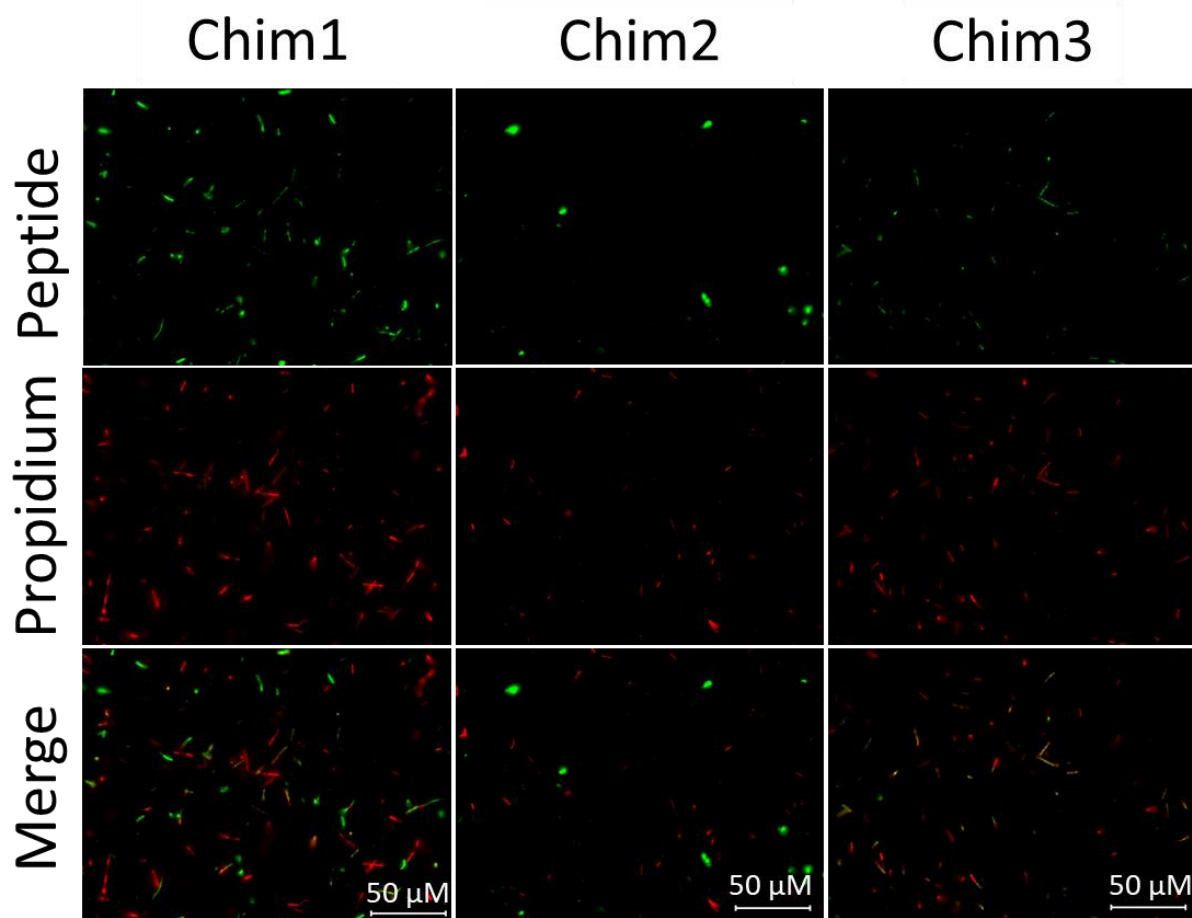


Figure 34: Fluorescence microscopy of the three chimeric peptides using *B. subtilis* after incubation with 1 μM peptide at 37 $^{\circ}\text{C}$ for 30 minutes. Peptides were marked with (5/6)-carboxylfluorescein. Dead bacteria were stained with propidium iodide.

To have a further insight into these interactions, the experiment was repeated for *B. subtilis* with 1 μM peptide concentration (**Figure 34**). Herein, the peptides **Chim1** and **Chim3** have definitive green peptide staining, mostly co-localizing with the red stained dead bacteria. Nonetheless, some examples of green stained bacteria were visible for **Chim2**, though they were not colocalizing with any PI-stained bacteria, but within clusters of bacteria. Already after 30-minute incubation with 1 μM peptide concentration, the chimeras were able to kill most, if not all bacteria present. Furthermore, this indicates not only a rapid method of action, but also emphasizes a membrane lysing mechanism that allows widespread invasion of PI into the cells.

7.4. Immobilized chimeric peptides

7.4.1. Immobilization and elemental analysis

To investigate the potential of the novel chimeric peptides as antimicrobial coating agents for medical surfaces, they were immobilized onto metal surfaces. Therefore, a simple immersion-based coating method was used to attach the chimeric peptides onto freshly cleaned and UV-sterilized small titanium plates (1 cm x 1cm).

To prove the successful immobilization of chimeric peptides onto the metallic surface, chemical elemental composition analysis of selected samples was performed using X-ray photoelectron spectroscopy (XPS) (performed by Michael Wilhelm, AG Prof. Mathur, Institute of Inorganic Chemistry, University of Cologne). The focus lied primarily on the content of nitrogen in comparison to oxygen and carbon (**Table 15, Supplementary 14**), as the other elements were known as common impurities on titanium and similar surfaces caused by oxidation and atmospheric dust. ^[205,206]

Table 15: *Relative abundances of elements (%) determined by XPS of Ti surfaces either treated with the respective chimeric peptides or not (w/o). Averages and deviations were calculated from two independent measurements.*

Element (%)	w/o	Chim1	Chim2	Chim3
Oxygen	23.5 ± 2.4	26.7 ± 1.9	27.1 ± 1.2	22.2 ± 5.7
Carbon	66.6 ± 1.4	57.6 ± 3.9	57.8 ± 2.4	65.5 ± 10.5
Nitrogen	2.6 ± 1.3	6.4 ± 1.8	7.3 ± 2.0	6.5 ± 3.8

The resulting data of XPS analysis showed that the major abundant components were indeed oxygen, carbon, and nitrogen (**Table 15**). Furthermore, a significant increase in relative elemental abundance of nitrogen in comparison to oxygen and carbon was detected. Overall, the three chimeras produced an increase of nitrogen content from 2.6 % in the untreated sample to more than 6.4 % (**Chim1**) and up to 7.3 % for **Chim2**. This more than 2-fold increase pointed to a serious number of peptides successfully

attached onto the surface. The comparably high amounts of oxygen and carbon might indicate impurities derived from the freshly prepared samples, a phenomenon that is often described for different surface materials. [205,206] In general, the tested chimeric peptides were efficiently immobilized onto the surface.

7.4.2. Surface activity assay

After successfully attaching the peptides on the titanium plates, it was tested if the modified surfaces would prevent bacterial adhesion. Therefore, the metal pieces were covered with bacterial culture of *B. subtilis* and incubated for 6 h. Afterwards, a sample was taken and spread onto agar plates to proliferate overnight.

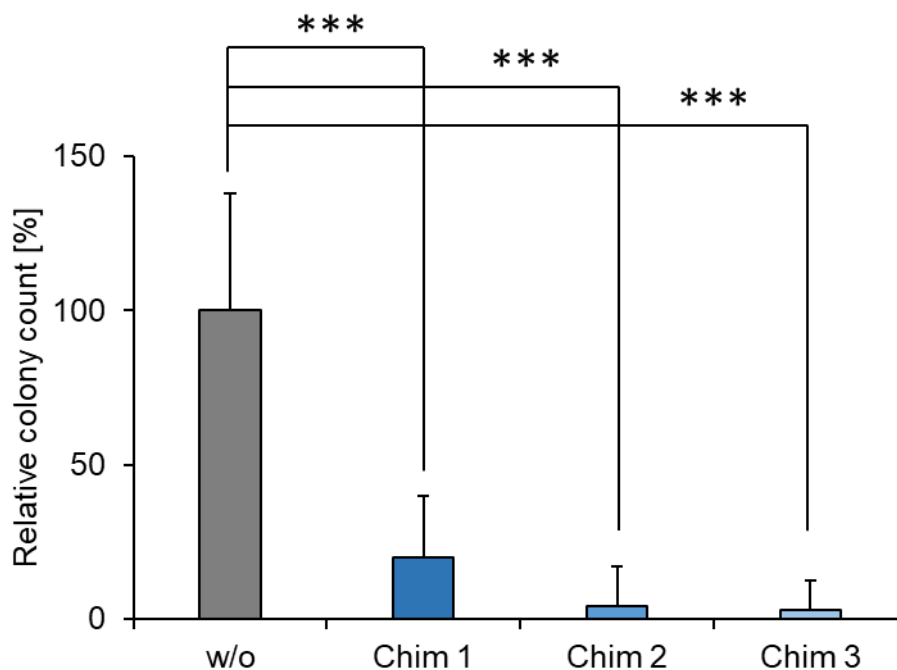


Figure 35: Relative amount of *B. subtilis* colonies counted after incubation of bacteria for 6 hours at 37 °C on small titanium plates, either pure (w/o) or plates coated with chimeric peptides. Statistical significance in relation to pure titanium plates was calculated with *t*-test: ns: $P > 0.05$; *: $P \leq 0.05$; **: $P \leq 0.01$; ***: $P \leq 0.001$.

Counting the number of generated colonies, a significant decrease of colonies was detected for all samples that were taken from the modified titanium plates (**Figure 35**) in comparison to the untreated samples. Notably, the effect was less pronounced in Chim1, where a decrease in colony formation of about 80 % was observed, compared to the other two chimeras, where colony formation decreased by almost 97 %. The higher activity of **Chim2** in preventing bacterial adhesion might come from better attachment to the titanium surface. This way it could also be explained, why the **Chim1** is less effective compared to the other two peptides despite similar antimicrobial profile in solution. Yet further experiments need to be performed on determining immobilization efficiency to confirm this possibility.

In conclusion, all tested chimeric peptides showed great potency and thus might function as a promising tool in the development of surface coating agents preventing biofilm formation on medical titanium surfaces. Notably, in comparison to similar studies where such bifunctional peptides were used, the novel chimeras showed comparable activity when immobilized^[101,122,130].

7.5. Conclusion

Three new chimeric peptides were created by combining **AMP4b**, the most promising antimicrobial sequence from former studies, with three different titanium binding sequences, respectively. The bifunctionality of the novel peptides showed no significant decrease in their antimicrobial activity, even against common pathogens *Staphylococcus aureus* and MRSA. Furthermore, these chimeric peptides showed no haemolytic activity against human red blood cells, supporting their interest for further research.

Upon immobilization of the bifunctional peptides onto small titanium plates through simple immersion coating, a change in relative abundance of nitrogen in their elemental surface composition was observable. This indicated a successful immobilization of the peptides onto the metal substrates. Finally, the potential of the new chimeric peptide coatings to prevent bacterial attachment on prepared metal surfaces was assessed. Herein the colony forming units of *Bacillus subtilis* that adhered onto the titanium surfaces decreased up to 97 %.

Overall, the three chimeric peptides are promising tools for antimicrobial coating onto titanium medical devices, e.g. artificial implants. Especially **Chim3** seemed to be the variant with the highest effect. Still, further work must be done into this field to better evaluate the immobilization efficiency and the impact such coatings would have to the tissue as for example osseointegration and cytotoxicity of the implants to the hosts bone structure.

8. Thesis Conclusion and Outlook

To summarize the findings of this work, different series of peptides, based on the cell penetrating peptide **sC18**, were designed and further developed to optimize their antimicrobial activity.

At first, specific substitutions with phenylalanine and unnatural fluorinated phenylalanine enhanced the antimicrobial activity by a mechanism of membrane disruption and led to high antibacterial activity in low micromolar range. These peptides also showed promising selectivity between bacterial and mammalian cells, and they also expressed potential as anticancer peptides. The novel fluorinated peptides have not shown significant increases in protease stability, but the findings suggest a rapid membrane disruptive mechanism which occurs before the peptides are degraded by extracellular proteases. Due to the combination of potent antibacterial activity with low cytotoxicity against mammalian cells, the novel peptide **AMP4b** was classified as the most promising bacterio-selective AMP.

In a second attempt to enhance the antimicrobial properties of **sC18**, through specific substitutions, two series of peptides using exchanges of cationic arginine and hydrophobic leucine were designed. The first series focussed on the length of the AMP, as they were based on **sC18***, **sC18** and **sC18ΔE**, respectively. Herein a clear correlation was found between the peptide's length and the antimicrobial activity, potentially based on stabilization of alpha helical structures or the ability of longer peptides to easier traverse the complete lipid bilayer to form pores. The second series of peptides based on **sC18*** has proven that increasing the hydrophobicity yielded higher activity, more so than increasing the peptides positive net charge. Overall, also these peptides expressed a potent antimicrobial activity without inducing haemolysis and thus, offer novel alternative AMP sequences.

Based on the antimicrobial peptide **AMP4b**, three chimeric peptides were designed by fusion with different titanium binding sequences. The latter did not negatively impact helical folding, antimicrobial activity, or haemolytic potential to significant extent. These chimeric peptides were indeed useful for modifying titanium surfaces, where they inhibited the bacterial adhesion of *B. subtilis*. Thus, these chimeric peptides are promising candidates for further research on AMP based surface functionalizing on medical devices. Further experiments need to be done to quantify immobilization efficiency and the influence of the novel chimera on mammalian cells.

The newly discussed peptides can be seen as promising steps in the development of further antimicrobial peptides, for instance **AMP4b** as antibiotic drug to fight multi-drug resistant bacteria, or **Chim3** as new candidate for antibiofilm coatings.

In further studies, two aspects should be investigated. First, the cytotoxic behaviour towards eukaryotic cells must be analysed to define the cellular selectivity of the novel AMPs and to determine the therapeutic window of concentrations regarding different cell types. Also, experiments with the peptide immobilized titanium plates are needed, to assess the biocompatibility for these as implant coating to host tissue. Lastly, the mechanism of these peptides can be further investigated. So far it is evident that the peptides perform a rapid membrane disruptive mechanism onto the negatively charged lipid layer. Yet there are different methods of pore formation in cationic antimicrobial peptides and until now it is not defined, which one is utilized by the novel antimicrobial peptides.

Overall, the utilization of rational designed peptides can offer a wide range of different applications. Within these studies, it was proven that simple change in the amino acid sequence can yield potent activities, without conjugation of bioactive components.

9. References

- [1] C. Tropini, K. A. Earle, K. C. Huang, J. L. Sonnenburg, *Cell Host Microbe* **2017**, 21, 433.
- [2] C. J. Murray, K. S. Ikuta, F. Sharara, L. Swetschinski, G. Robles Aguilar, A. Gray, C. Han, C. Bisignano, P. Rao, E. Wool, et al., *Lancet* **2022**, 399, 629–655.
- [3] “Prokaryotes vs Eukaryotes: What Are the Key Differences? | Technology Networks,” can be found under <https://www.technologynetworks.com/cell-science/articles/prokaryotes-vs-eukaryotes-what-are-the-key-differences-336095>, **n.d.**
- [4] A. J. Roger, S. A. Muñoz-Gómez, R. Kamikawa, *Curr. Biol.* **2017**, 27, R1177–R1192.
- [5] H. Strahl, J. Errington, <https://doi.org/10.1146/annurev-micro-102215-095630> **2017**, 71, 519–538.
- [6] I. Neundorff, *Adv. Exp. Med. Biol.* **2019**, 1117, 93–109.
- [7] K. Látrová, N. Havlová, R. Večeřová, D. Pinkas, K. Bogdanová, M. Kolář, R. Fišer, I. Konopásek, D. D. Do Pham, D. Rejman, et al., *Sci. Reports* **2021**, 11, 1–16.
- [8] A. A. Baxter, F. T. Lay, I. K. H. Poon, M. Kvansakul, M. D. Hulett, *Cell. Mol. Life Sci.* **2017**, 74, 3809–3825.
- [9] D. Megrian, N. Taib, J. Witwinowski, C. Beloin, S. Gribaldo, *Mol. Microbiol.* **2020**, 113, 659–671.
- [10] F. Ranklin, D. L. Owy, <https://doi.org/10.1056/NEJM199808203390806> **1998**, 339, 520–532.
- [11] P. D. Lister, D. J. Wolter, N. D. Hanson, *Clin. Microbiol. Rev.* **2009**, 22, 582.
- [12] G. W. Fish, M. M. Hand, J. W. Franklin Keim, *Am. J. Pathol.* **1937**, 13, 121.
- [13] J. Reynolds, R. B. Moyes, D. P. Breakwell, *Curr. Protoc. Microbiol.* **2009**, 15, A.3H.1-A.3H.5.
- [14] J. Parkin, B. Cohen, *Lancet* **2001**, 357, 1777–1789.

- [15] S. Veerachamy, T. Yarlagadda, G. Manivasagam, P. K. Yarlagadda, *Proc. Inst. Mech. Eng. Part H J. Eng. Med.* **2014**, 228, 1083–1099.
- [16] G. P. Sakala, M. Reches, *Adv. Mater. Interfaces* **2018**, 5, 1800073.
- [17] I. Francolini, G. Donelli, *FEMS Immunol. Med. Microbiol.* **2010**, 59, 227–238.
- [18] S. S. Magill, J. R. Edwards, W. Bamberg, Z. G. Beldavs, G. Dumyati, M. A. Kainer, R. Lynfield, M. Maloney, L. McAllister-Hollod, J. Nadle, et al., *N. Engl. J. Med.* **2014**, 370, 1198.
- [19] O. Camps-Font, R. Figueiredo, E. Valmaseda-Castellón, C. Gay-Escoda, *Implant Dent.* **2015**, 24, 713–719.
- [20] R. Nolan, M. Kemmoona, I. Polyzois, N. Claffey, *Clin. Oral Implants Res.* **2014**, 25, 252–259.
- [21] M. Abu-Ta'a, M. Quirynen, W. Teughels, D. Van Steenberghe, *J. Clin. Periodontol.* **2008**, 35, 58–63.
- [22] S. A. Khan, C. S. Lee, *Acta Biomater.* **2020**, 113, 101–118.
- [23] S. S. Talsma, *Home Healthc. Nurse* **2007**, 25, 589–594.
- [24] C. Wisdom, C. Chen, E. Yuca, Y. Zhou, C. Tamerler, M. L. Snead, *JOM* **2019**, 71, 1271–1280.
- [25] K. Gould, *J. Antimicrob. Chemother.* **2016**, 71, 572–575.
- [26] K. I. Mohr, *Curr. Top. Microbiol. Immunol.* **2016**, 398, 237–272.
- [27] D. Duschinsky, *DMW - Dtsch. Medizinische Wochenschrift* **2009**, 36, 2437–2438.
- [28] A. Fleming, **n.d.**
- [29] M. A. Cook, G. D. Wright, *Sci. Transl. Med.* **2022**, 14, eabo7793.
- [30] T. M. Wassenaar, <http://dx.doi.org/10.1080/10408410591005110> **2008**, 31, 155–169.
- [31] P. S. McManus, V. O. Stockwell, G. W. Sundin, A. L. Jones, <http://dx.doi.org/10.1146/annurev.phyto.40.120301.093927> **2003**, 40, 443–465.
- [32] J. Nemeth, G. Oesch, S. P. Kuster, *Nemeth, Johannes; Oesch, Gabriela;*

- Kuster, Stefan P (2015). *Bacteriostatic versus bactericidal Antibiot. patients with serious Bact. Infect. Syst. Rev. meta-analysis. J. Antimicrob. Chemother.* 70(2)382-395. **2015**, 70, 382–395.
- [33] R. Aminov, *Biochem. Pharmacol.* **2017**, 133, 4–19.
- [34] T. Maxson, D. A. Mitchell, *Tetrahedron* **2016**, 72, 3609–3624.
- [35] E. B. Chahine, J. A. Dougherty, K. A. Thornby, E. H. Guirguis, <https://doi.org/10.1177/10600280211031390> **2021**, 56, 441–462.
- [36] A. R. Coates, G. Halls, Y. Hu, *Br. J. Pharmacol.* **2011**, 163, 184.
- [37] “A Brief Overview of Classes of Antibiotics – Compound Interest,” can be found under <https://www.compoundchem.com/2014/09/08/antibiotics/>, **n.d.**
- [38] L. Brinkac, A. Voorhies, A. Gomez, K. E. Nelson, *Microb. Ecol.* **2017**, 74, 1001.
- [39] J. L. Martinez, F. Baquero, *Antimicrob. Agents Chemother.* **2000**, 44, 1771.
- [40] B. H. Ter Kuile, N. Kraupner, S. Brul, *FEMS Microbiol. Lett.* **2016**, 363, 210.
- [41] C. Manyi-Loh, S. Mamphweli, E. Meyer, A. Okoh, *Mol. A J. Synth. Chem. Nat. Prod. Chem.* **2018**, 23, DOI 10.3390/MOLECULES23040795.
- [42] M. Murray, G. Salvatierra, A. Dávila-Barclay, B. Ayzanoa, C. Castillo-Vilcahuaman, M. Huang, M. J. Pajuelo, A. G. Lescano, L. Cabrera, M. Calderón, et al., *Front. Microbiol.* **2021**, 12, DOI 10.3389/FMICB.2021.635871.
- [43] K. Hegstad, H. Mylvaganam, J. Janice, E. Josefsen, A. Sivertsen, D. Skaare, *mSphere* **2020**, 5, DOI 10.1128/MSPHERE.00969-19.
- [44] N. A. Lermينياux, A. D. S. Cameron, *Can. J. Microbiol.* **2019**, 65, 34–44.
- [45] M. S. Mulani, E. E. Kamble, S. N. Kumkar, M. S. Tawre, K. R. Pardesi, *Front. Microbiol.* **2019**, 10, 539.
- [46] D. M. P. De Oliveira, B. M. Forde, T. J. Kidd, P. N. A. Harris, M. A. Schembri, S. A. Beatson, D. L. Paterson, M. J. Walker, *Clin. Microbiol. Rev.* **2020**, 33, DOI 10.1128/CMR.00181-19.
- [47] S. Santajit, N. Indrawattana, *Biomed Res. Int.* **2016**, 2016, DOI 10.1155/2016/2475067.

- [48] M. Mahlapuu, J. Håkansson, L. Ringstad, C. Björn, *Front. Cell. Infect. Microbiol.* **2016**, *6*, 194.
- [49] F. Gayraud, M. Klußmann, I. Neundorf, *Molecules* **2021**, *26*, DOI 10.3390/MOLECULES26061591.
- [50] R. Mhidia, A. Vallin, N. Ollivier, A. Blanpain, G. Shi, R. Christiano, L. Johannes, O. Melnyk, *Bioconjug. Chem.* **2010**, *21*, 219–228.
- [51] K. Klabenkova, A. Fokina, D. Stetsenko, *Molecules* **2021**, *26*, DOI 10.3390/MOLECULES26175420.
- [52] K. Cleal, L. He, P. D. Watson, A. T. Jones, *Curr. Pharm. Des.* **2013**, *19*, 2878–2894.
- [53] J. D. Ramsey, N. H. Flynn, *Pharmacol. Ther.* **2015**, *154*, 78–86.
- [54] S. Noorian, R. K. Oskuee, A. Jalili, *Int. J. Pept. Res. Ther.* **2021**, *27*, 1205–1220.
- [55] A. Bin Hafeez, X. Jiang, P. J. Bergen, Y. Zhu, *Int. J. Mol. Sci.* **2021**, *Vol. 22*, Page 11691 **2021**, *22*, 11691.
- [56] Y. H. Ho, P. Shah, Y. W. Chen, C. S. Chen, *Mol. Cell. Proteomics* **2016**, *15*, 1837–1847.
- [57] J. K. Boparai, P. K. Sharma, *Protein Pept. Lett.* **2020**, *27*, 4.
- [58] S. Bobone, L. Stella, in *Adv. Exp. Med. Biol.*, Springer, Singapore, **2019**, pp. 175–214.
- [59] I. N. Hsieh, K. L. Hartshorn, *Pharmaceuticals* **2016**, *9*, DOI 10.3390/PH9030053.
- [60] M. Bondaryk, M. Staniszevska, P. Zielińska, Z. Urbańczyk-Lipkowska, *J. Fungi* **2017**, *3*, DOI 10.3390/JOF3030046.
- [61] J. Vizioli, M. Salzet, *Trends Parasitol.* **2002**, *18*, 475–476.
- [62] L. Feni, I. Neundorf, *Adv. Exp. Med. Biol.* **2017**, *1030*, 279–295.
- [63] D. Gaspar, A. Salomé Veiga, M. A. R. B. Castanho, *Front. Microbiol.* **2013**, *4*, 294.

- [64] D. W. Hoskin, A. Ramamoorthy, *Biochim. Biophys. Acta - Biomembr.* **2008**, 1778, 357–375.
- [65] H. Derakhshankhah, S. Jafari, *Biomed. Pharmacother.* **2018**, 108, 1090–1096.
- [66] Y. Luo, Y. Song, *Int. J. Mol. Sci.* 2021, Vol. 22, Page 11401 **2021**, 22, 11401.
- [67] K. Matsuzaki, *Biochim. Biophys. Acta - Biomembr.* **2009**, 1788, 1687–1692.
- [68] J. Garner, M. M. Harding, *Org. Biomol. Chem.* **2007**, 5, 3577–3585.
- [69] C. J. Bowerman, B. L. Nilsson, *Biopolymers* **2012**, 98, 169–184.
- [70] P. V Panteleev, I. A. Bolosov, S. V Balandin, T. V Ovchinnikova, M. M. Shemyakin, Y. A. Ovchinnikov, *Structure and Biological Functions of β -Hairpin Antimicrobial Peptides*, **2015**.
- [71] L. T. Nguyen, E. F. Haney, H. J. Vogel, *Trends Biotechnol.* **2011**, 29, 464–472.
- [72] D. Takahashi, S. K. Shukla, O. Prakash, G. Zhang, *Biochimie* **2010**, 92, 1236–1241.
- [73] F. G. Avci, B. S. Akbulut, E. Ozkirimli, *Biomolecules* **2018**, 8, DOI 10.3390/BIOM8030077.
- [74] Q. Y. Zhang, Z. Bin Yan, Y. M. Meng, X. Y. Hong, G. Shao, J. J. Ma, X. R. Cheng, J. Liu, J. Kang, C. Y. Fu, *Mil. Med. Res.* 2021 81 **2021**, 8, 1–25.
- [75] T. Yacoub, M. Rima, M. Karam, J. M. Sabatier, Z. Fajloun, *Molecules* **2020**, 25, DOI 10.3390/MOLECULES25102402.
- [76] R. E. W. Hancock, M. G. Scott, *Proc. Natl. Acad. Sci. U. S. A.* **2000**, 97, 8856–8861.
- [77] R. Lai, H. Liu, W. Hui Lee, Y. Zhang, *Biochem. Biophys. Res. Commun.* **2002**, 295, 796–799.
- [78] X. He, S. Yang, L. Wei, R. Liu, R. Lai, M. Rong, *Amino Acids* **2013**, 44, 481–487.
- [79] M. L. Mangoni, B. Casciaro, *Antibiotics* **2020**, 9, 1–4.
- [80] M. Zasloff, *Proc. Natl. Acad. Sci. U. S. A.* **1987**, 84, 5449.
- [81] Y. S. Chan, R. C. F. Cheung, L. Xia, J. H. Wong, T. B. Ng, W. Y. Chan, *Appl.*

- Microbiol. Biotechnol.* **2016**, *100*, 6165–6181.
- [82] W. Chen, B. Yang, H. Zhou, L. Sun, J. Dou, H. Qian, W. Huang, Y. Mei, J. Han, *Peptides* **2011**, *32*, 2497–2503.
- [83] Y. Wang, J. Hong, X. Liu, H. Yang, R. Liu, J. Wu, A. Wang, D. Lin, R. Lai, *PLoS One* **2008**, *3*, DOI 10.1371/JOURNAL.PONE.0003217.
- [84] P. I. Silva, S. Daffre, P. Bulet, *J. Biol. Chem.* **2000**, *275*, 33464–33470.
- [85] V. N. Lazarev, M. M. Shkarupeta, N. F. Polina, E. S. Kostjukova, A. A. Vassilevski, S. A. Kozlov, E. V. Grishin, V. M. Govorun, *Arch. Microbiol.* **2013**, *195*, 173–179.
- [86] P. Wadhvani, S. Sekaran, E. Strandberg, J. Bürck, A. Chugh, A. S. Ulrich, *Int. J. Mol. Sci.* **2021**, *22*, DOI 10.3390/IJMS221810156/S1.
- [87] G. Liu, F. Yang, F. Li, Z. Li, Y. Lang, B. Shen, Y. Wu, W. Li, P. L. Harrison, P. N. Strong, et al., *Front. Microbiol.* **2018**, *9*, 1159.
- [88] P. L. Harrison, M. A. Abdel-Rahman, K. Miller, P. N. Strong, *Toxicon* **2014**, *88*, 115.
- [89] K. Luna-Ramírez, M. A. Sani, J. Silva-Sanchez, J. M. Jiménez-Vargas, F. Reyna-Flores, K. D. Winkel, C. E. Wright, L. D. Possani, F. Separovic, *Biochim. Biophys. Acta - Biomembr.* **2014**, *1838*, 2140–2148.
- [90] A. Khalil, B. H. Elesawy, T. M. Ali, O. M. Ahmed, *Molecules* **2021**, *26*, DOI 10.3390/MOLECULES26164941.
- [91] I. Rady, I. A. Siddiqui, M. Rady, H. Mukhtar, *Cancer Lett.* **2017**, *402*, 16.
- [92] H. Memariani, M. Memariani, H. Moravvej, M. Shahidi-Dadras, *Eur. J. Clin. Microbiol. Infect. Dis.* **2020**, *39*, 5.
- [93] W. Shi, C. Li, M. Li, X. Zong, D. Han, Y. Chen, *Appl. Microbiol. Biotechnol.* **2016**, *100*, 5059.
- [94] J. W. Larrick, M. Hirata, Y. Shimomoura, M. Yoshida, H. Zheng, J. Zhong, S. C. Wright, *Antimicrob. Agents Chemother.* **1993**, *37*, 2534–2539.
- [95] S. T. Henriques, N. Lawrence, S. Chaousis, A. S. Ravipati, O. Cheneval, A. H. Benfield, A. G. Elliott, A. M. Kavanagh, M. A. Cooper, L. Y. Chan, et al., *ACS*

- Chem. Biol.* **2017**, *12*, 2324–2334.
- [96] A. R. Mitchell, *Pept. Sci.* **2008**, *90*, 175–184.
- [97] R. C. Sheppard, *Nature* **1984**, *311*, 699.
- [98] R. A. Lerner, *Science (80-.)*. **2006**, *313*, 57.
- [99] R. Behrendt, P. White, J. Offer, *J. Pept. Sci.* **2016**, *22*, 4.
- [100] D. F. H. Winkler, *Methods Mol. Biol.* **2020**, *2103*, 59–94.
- [101] H. Yazici, M. B. O'Neill, T. Kacar, B. R. Wilson, E. E. Oren, M. Sarikaya, C. Tamerler, *ACS Appl. Mater. Interfaces* **2016**, *8*, 5070–5081.
- [102] L. I. Fedoreyeva, I. I. Kireev, V. K. Khavinson, B. F. Vanyushin, *Biochem. 2011 7611* **2011**, *76*, 1210–1219.
- [103] B. J. Evans, A. T. King, A. Katsifis, L. Matesic, J. F. Jamie, *Molecules* **2020**, *25*, DOI 10.3390/MOLECULES25102314.
- [104] J. Lu, H. Xu, J. Xia, J. Ma, J. Xu, Y. Li, J. Feng, *Front. Microbiol.* **2020**, *11*, 2869.
- [105] S. C. Setty, S. Horam, M. Pasupuleti, W. Haq, *Int. J. Pept. Res. Ther.* **2017**, *23*, 213–225.
- [106] M. D. Díaz, M. Palomino-Schätzlein, F. Corzana, C. Andreu, R. J. Carbajo, M. Del Olmo, A. Canales-Mayordomo, A. Pineda-Lucena, G. Asensio, J. Jiménez-Barbero, *ChemBioChem* **2010**, *11*, 2424–2432.
- [107] M. Esposito, M. G. Grusovin, M. Talati, P. Coulthard, R. Oliver, H. V. Worthington, *Cochrane Database Syst. Rev.* **2008**, doi.org/10.1002/14651858.CD004152.pub2.
- [108] J. L. Harding, M. M. Reynolds, *Trends Biotechnol.* **2014**, *32*, 140–146.
- [109] J. M. Anderson, *Regen. Biomater.* **2016**, *3*, 73.
- [110] C. R. Arciola, D. Campoccia, L. Montanaro, *Nat. Rev. Microbiol.* **2018**, *16*, 397–409.
- [111] X. W. Tan, T. W. Goh, P. Saraswathi, C. L. Nyein, M. Setiawan, A. Riau, R. Lakshminarayanan, S. Liu, D. Tan, R. W. Beuerman, et al., *Antimicrob. Agents*

- Chemother.* **2014**, *58*, 5229–5238.
- [112] M. Riool, A. de Breij, J. W. Drijfhout, P. H. Nibbering, S. A. J. Zaat, *Front. Chem.* **2017**, *AUG*, 63.
- [113] P. Devasconcellos, S. Bose, H. Beyenal, A. Bandyopadhyay, L. G. Zirkle, *Mater. Sci. Eng. C* **2012**, *32*, 1112–1120.
- [114] R. M. Ortí-Lucas, J. Muñoz-Miguel, *Antimicrob. Resist. Infect. Control* **2017**, *6*, 61.
- [115] S. He, P. Zhou, L. Wang, X. Xiong, Y. Zhang, Y. Deng, S. Wei, *J. R. Soc. Interface* **2014**, *11*, doi.org/10.1098/rsif.2014.0169.
- [116] L. Zhou, H. M. Wong, Y. Y. Zhang, Q. L. Li, *ACS Appl. Mater. Interfaces* **2020**, *12*, 3021–3031.
- [117] M. Pihl, S. Galli, R. Jimbo, M. Andersson, *J. Biomed. Mater. Res. - Part B Appl. Biomater.* **2021**, *109*, 1787–1795.
- [118] X. Meng, J. Zhang, J. Chen, B. Nie, B. Yue, W. Zhang, Z. Lyu, T. Long, Y. Wang, *J. Mater. Chem. B* **2020**, *8*, 10190–10204.
- [119] B. G. X. Zhang, D. E. Myers, G. G. Wallace, M. Brandt, P. F. M. Choong, *Int. J. Mol. Sci.* **2014**, *15*, 11878.
- [120] M. G. Drexelius, I. Neundorf, *Int. J. Mol. Sci.* **2021**, *Vol. 22*, Page 13212 **2021**, *22*, 13212.
- [121] C. Wisdom, S. K. VanOosten, K. W. Boone, D. Khvostenko, P. M. Arnold, M. L. Snead, C. Tamerler, *J. Mol. Eng. Mater.* **2016**, *4*, 1640005.
- [122] Z. Liu, S. Ma, S. Duan, D. Xuliang, Y. Sun, X. Zhang, X. Xu, B. Guan, C. Wang, M. Hu, et al., *ACS Appl. Mater. Interfaces* **2016**, *8*, 5124–5136.
- [123] A. Saha, S. Nir, M. Reches, *Langmuir* **2020**, *36*, 4201–4206.
- [124] H. Geng, Y. Yuan, A. Adayi, X. Zhang, X. Song, L. Gong, X. Zhang, P. Gao, *Mater. Sci. Eng. C* **2018**, *82*, 141–154.
- [125] A. Care, P. L. Bergquist, A. Sunna, *Adv. Exp. Med. Biol.* **2017**, *1030*, 21–36.
- [126] R. Zuo, D. Örnek, T. K. Wood, *Appl. Microbiol. Biotechnol.* **2005**, *68*, 505–509.

- [127] D. E. Chico, R. L. Given, B. T. Miller, *Peptides* **2003**, *24*, 3–9.
- [128] H. Yazici, H. Fong, B. Wilson, E. E. Oren, F. A. Amos, H. Zhang, J. S. Evans, M. L. Snead, M. Sarikaya, C. Tamerler, *Acta Biomater.* **2013**, *9*, 5341.
- [129] E. C. Wisdom, Y. Zhou, C. Chen, C. Tamerler, M. L. Snead, *ACS Biomater. Sci. Eng.* **2020**, *6*, 2682–2695.
- [130] X. Zhang, H. Geng, L. Gong, Q. Zhang, H. Li, X. Zhang, Y. Wang, P. Gao, *Int. J. Nanomedicine* **2018**, *13*, 5361.
- [131] L. Gong, H. Geng, X. Zhang, P. Gao, *RSC Adv.* **2019**, *9*, 26276–26282.
- [132] L. Townsend, R. L. Williams, O. Anuforom, M. R. Berwick, F. Halstead, E. Hughes, A. Stamboulis, B. Oppenheim, J. Gough, L. Grover, et al., *J. R. Soc. Interface* **2017**, *14*, DOI 10.1098/rsif.2016.0657.
- [133] Z. Trzcińska, M. Bruggeman, H. Ijakipour, N. J. Hodges, J. Bowen, A. Stamboulis, *Materials (Basel)*. **2020**, *13*, DOI 10.3390/MA13173714.
- [134] J. H. Ryu, P. B. Messersmith, H. Lee, *ACS Appl. Mater. Interfaces* **2018**, *10*, 7523–7540.
- [135] X. W. Tan, T. W. Goh, P. Saraswathi, C. L. Nyein, M. Setiawan, A. Riau, R. Lakshminarayanan, S. Liu, D. Tan, R. W. Beuerman, et al., *Antimicrob. Agents Chemother.* **2014**, *58*, 5229–5238.
- [136] J. Zhan, L. Wang, Y. Zhu, H. Gao, Y. Chen, J. Chen, Y. Jia, J. He, Z. Fang, Y. Zhu, et al., *ACS Appl. Mater. Interfaces* **2018**, *10*, 35830–35837.
- [137] N. G. Fischer, D. G. Moussa, E. P. Skoe, D. A. De Jong, C. Aparicio, *ACS Biomater. Sci. Eng.* **2020**, *6*, 4929–4939.
- [138] V. P. Koidou, P. P. Argyris, E. P. Skoe, J. Mota Siqueira, X. Chen, L. Zhang, J. E. Hinrichs, M. Costalonga, C. Aparicio, *Biomater. Sci.* **2018**, *6*, 1936–1945.
- [139] B. Mishra, G. Wang, *Biofouling* **2017**, *33*, 544–555.
- [140] X. Chen, L. Zhou, D. Wu, W. Huang, Y. Lin, B. Zhou, J. Chen, *Biomed Res. Int.* **2020**, *2020*, DOI 10.1155/2020/2327034.
- [141] J. Chen, Y. Zhu, M. Xiong, G. Hu, J. Zhan, T. Li, L. Wang, Y. Wang, *ACS Biomater. Sci. Eng.* **2019**, *5*, 1034–1044.

- [142] M. Kazemzadeh-Narbat, J. Kindrachuk, K. Duan, H. Jenssen, R. E. W. Hancock, R. Wang, *Biomaterials* **2010**, *31*, 9519–9526.
- [143] H. Yazici, G. Habib, K. Boone, M. Urgan, F. S. Utku, C. Tamerler, *Mater. Sci. Eng. C* **2019**, *94*, 333–343.
- [144] S. Acosta, A. Ibañez-Fonseca, C. Aparicio, J. C. Rodríguez-Cabello, *Biomater. Sci.* **2020**, *8*, 2866–2877.
- [145] T. Li, N. Wang, S. Chen, R. Lu, H. Li, Z. Zhang, *Int. J. Nanomedicine* **2017**, *12*, 2995–3007.
- [146] J. Chen, X. Shi, Y. Zhu, Y. Chen, M. Gao, H. Gao, L. Liu, L. Wang, C. Mao, Y. Wang, *Theranostics* **2020**, *10*, 109–122.
- [147] X. Shen, M. A. Al-Baadani, H. He, L. Cai, Z. Wu, L. Yao, X. Wu, S. Wu, M. Chen, H. Zhang, et al., *Int. J. Nanomedicine* **2019**, *14*, 3043–3054.
- [148] Y. Zhang, L. Zhang, B. Li, Y. Han, *ACS Appl. Mater. Interfaces* **2017**, *9*, 9449–9461.
- [149] A. Volejníková, P. Melicherčík, O. Nešuta, E. Vaňková, L. Bednárová, J. Rybáček, V. Čeřovský, *J. Med. Microbiol.* **2019**, *68*, 961–972.
- [150] H. W. Liu, D. X. Wei, J. Z. Deng, J. J. Zhu, K. Xu, W. H. Hu, S. H. Xiao, Y. G. Zhou, *Artif. Cells, Nanomedicine Biotechnol.* **2018**, *46*, S460–S470.
- [151] Y. He, C. Mu, X. Shen, Z. Yuan, J. Liu, W. Chen, C. Lin, B. Tao, B. Liu, K. Cai, *Acta Biomater.* **2018**, *80*, 412–424.
- [152] A. de L. Rodríguez López, M. R. Lee, B. J. Ortiz, B. D. Gastfriend, R. Whitehead, D. M. Lynn, S. P. Palecek, *Acta Biomater.* **2019**, *93*, 50–62.
- [153] L. Zhang, Y. Xue, S. Gopalakrishnan, K. Li, Y. Han, V. M. Rotello, *ACS Appl. Mater. Interfaces* **2021**, *13*, 28764–28773.
- [154] J. Shi, Y. Liu, Y. Wang, J. Zhang, S. Zhao, G. Yang, *Sci. Rep.* **2015**, *5*, 1–15.
- [155] H. Cheng, K. Yue, M. Kazemzadeh-Narbat, Y. Liu, A. Khalilpour, B. Li, Y. S. Zhang, N. Annabi, A. Khademhosseini, *ACS Appl. Mater. Interfaces* **2017**, *9*, 11428–11439.
- [156] I. Neundorff, R. Rennert, J. Hoyer, F. Schramm, K. Löbner, I. Kitanovic, S.

- Wölfl, *Pharmaceuticals* **2009**, 2, 49.
- [157] T. Lützenburg, N. Burdina, M. S. Scholz, I. Neundorf, *Pharmaceutics* **2021**, 13, DOI 10.3390/PHARMACEUTICS13122075/S1.
- [158] T. Lützenburg, I. Neundorf, M. Scholz, *Chem. Phys. Lipids* **2018**, 213, 62–67.
- [159] A. Haseloer, T. Lützenburg, J. P. Strache, J. Neudörfl, I. Neundorf, A. Klein, *Chembiochem* **2021**, 22, 694.
- [160] M. Horn, I. Neundorf, *Sci. Rep.* **2018**, 8, DOI 10.1038/S41598-018-34684-1.
- [161] A. Gronewold, M. Horn, I. Neundorf, *Beilstein J. Org. Chem.* **2018**, 14, 1378.
- [162] M. Horn, F. Reichart, S. Natividad-Tietz, D. Diaz, I. Neundorf, *Chem. Commun.* **2016**, 52, 2261–2264.
- [163] André Reinhardt, *Inaug. Diss.* **2017**.
- [164] A. Reinhardt, M. Horn, J. Pieper Gen Schmauck, A. Bröhl, R. Giernoth, C. Oelkrug, A. Schubert, I. Neundorf, *Bioconjug. Chem.* **2014**, 25, 2166–2174.
- [165] “HeliQuest ComputParam form version3,” can be found under <https://heliquest.ipmc.cnrs.fr/cgi-bin/ComputParams.py>, **n.d.**
- [166] J. Rappsilber, M. Mann, Y. Ishihama, *Nat. Protoc.* **2007**, 2, 1896–1906.
- [167] S. Beck, A. Michalski, O. Raether, M. Lubeck, S. Kaspar, N. Goedecke, C. Baessmann, D. Hornburg, F. Meier, I. Paron, et al., *Mol. Cell. Proteomics* **2015**, 14, 2014–2029.
- [168] S. Tyanova, T. Temu, J. Cox, *Nat. Protoc.* **2016**, 11, 2301–2319.
- [169] S. Tyanova, T. Temu, P. Sinitcyn, A. Carlson, M. Y. Hein, T. Geiger, M. Mann, J. Cox, *Nat. Methods* **2016**, 13, 731–740.
- [170] K. D. Saint Jean, K. D. Henderson, C. L. Chrom, L. E. Abiuso, L. M. Renn, G. A. Caputo, *Probiotics Antimicrob. Proteins* **2018**, 10, 408–419.
- [171] M. Drexelius, A. Reinhardt, J. Grabeck, T. Cronenberg, F. Nitsche, P. F. Huesgen, B. Maier, I. Neundorf, *Biochem. J.* **2021**, 478, 63–78.
- [172] J. Grabeck, *Bachelor thesis* **2019**.
- [173] M. G. Drexelius, *Master thesis* **2018**.

- [174] **N.d.**
- [175] Y. Huang, L. He, G. Li, N. Zhai, H. Jiang, Y. Chen, *Protein Cell* **2014**, 5, 631–642.
- [176] H. Meng, K. Kumar, *J. Am. Chem. Soc.* **2007**, 129, 15615–15622.
- [177] G. Carmona, A. Rodriguez, D. Juarez, G. Corzo, E. Villegas, *Protein J.* **2013**, 32, 456–466.
- [178] B. J. Moncla, K. Pryke, L. C. Rohan, P. W. Graebing, *Adv. Biosci. Biotechnol.* **2011**, 2, 404–408.
- [179] S. B. Leslie, E. Israeli, B. Lighthart, J. H. Crowe, L. M. Crowe, *Appl. Environ. Microbiol.* **1995**, 61, 3592–3597.
- [180] M. Bacalum, M. Radu, *Int. J. Pept. Res. Ther.* **2015**, 21, 47–55.
- [181] L. M. Yin, M. A. Edwards, J. Li, C. M. Yip, C. M. Deber, *J. Biol. Chem.* **2012**, 287, 7738.
- [182] I. Ruseska, A. Zimmer, *Beilstein J. Nanotechnol.* **2020**, 11, 101–123.
- [183] N. Raheem, S. K. Straus, *Front. Microbiol.* **2019**, 10, 2866.
- [184] C. F. Le, C. M. Fang, S. D. Sekaran, *Antimicrob. Agents Chemother.* **2017**, 61, DOI 10.1128/AAC.02340-16.
- [185] S. Clark, T. A. Jowitt, L. K. Harris, C. G. Knight, C. B. Dobson, *Commun. Biol.* **2021**, 41 **2021**, 4, 1–14.
- [186] K. J. Cutrona, B. A. Kaufman, D. M. Figueroa, D. E. Elmore, *FEBS Lett.* **2015**, 589, 3915.
- [187] T. Lützenburg, *Inaug. Diss.* **2021**.
- [188] L. Buchwald, *Bachelor thesis* **2020**.
- [189] M. (Universita D. S. F. Garsoria, *Master thesis* **2021**.
- [190] S. Köster, K. Van Pee, Ö. Yildiz, *Methods Enzymol.* **2015**, 557, 149–166.
- [191] M. C. Gagnon, E. Strandberg, A. Grau-Campistany, P. Wadhvani, J. Reichert, J. Bürck, F. Rabanal, M. Auger, J. F. Paquin, A. S. Ulrich, *Biochemistry* **2017**, 56, 1680–1695.

- [192] A. I. Dragan, C. Crane-Robinson, P. L. Privalov, *Eur. Biophys. J.* **2021**, *50*, 787.
- [193] L. PAULING, R. B. COREY, H. R. BRANSON, *Proc. Natl. Acad. Sci. U. S. A.* **1951**, *37*, 205.
- [194] K. Andreev, M. W. Martynowycz, M. L. Huang, I. Kuzmenko, W. Bu, K. Kirshenbaum, D. Gidalevitz, *Biochim. Biophys. Acta* **2018**, *1860*, 1414.
- [195] R. Arnold, *Bachelor thesis* **2022**.
- [196] L. Zhong, W. C. Johnson, *Biophysics (Oxf)*. **1992**, *89*, 4462–4465.
- [197] A. K. Mahalka, P. K. J. Kinnunen, *Biochim. Biophys. Acta - Biomembr.* **2009**, *1788*, 1600–1609.
- [198] M. C. Manning, R. W. Woody, *Biopolymers* **1991**, *31*, 569–586.
- [199] M. Otto, *Curr. Top. Microbiol. Immunol.* **2008**, *322*, 207.
- [200] J. Wei, X. Cao, J. Qian, Z. Liu, X. Wang, Q. Su, Y. Wang, R. Xie, X. Li, *Med. (United States)* **2021**, *100*, DOI 10.1097/MD.00000000000027426.
- [201] B. Mishra, R. M. Golla, K. Lau, T. Lushnikova, G. Wang, *ACS Med. Chem. Lett.* **2016**, *7*, 117–121.
- [202] D. T. Yucesoy, M. Hnilova, K. Boone, P. M. Arnold, M. L. Snead, C. Tamerler, *JOM (1989)*. **2015**, *67*, 754.
- [203] Z. Lu, Y. Wu, Z. Cong, Y. Qian, X. Wu, N. Shao, Z. Qiao, H. Zhang, Y. She, K. Chen, et al., *Bioact. Mater.* **2021**, *6*, 4531.
- [204] K. E. Ridyard, J. Overhage, *Antibiotics* **2021**, *10*, DOI 10.3390/ANTIBIOTICS10060650.
- [205] S. Evans, *Surf. INTERFACE Anal.* **1997**, *25*, 924–930.
- [206] A. Champion, V. Hallmark, G. L. Richmond, P. Chu, R. Adzic, M. Hanson, E. Yeager, A. Hamelin, G. Valette, D. Mullins, et al., *J. Electroanal. Chem* **1978**, *23*, 2401–2408.

10. Attachments

10.1. List of abbreviations

ACN	Acetonitrile
ACP	Anticancer peptide
AMP	Antimicrobial peptide
AMR	Antimicrobial resistances
CD	Circular Dichroism
CF	5/6-Carboxyfluorescein
CPP	Cell penetrating peptide
DCM	Dichlormethane
DIC	N,N'-diisopropylcarbodiimide
DIPEA	N,N-diisopropylethylamine
DMF	N,N-dimethylformamid
DMSO	Dimethyl sulfoxide
EDT	Ethane-1,2-dithiol
EDTA	Ethylendiamintetraacetat
eq	Equivalents
ESI-MS	Electrospray ionization mass-spectrometry
FA	Formic acid
FACS	Fluorescence assisted cell sorting
FBS	Fetal Bovine Serum
Fmoc	Fluorenyl-9-methoxycarbonyl
HATU	N-methylmethanaminium hexafluorophosphate N-oxide
h-RBC	human red blood cells
INT	Iodnitrotetrazolium
LDH	Lactatdehydrogenase
MHB	Müller-Hinton broth
MIC	Minimal inhibitory concentration with no bacterial viability
MIC ₅₀	Minimal inhibitory concentration of 50% bacterial viability
MRSA	Methicillin resistant <i>Staphylococcus aureus</i>

OD	Optical density
Oxyrna	Ethyl cyano(hydroxyimino) acetate
PBS	Phosphate buffered saline
PD	Polydopamine
PI	Propidiumiodide
PMSF	Phenylmethylsulfonylfluorid
RP-HPLC	Reversed-phase high-performance liquid chromatography
S1	Biosafety level 1 microorganism (non-pathogenic to humans)
S2	Biosafety level 2 microorganism (pathogenic to humans, mild diseases)
SD	Standard deviation
SEM	Scanning electron microscopy
SI	Selectivity index
SPPS	Solid phase peptide synthesis
TBP	Titanium binding peptide
TFA	Trifluoroacetic acid
TFE	2,2,2-trifluoroethanol
THA	Thioanisol
Ti	Titanium
TIS	Triisopropylsilane
XPS	X-ray photoelectron spectroscopy

10.2. List of amino acids

Name	1-letter code	3-letter code
Alanine	A	Ala
Cysteine	C	Cys
Aspartate	D	Asp
Glutamate	E	Glu
Phenylalanine	F	Phe
Glycine	G	Gly
Histidine	H	His
Isoleucine	I	Ile
Lysine	K	Lys
Leucine	L	Leu
Methionine	M	Met
Asparagine	N	Asn
Proline	P	Pro
Glutamine	Q	Gln
Arginine	R	Arg
Serine	S	Ser
Threonine	T	Thr
Valine	V	Val
Tryptophane	W	Trp
Tyrosine	Y	Tyr
4-fluorphenylalanine	X ₁	/
3,5-difluorphenylalanine	X ₂	/
pentafluorphenylalanine	X ₃	/

10.3. Register of figures

Figure 1: Differences in eukaryotic and prokaryotic cell structures. ^[3]	1
Figure 2: Composition of membranes and other types of bilayers in gram-positive and gram-negative bacterial surfaces.....	2
Figure 3: Schematic bacterial infection in mammalian tissue leading to inflammation and immune responses from proteins (enzymes and peptides) as well as direct immune cell and antibody involvement.	3
Figure 4: Mechanism of antimicrobial peptides. Top: Attachment of approaching antimicrobial peptides onto bacterial membrane by electrostatic interaction. Peptide coiling through interaction with membrane and either translocation to reach intracellular targets or perturbing the membrane to reach bacterial lysis. Bottom: The three main mechanisms of bacterial membrane perturbation by antimicrobial peptides through pore formation with the barrel-stave, toroidal or carpet mechanism ^[57,73,74]	10
Figure 5: The three main strategies of antimicrobial surface coatings to prevent biofilm formation. ^[120]	14
Figure 6: Helical wheel projection ^[165] for prognosis of crucial substitution positions with isoleucine in sC18 to enhance antibacterial activity by widening the hydrophobic site (R10 and K16) or removing the negative charge (E15).....	18
Figure 7: Versatility of activity in rational designed peptides.	22
Figure 8: Circular dichroism spectroscopy of the generation four antimicrobial peptides in phosphate buffer (top) and buffer with the addition of trifluoroethanol (bottom). 41	41
Figure 9: Screening generation four peptides for their antimicrobial activity against seven bacterial strains. Bacteria were incubated for 6 h at 37°C. Data represent the mean \pm SD of $n \geq 3$ performed in triplicate. Negative control (water) was set to 100% to calculate the relative quantity of living cells.	42
Figure 10: Antimicrobial activity of the peptides AMP3g , AMP4b and AMP4e against <i>Pseudomonas aeruginosa</i> in comparison to common antibiotic Gentamycin. 44	44
Figure 11: Antimicrobial activity (6 h, 37°C incubation) of the identified peptide fragments against <i>B. subtilis</i> and <i>P. fluorescens</i>	46
Figure 12: Proteome evaluation of <i>B. subtilis</i> treated with AMP4e	47
Figure 13: Antimicrobial assay (6 h, 37 °C incubation) using <i>B. subtilis</i> and AMP4a , AMP4b and AMP4e at minimal inhibitory concentration, with preceding 18 h treatment	

in fresh growth medium (full colour) or bacterial cell culture supernatant (dashed). Data represent mean \pm SD of $n \geq 3$ performed in triplicate. Statistical significance was calculated with t-test: ns: $P > 0.05$; ***: $P \leq 0.001$ 48

Figure 14: Haemolysis assay of the generation three and four antimicrobial peptides using human red blood cells (hRBC). The erythrocytes were incubated with peptides for 24 h at 37°C. Negative control was water and positive control 1% Triton X-100. Data represent mean \pm SD of $n \geq 3$ performed in triplicate. Statistical significance was calculated with t-test: *: $P \leq 0.05$ 50

Figure 15: Cytotoxicity of the generation three and four peptides towards non-cancerous cell line HEK293 for 24 hours at 37 °C. Negative control (water) was set to 100% to calculate relative cell viability. Data represent mean \pm SD of $n \geq 3$ performed in triplicate. Statistical significance was calculated with t-test: *: $P \leq 0.05$; **: $P \leq 0.01$; ***: $P \leq 0.001$ 50

Figure 16: Cytotoxicity of the generation three and four peptides towards cancerous cell lines. (left: HeLa, right: MCF7) for 24 hours at 37 °C. Negative control (water) was set to 100% to calculate relative cell viability. Data represent mean \pm SD of $n \geq 3$ performed in triplicate. Statistical significance was calculated with t-test: *: $P \leq 0.05$; **: $P \leq 0.01$; ***: $P \leq 0.001$ 52

Figure 17: Cellular internalization experiment in HeLa and HEK293 cells using the third and fourth generation peptides. The sub-lethal concentrations used were 10 μ M for generation 3 peptides and 5 μ M for generation four peptides. 10.000 cells were counted, and data normalized to sC18, representing the mean \pm SD of $n \geq 2$ performed in triplicate. Statistical significance was calculated with t-test: ns: $P > 0.05$; *: $P \leq 0.05$; **: $P \leq 0.01$; ***: $P \leq 0.001$ 53

Figure 18: Lactate dehydrogenase release assay of selected peptides to investigate the membrane disruption process. Peptides were incubated with HeLa cells for 1 hour. Data represent mean \pm SD of $n \geq 2$ performed in triplicate. Statistical significance was calculated with t-test: ns: $P > 0.05$; ***: $P \leq 0.001$ 54

Figure 19: Characterization of morphological changes in different bacteria after peptide incubation using scanning electron microscopy. Incubation: 90 minutes at 37 °C with 4xMIC₅₀ of antimicrobial peptides or water (control)..... 56

Figure 20: Helical wheel projections^[165] for peptides **sC18**, **sC18 Δ E** and **sC18*** as well as **RL-sC18**, **RL-sC18 Δ E** and **RL-sC18***..... 59

Figure 21: CD-spectroscopy of peptides RL-sc18 , RL-sC18ΔE and RL-sC18* in phosphate buffer (top) or phosphate buffer with TFE (bottom). R-values were calculated from the intensities at 208 and 222 nm.....	61
Figure 22: Iodnitrotetrazolium chloride assay using the RL-sC18 variants and testing them against <i>B. subtilis</i> , <i>M. luteus</i> , <i>C. glutamicum</i> , <i>P. fluorescens</i> , <i>S. typhimurium</i> , <i>E. coli</i> and <i>M. phlei</i> , respectively.....	62
Figure 23: Haemolysis assay of the three RL-sC18 variants, normalized to Triton X-100. Incubation: 24 hours at 37 °C.....	63
Figure 24: Helical wheel projection ^[165] indicating the specific substitutions of arginine and leucine to the sequence of sC18* resulting in the RL-screen peptides to achieve peptides RL-1 to RL-4	64
Figure 25: Iodnitrotetrazolium chloride assay using RL-peptides and testing them against <i>Bacillus subtilis</i> . Top: Mono-substitutions, middle: double-substitutions, Bottom: Triple-substitutions.	67
Figure 26: Iodnitrotetrazolium chloride assay using selected RL-peptides and testing them against <i>M. luteus</i> , <i>C. glutamicum</i> , <i>S. typhimurium</i> , <i>P. fluorescens</i> , <i>M. phlei</i> and <i>E. coli</i> . 68	68
Figure 27: Haemolysis assay for the four selected RL-screen peptides, normalized to Triton X-100. Incubation: 24 hours at 37 °C.....	69
Figure 28: Efficiency of immobilized antimicrobial peptides AMP3g , AMP4b and AMP4e on preventing the adhesion of <i>B. subtilis</i> on titanium plates. Data represent mean ± SD of $n \geq 3$ performed in triplicate. Statistical significance was calculated with t-test: *: $P \leq 0.05$; **: $P \leq 0.01$; ***: $P \leq 0.001$	72
Figure 29: Helical wheel projections ^[165] and hydrophobic momentum of AMP4b and the chimeric peptides Chim1 , Chim2 and Chim3	74
Figure 30: Circular dichroism spectroscopy of the three chimeric peptides in phosphate buffer with variable content of trifluoroethanol (TFE).	75
Figure 31: Antimicrobial activity assay of chimeric peptides with <i>B. subtilis</i> , <i>P. fluorescens</i> and <i>S. typhimurium</i> . Incubation for 6 h at 37°C. Data represent mean ± SD of $n = 3$ performed in triplicate. To calculate the relative quantity of living cells, negative control (water) was set to 100%.	78
Figure 32: Antimicrobial activity assay of chimeric peptides, AMP4b , and control peptide LL37 using <i>S. aureus</i> and methicillin resistant <i>S. aureus</i> (MRSA). Bacteria were incubated for 6 h at 37°C. Data represent mean ± SD of $n = 1$ performed in	

triplicate. To calculate the relative quantity of living cells, negative control (water) was set to 100%..... 81

Figure 33: Haemolysis assay using the three chimeric peptides and LL37. Purified human red blood cells (hRBC) were incubated for 24 h at 37°C. Positive control 1% Triton X-100 and negative control was water. Data represents mean ± SD of n = 3 performed in triplicate. Statistical significance in relation to LL37 was calculated with t-test: ***: $P \leq 0.001$ 82

Figure 34: Fluorescence microscopy of the three chimeric peptides using *B. subtilis* after incubation with 1 µM peptide at 37 °C for 30 minutes. Peptides were marked with (5/6)-carboxylfluorescein. Dead bacteria were stained with propidium iodide. 84

Figure 35: Relative amount of *B. subtilis* colonies counted after incubation of bacteria for 6 hours at 37 °C on small titanium plates, either pure (w/o) or plates coated with chimeric peptides. Statistical significance in relation to pure titanium plates was calculated with t-test: ns: $P > 0.05$; *: $P \leq 0.05$; **: $P \leq 0.01$; ***: $P \leq 0.001$ 86

10.4. Register of tables

Table 1:	List of common antibiotics, their antibiotic class and mechanism to affect bacterial viability ^[36,37]	6
Table 2:	Prominent antimicrobial peptides derived from natural sources.	11
Table 3:	MIC ₅₀ values [μ M] for the generation two and three peptides tested against seven different bacterial strains. Incubation time was 6 h at 37°C.	20
Table 4:	Laboratory equipment used for the experiments in this work.	23
Table 5:	Sequences of all peptides investigated in this work.	26
Table 6:	Sequences and physicochemical properties of the generation three and four antimicrobial peptides. Physicochemical values were calculated with the thermofisher peptide analysis tool. ^[174]	39
Table 7:	MIC ₅₀ values [μ M] for the generation four peptides tested against seven different bacterial strains. Incubation time was 6 h at 37°C.	43
Table 8:	Enzymatic stability of peptides AMP4a , AMP4b and AMP4e after incubation with 1:50 trypsin. Cleavage-sites of peptides over time determined by LC–MS. N-terminal (A) and C-terminal (B) fragments were identified by their mass signature in ESI-MS.	45
Table 9:	Selectivity index calculation between bacterial and mammalian cells. Calculation (CC ₁₀₀ /MIC ₁₀₀) was performed with the experimental values of <i>B. subtilis</i> and <i>P. fluorescens</i> , as well as CC ₁₀₀ values of HEK293 cells.	51
Table 10:	Sequences and physicochemical properties of the RL-sC18 variants. Physicochemical values were calculated with the thermofisher peptide analysis tool ^[174]	60
Table 11:	Peptide sequences and physicochemical values (calculated with the thermofisher peptide analysis tool ^[174]) of novel R,L-peptides.	65
Table 12:	Peptide sequences and physicochemical properties of the three chimeric peptides and LL37, used as control in this work. Physicochemical values were calculated by Thermofisher peptide analysis tool. ^[174] R-values were calculated by taking the ratio between the molar ellipticity at 220 nm and 208 nm (R-value = $[\Theta]_{220} / [\Theta]_{208}$).	73
Table 13:	Calculated R-values for the three chimeric peptides ($\Theta_{222} / \Theta_{208}$).	76
Table 14:	MIC ₅₀ values [μ M] for peptides Chim1-3 when in presence of different bacterial strains as determined by a colorimetric iodnitrotetrazolium assay. bacteria	

were incubated for 6 h at 37 °C with different peptide concentrations, respectively. Standard deviations were calculated from the three separate experiments in triplicate.

79

Table 15: Relative abundances of elements (%) determined by XPS of Ti surfaces either treated with the respective chimeric peptides or not (w/o). Averages and deviations were calculated from two independent measurements..... 85

10.5. Register of Supplementary

Supplementary 1: UV-chromatogram and mass spectrometry analysis of peptides AMP3a, AMP3b, AMP3c and AMP3d	115
Supplementary 2: UV-chromatogram and mass spectrometry analysis of peptides AMP3e, AMP3f, AMP3g and AMP4a	116
Supplementary 3: UV-chromatogram and mass spectrometry analysis of peptides AMP4b, AMP4c, AMP4d and AMP4e	117
Supplementary 4: UV-chromatogram and mass spectrometry analysis of peptides RL-sC18, RL-sC18ΔE and RL-sC18*	118
Supplementary 5: UV-chromatogram and mass spectrometry analysis of peptides Chim1, Chim2 and Chim3	119
Supplementary 6: UV-chromatogram and mass spectrometry analysis of peptides CF-Chim1, CF-Chim2 and CF-Chim3	120
Supplementary 7: Preliminary work on AMP generation one (isoleucine screening) with three different bacterial strains. Bacteria were incubated for 6 h at 37°C with various peptide concentrations. Data represent mean ± SD of n (number of experiments) ≥ 1 performed in triplicate. Negative control (water) was set to 100% to calculate the relative quantity of living cells.	121
Supplementary 8: Screening generation two peptides (isoleucine substitution) for their antimicrobial activity against seven bacterial strains. Bacteria were incubated for 6 h at 37°C. Data represent mean ± SD of n ≥ 3 performed in triplicate. Negative control (water) was set to 100% to calculate the relative quantity of living cells.....	122
Supplementary 9: Screening generation three peptides (phenylalanine substitution) for their antimicrobial activity against seven bacterial strains. Bacteria were incubated for 6 h at 37°C. Data represent mean ± SD of n ≥ 3 performed in triplicate. Negative control (water) was set to 100% to calculate the relative quantity of living cells.	123
Supplementary 10: Dose response curves of the chimeric peptides with <i>S. typhimuiurm</i> , <i>P. fluorescens</i> and <i>B. subtilis</i>	124
Supplementary 11: Fluorescence microscopy of sC18, AMP4b and the three chimeric peptides using <i>B. subtilis</i> after incubation with 20 µM peptide at 37 °C for 30 minutes. Peptides were marked with (5/6)-carboxylfluorescein. Dead bacteria were stained with propidium iodide.	125
Supplementary 12: Fluorescence microscopy of sC18, AMP4b and the three chimeric peptides using <i>P. fluorescens</i> after incubation with 20 µM peptide at 37 °C for	

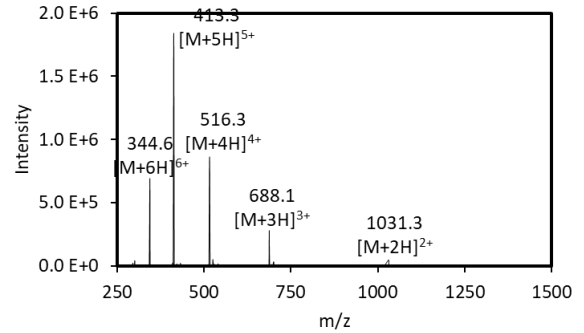
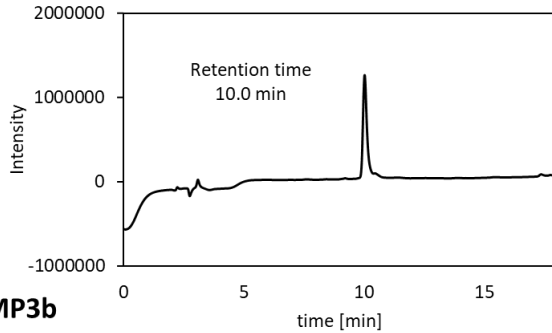
30 minutes. Peptides were marked with (5/6)-carboxylfluorescein. Dead bacteria were stained with propidium iodide. 126

Supplementary 13: Fluorescence microscopy of sC18, AMP4b and the three chimeric peptides using *S. typhimurium* after incubation with 20 µM peptide at 37 °C for 30 minutes. Peptides were marked with (5/6)-carboxylfluorescein. Dead bacteria were stained with propidium iodide. 127

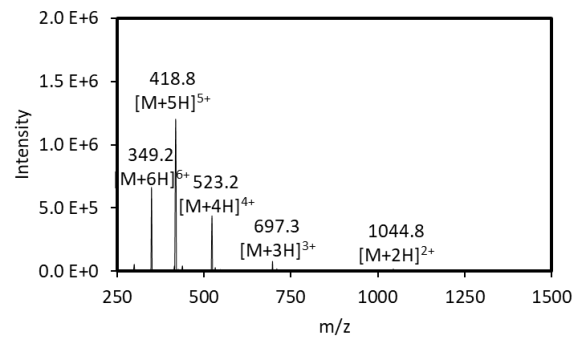
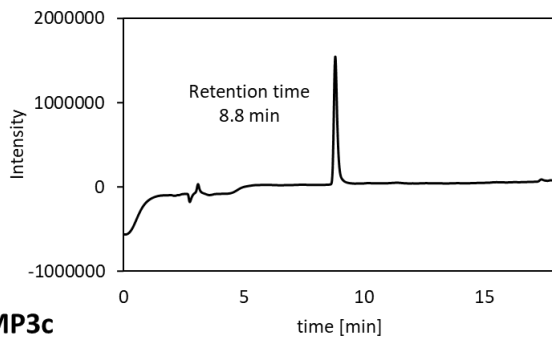
Supplementary 14: Spectra of XPS measurement for elemental analyses of titanium plates without coating (w/o) and immobilized with chimeric peptides (**Chim1**, **Chim2**, **Chim3**). 128

10.6. Peptide Analysis Spectra

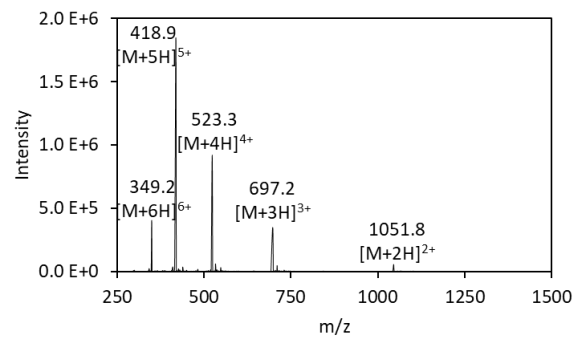
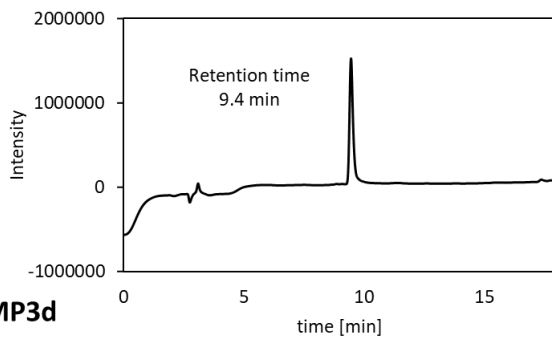
AMP3a



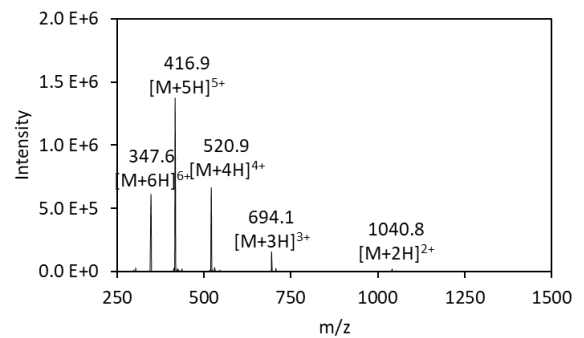
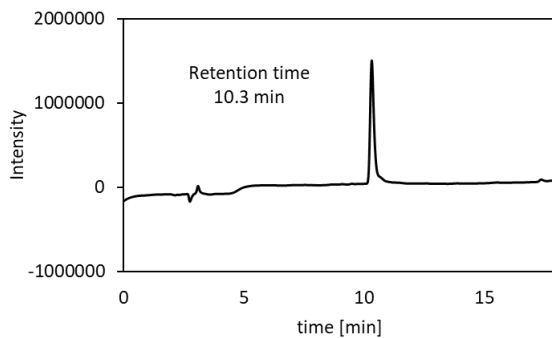
AMP3b



AMP3c

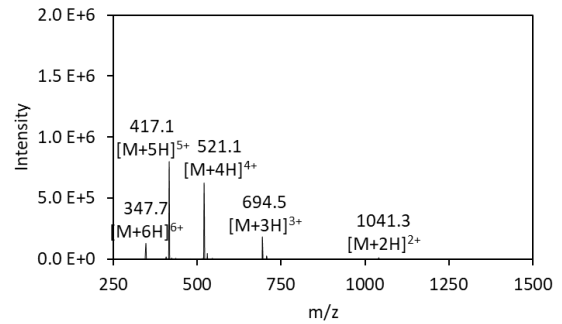
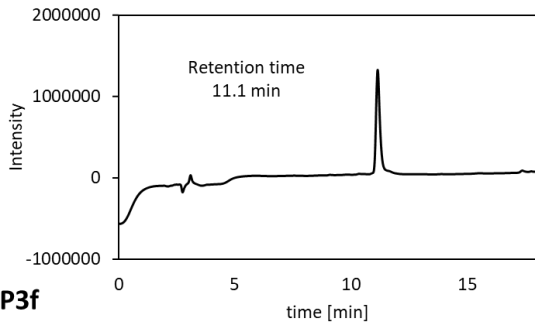


AMP3d

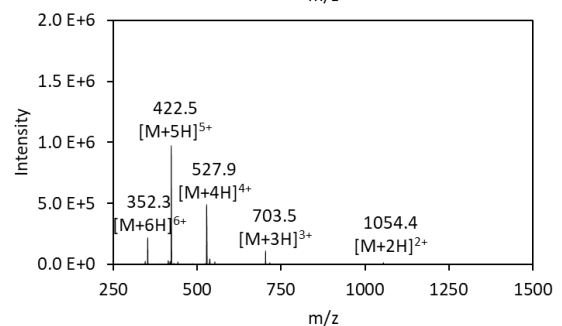
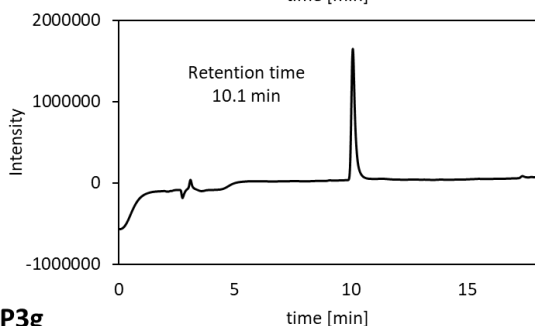


Supplementary 1: UV-chromatogram and mass spectrometry analysis of peptides AMP3a, AMP3b, AMP3c and AMP3d^[171].

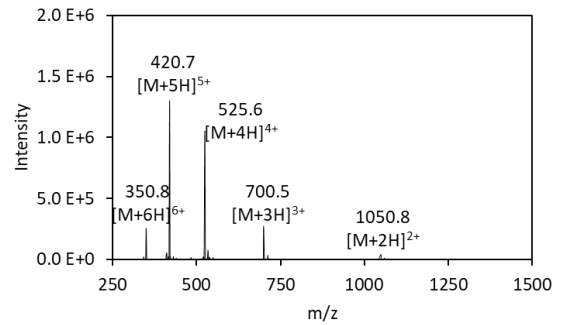
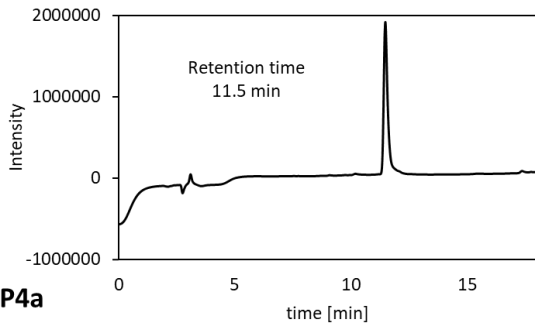
AMP3e



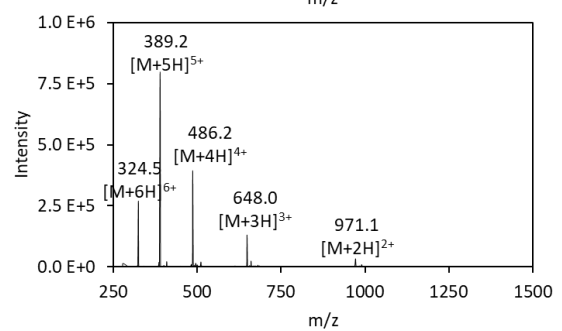
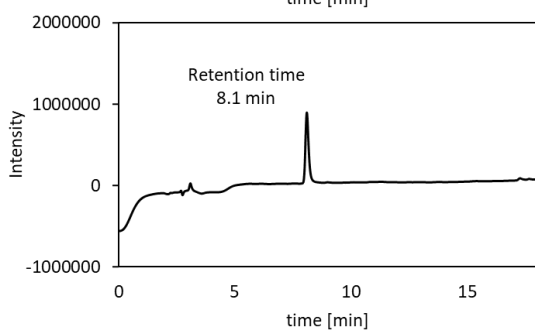
AMP3f



AMP3g

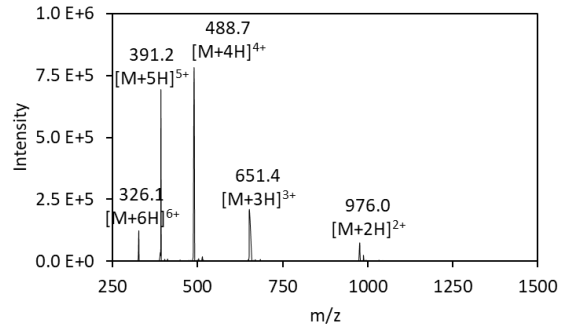
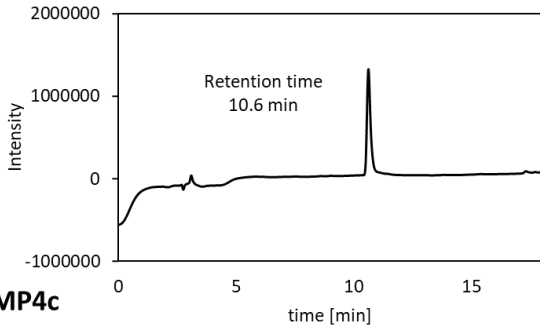


AMP4a

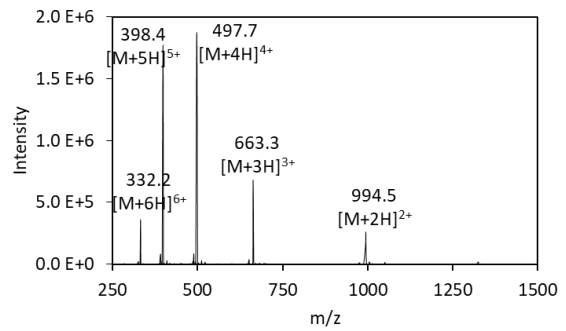
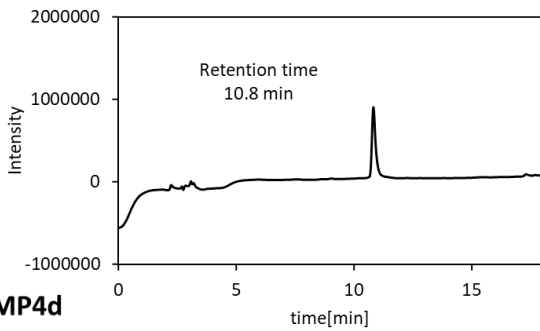


Supplementary 2: UV-chromatogram and mass spectrometry analysis of peptides AMP3e, AMP3f, AMP3g and AMP4a^[171].

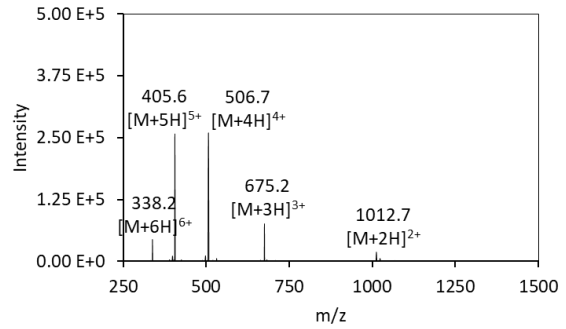
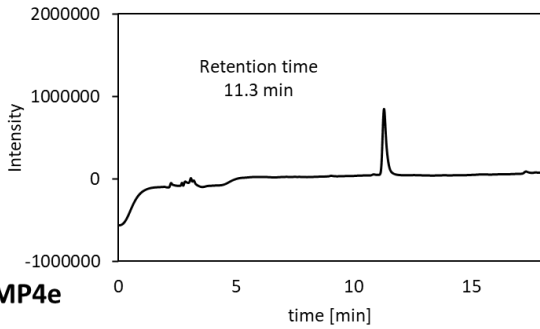
AMP4b



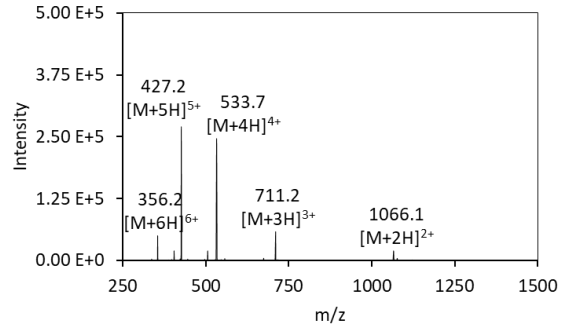
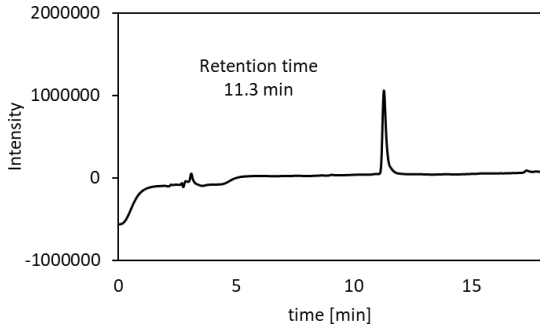
AMP4c



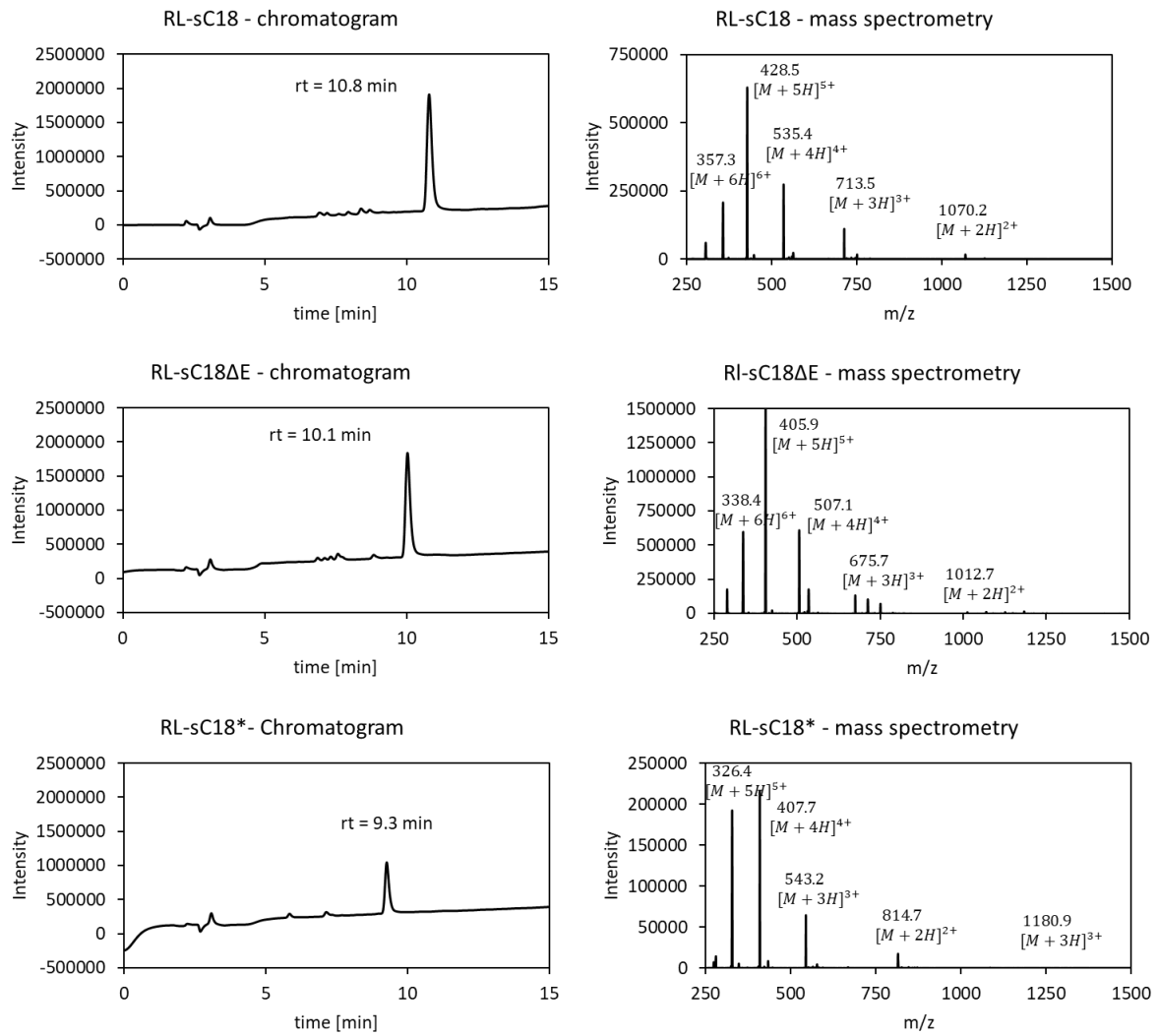
AMP4d



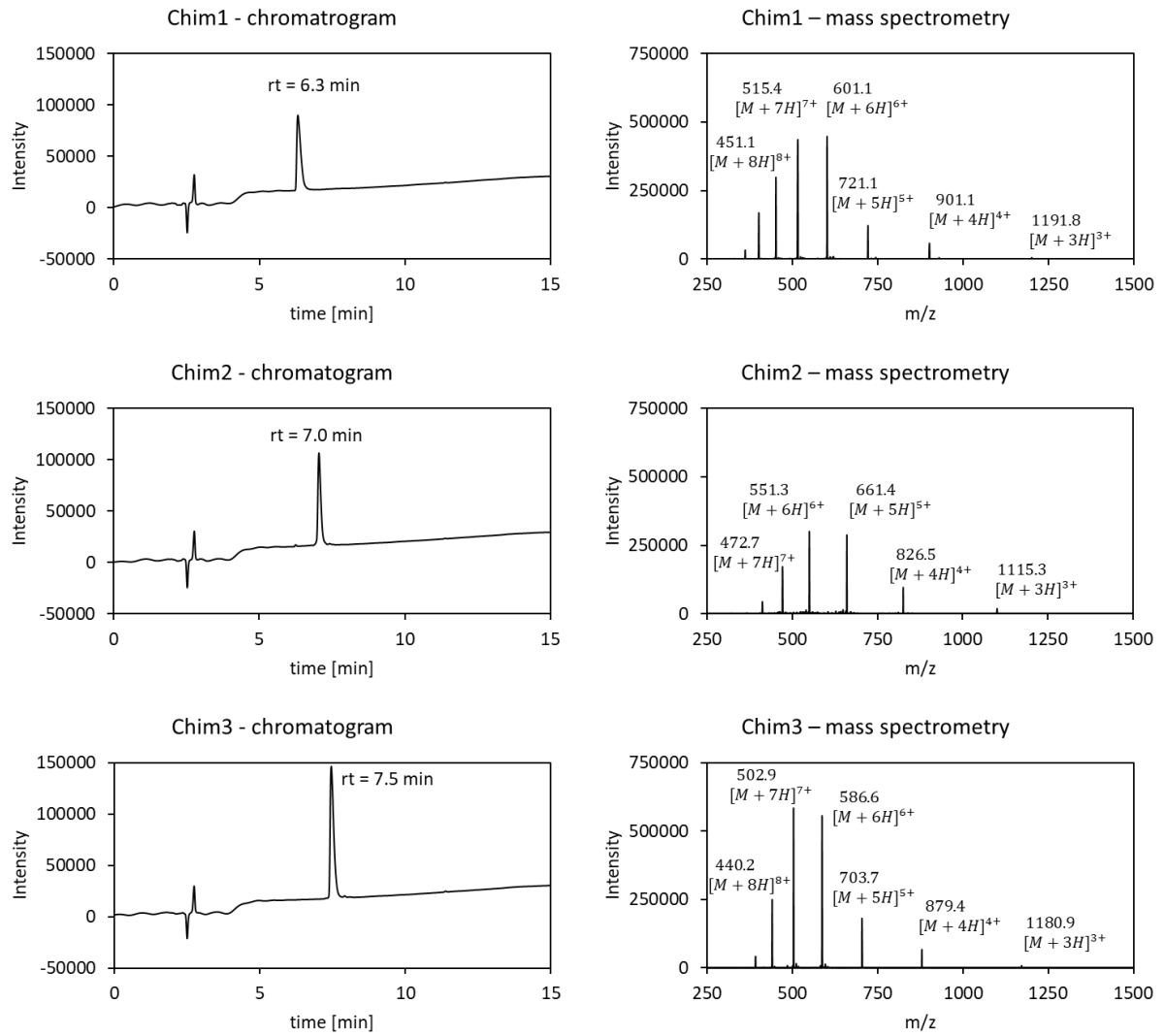
AMP4e



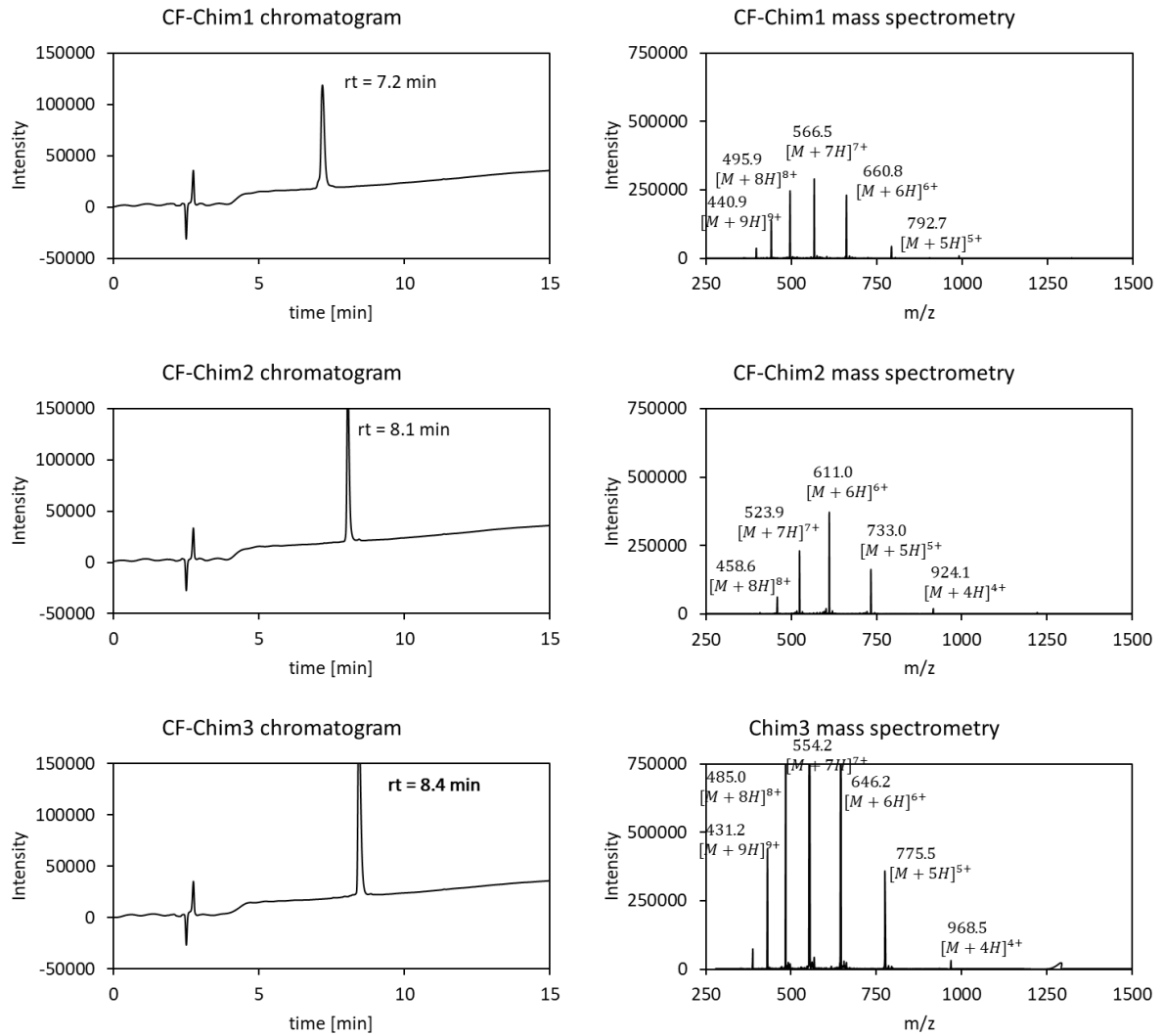
Supplementary 3: UV-chromatogram and mass spectrometry analysis of peptides AMP4b, AMP4c, AMP4d and AMP4e^[171].



Supplementary 4: UV-chromatogram and mass spectrometry analysis of peptides *RL-sC18*, *RL-sC18ΔE* and *RL-sC18.**

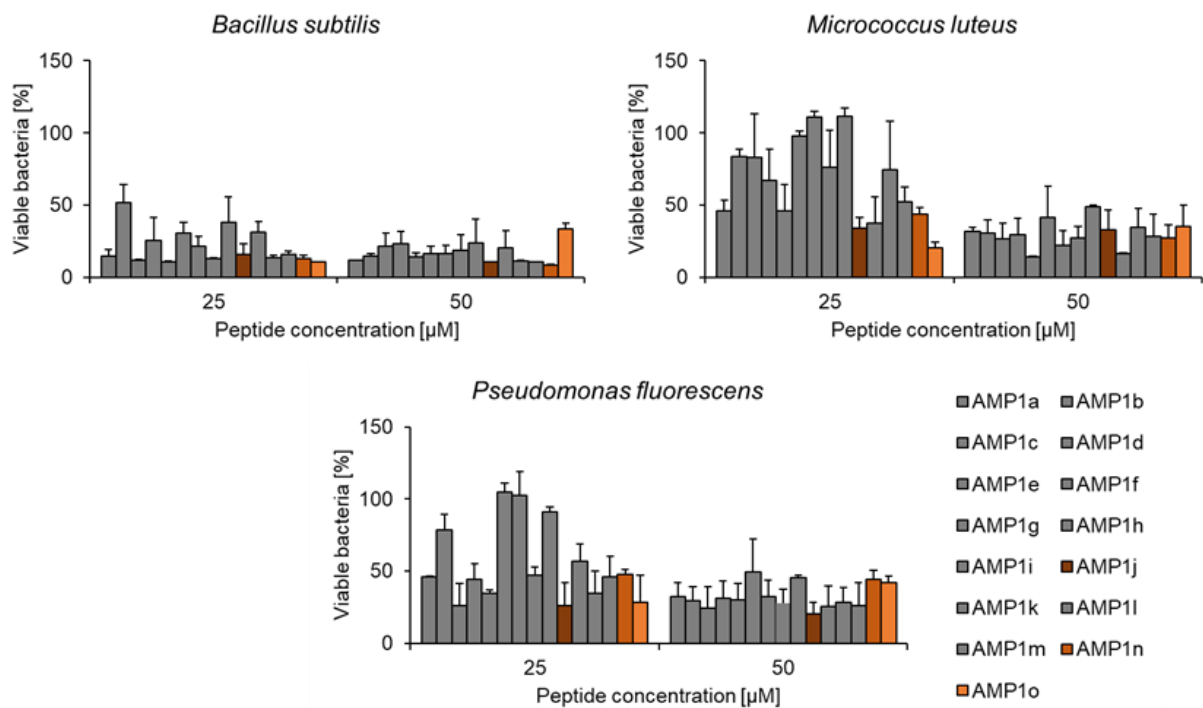


Supplementary 5: UV-chromatogram and mass spectrometry analysis of peptides *Chim1*, *Chim2* and *Chim3*.

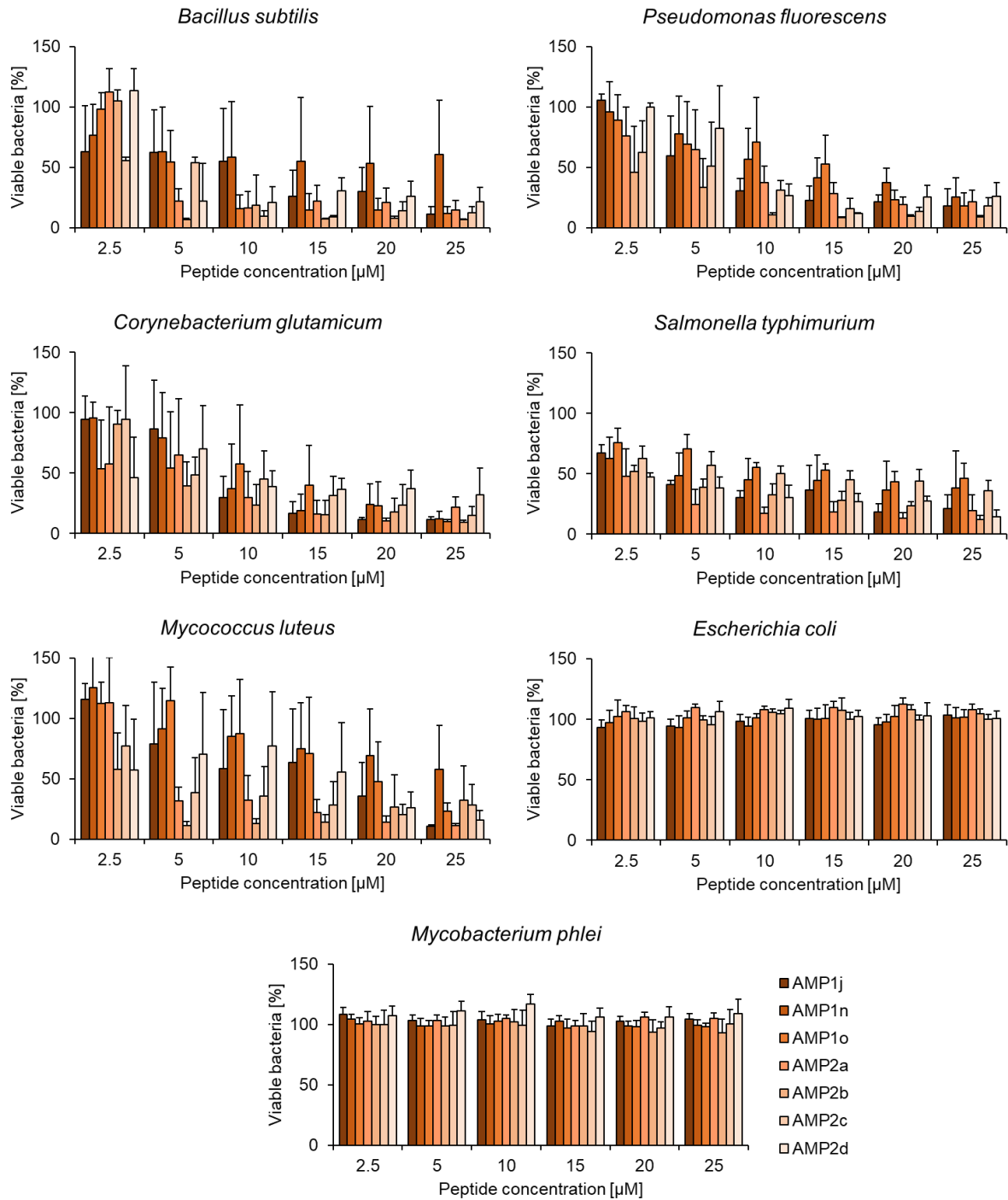


Supplementary 6: UV-chromatogram and mass spectrometry analysis of peptides CF-Chim1, CF-Chim2 and CF-Chim3.

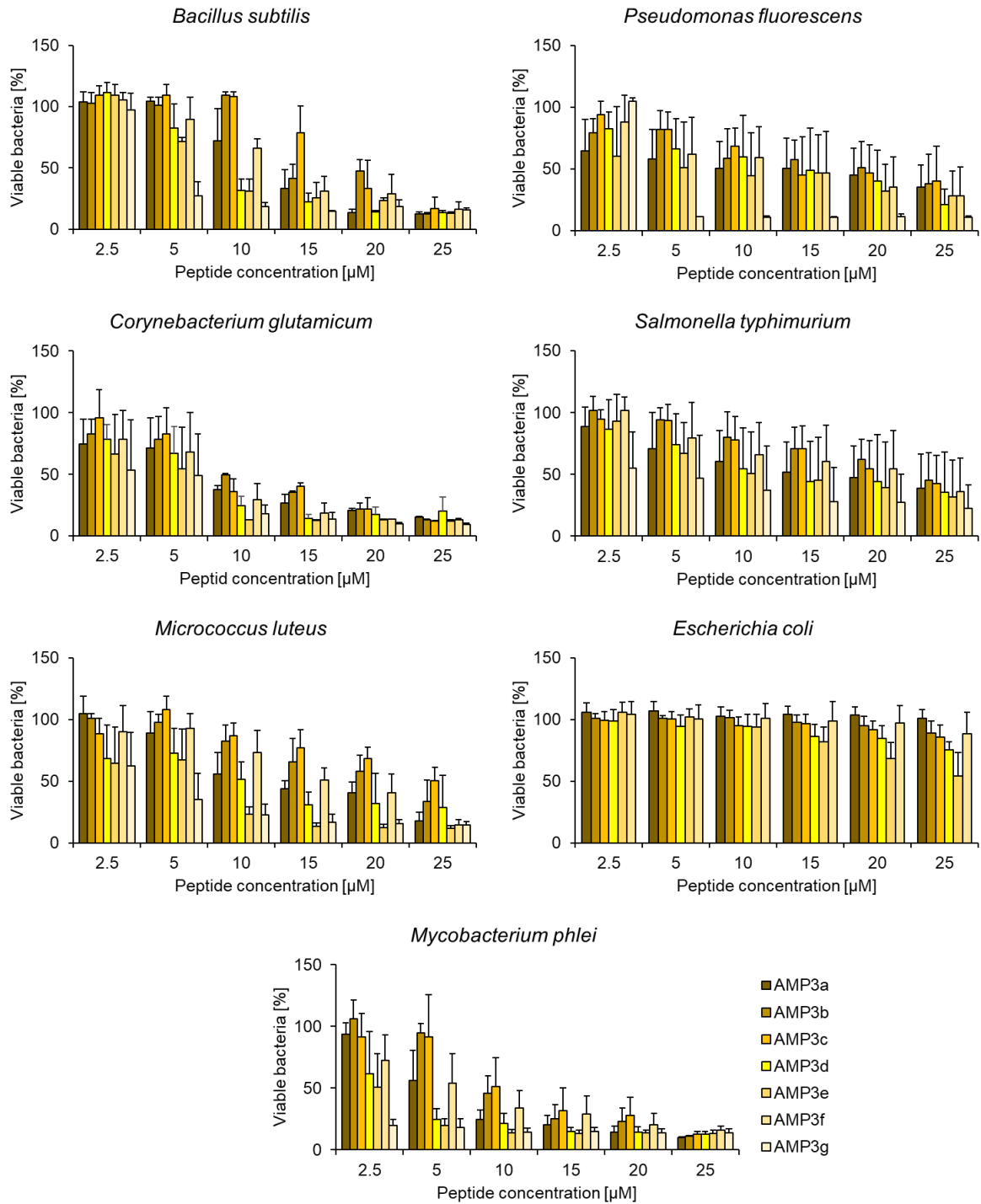
10.7. Preliminary antibacterial data



Supplementary 7: Preliminary work on AMP generation one (isoleucine screening) with three different bacterial strains^[163,171]. Bacteria were incubated for 6 h at 37°C with various peptide concentrations. Data represent mean \pm SD of n (number of experiments) ≥ 1 performed in triplicate. Negative control (water) was set to 100% to calculate the relative quantity of living cells.

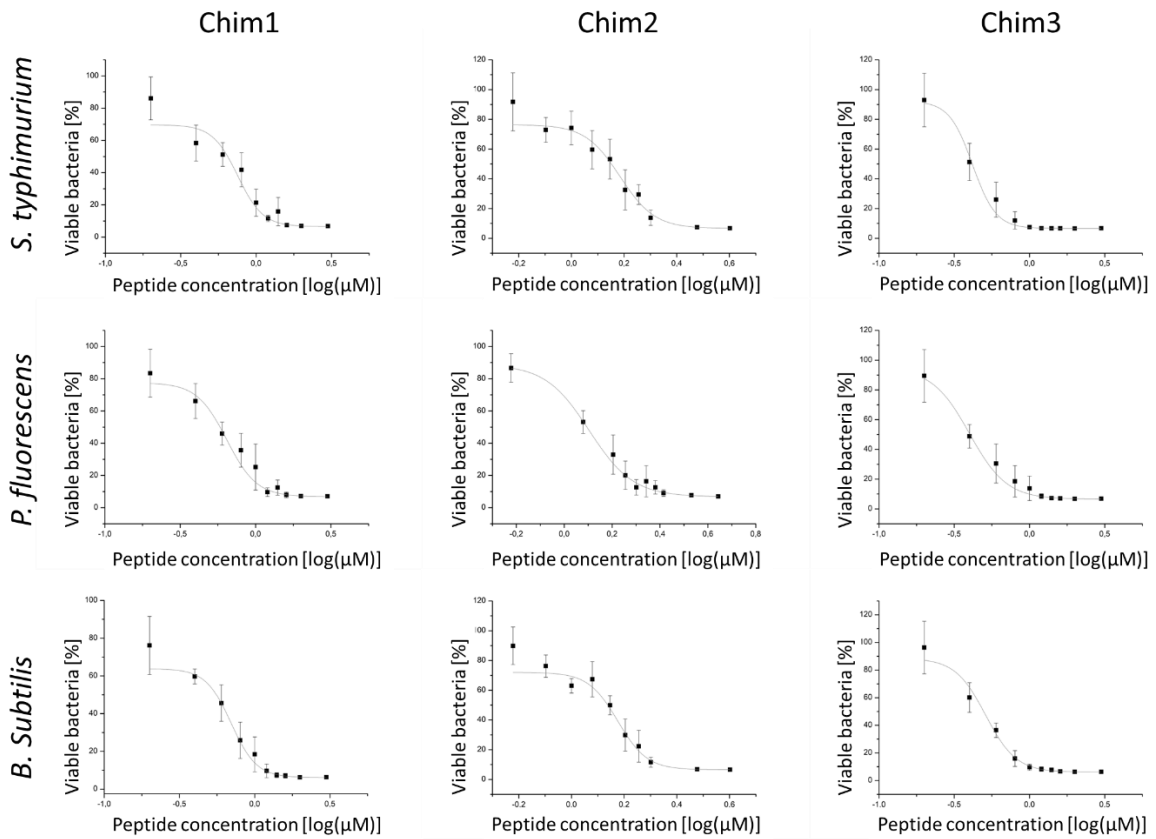


Supplementary 8: Preliminary screening generation two peptides (isoleucine substitution) for their antimicrobial activity against seven bacterial strains^[163,171]. Bacteria were incubated for 6 h at 37°C. Data represent mean \pm SD of $n \geq 3$ performed in triplicate. Negative control (water) was set to 100% to calculate the relative quantity of living cells.

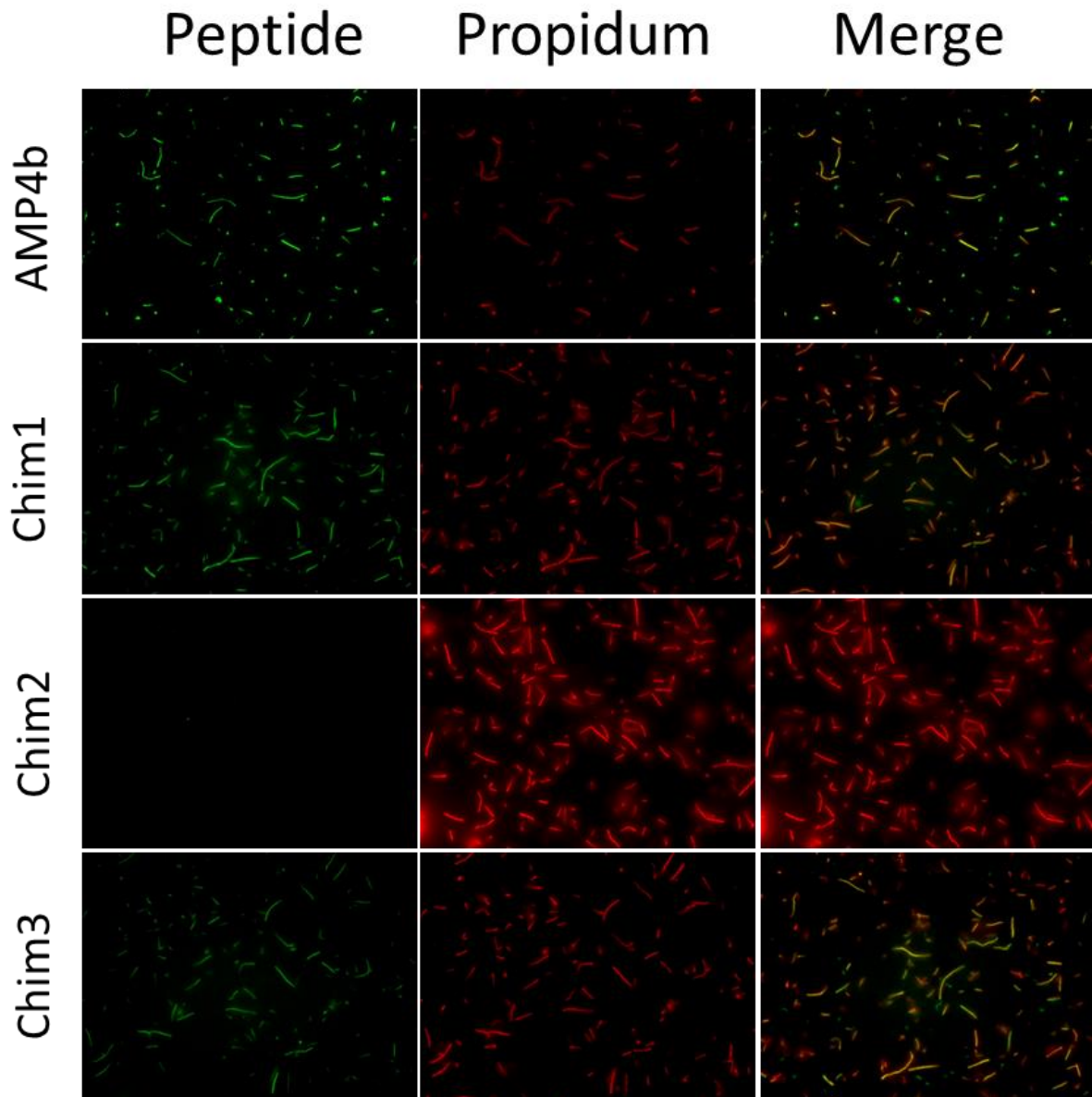


Supplementary 9: Preliminary screening generation three peptides (phenylalanine substitution) for their antimicrobial activity against seven bacterial strains^[163,171]. Bacteria were incubated for 6 h at 37°C. Data represent mean ± SD of $n \geq 3$ performed in triplicate. Negative control (water) was set to 100% to calculate the relative quantity of living cells.

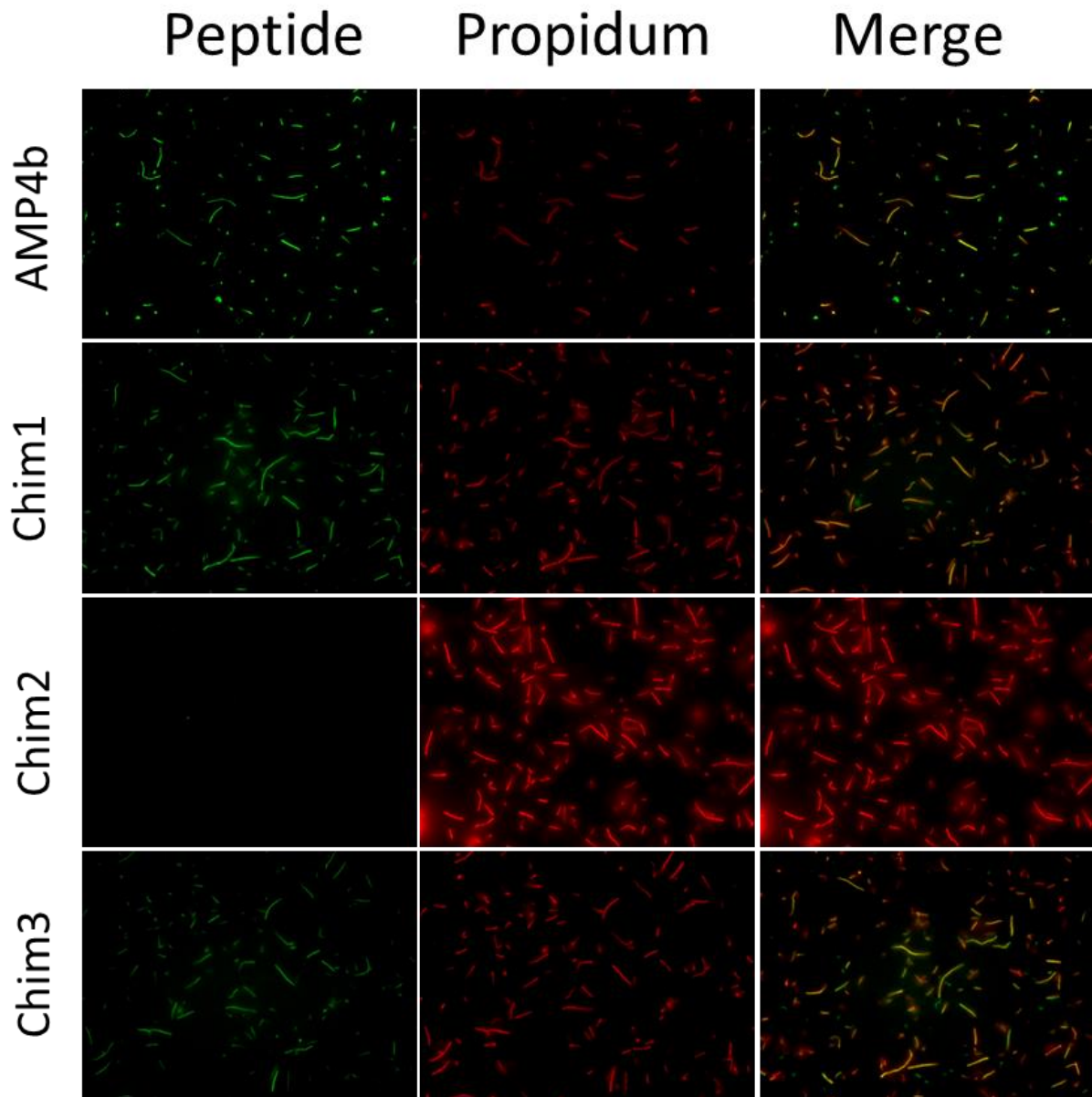
10.8. Dose response curves of chimeric peptides



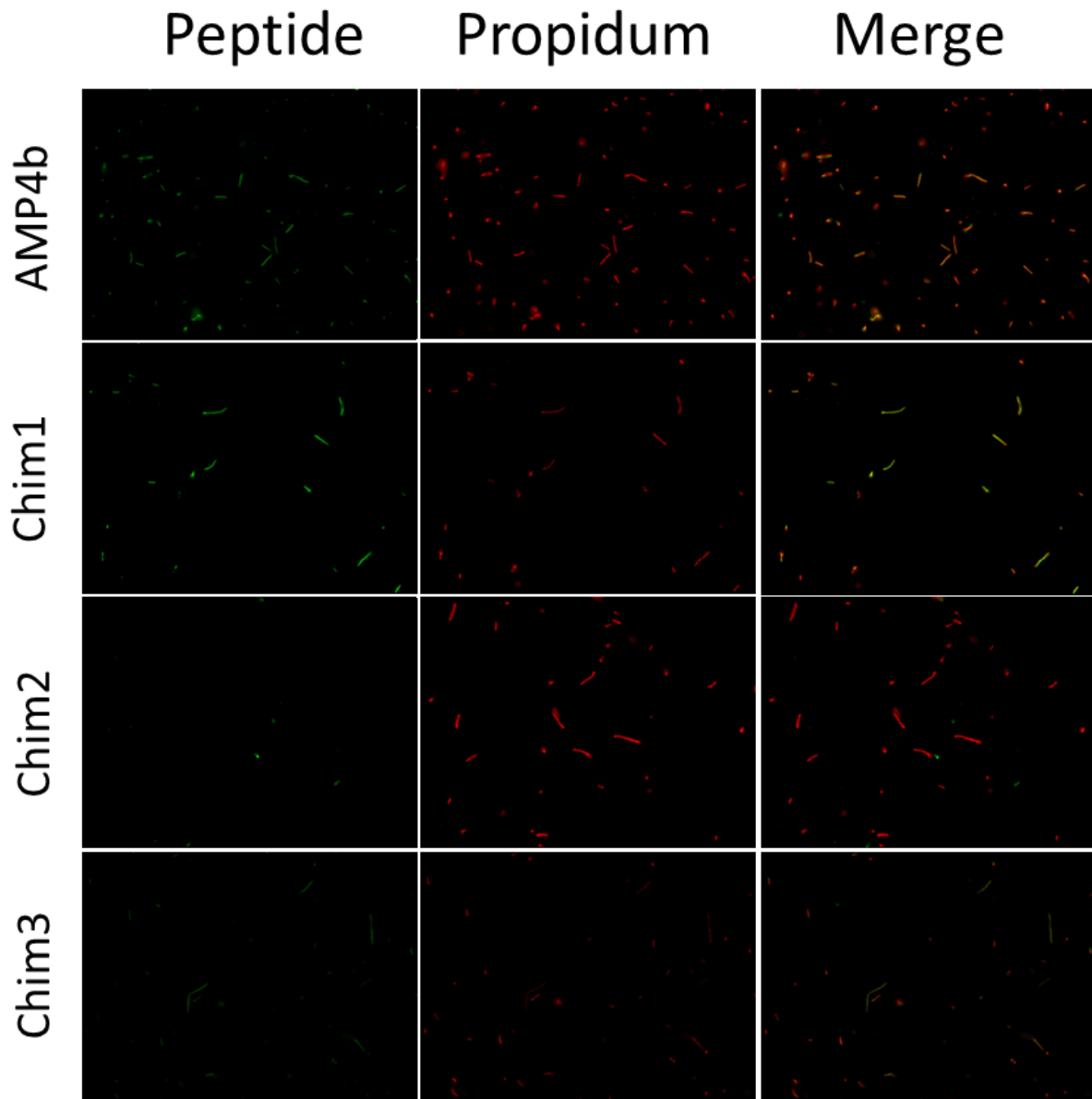
Supplementary 10: Dose response curves of the chimeric peptides with *S. typhimurium*, *P. fluorescens* and *B. subtilis*.

10.9. Fluorescence microscopy of chimeric peptides

Supplementary 11: Fluorescence microscopy of **AMP4b** and the three chimeric peptides using *B. subtilis* after incubation with 20 μ M peptide at 37 °C for 30 minutes. Peptides were marked with (5/6)-carboxylfluorescein. Dead bacteria were stained with propidium iodide.

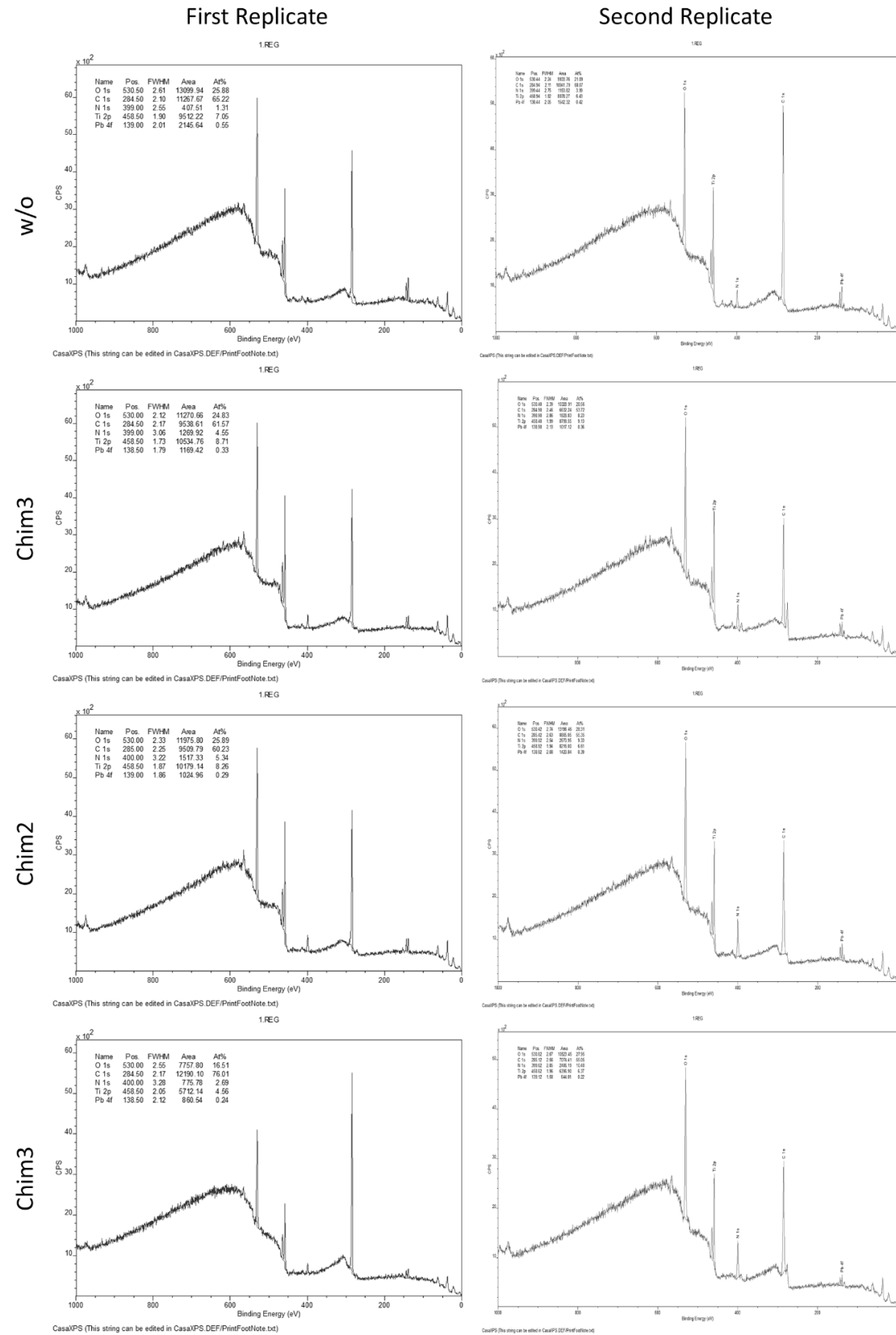


Supplementary 12: *Fluorescence microscopy of AMP4b and the three chimeric peptides using P. fluorescens after incubation with 20 μM peptide at 37 °C for 30 minutes. Peptides were marked with (5/6)-carboxylfluorescein. Dead bacteria were stained with propidium iodide.*



Supplementary 13: Fluorescence microscopy of **AMP4b** and the three chimeric peptides using *S. typhimurium* after incubation with 20 μ M peptide at 37 °C for 30 minutes. Peptides were marked with (5/6)-carboxylfluorescein. Dead bacteria were stained with propidium iodide.

10.10. XPS elemental analysis spectra



Supplementary 14: Spectra of XPS measurement for elemental analyses of titanium plates without coating (w/o) and immobilized with chimeric peptides (**Chim1**, **Chim2**, **Chim3**).

11. Danksagung

Ich möchte mich bei vielen Leuten bedanken, welche mich auf meinem Weg begleitet haben und diese Promotion erst möglich gemacht haben.

Mein erster Dank gilt selbstverständlich Frau Prof. Dr. Ines Neundorf, dafür dass sie meine Doktormutter war und mich in den vergangenen Jahren angeleitet hat. Dank ihr durfte ich dieses interessante Projekt erforschen und auch wenn wir beim Schreiben von Artikeln manchmal unterschiedliche Ansätze hatten, waren dies doch wertvolle Erfahrungen, an welchen ich gewachsen bin.

Mein nächster Dank gilt Herrn Prof. Dr. Ulrich Baumann, dafür dass er mein Mentor während der Promotion war und zudem die Rolle als mein Zweitprüfer übernommen hat. Schon in meinen vergangenen Studiengängen war es immer angenehm zusammen zu arbeiten, weswegen sie schon zum dritten Mal diese Rolle für mich einnehmen durften.

Aber ich muss mich nicht bloß bei den Professoren bedanken, sondern auch bei meinen Kollegen, ohne welche die vergangenen vier Jahre in der Arbeitsgruppe definitiv anders gewesen wären: Lucia, du warst immer ein Quell der Freude im Labor, auch wenn du mich nicht immer ganz verstanden hast, wenn ich mal wieder zu schnell sprach. Annika, du hast mir gezeigt, wie ich mit Zellen umgehen muss und uns regelmäßig die Zeit mit bester Latin-Musik und fantastischen Abendessen versüßt. Tamara, du warst meine Betreuerin während meiner ersten Zeit in der Gruppe und die weitere Zeit habe ich dich als meine große Arbeitsschwester gesehen, die nur ein Wort beschreiben kann: popular. Merlin, du bist unser Meister der schlechten Witze, auch wenn ich manchmal ehrlich das Lachen unterdrücken musste. Katharina, du bist das Herz der Gruppe nimmst dir zu viele Aufgaben auf, von Slack-Spammerin und Twitter-Trenderin bis zur Musik-Managerin und Bestellungen-Bevollmächtigten. Joshua, du warst mein erster Student und ich bin stolz, dass du nun als Doktorand mit bei uns im Büro sitzt, wenn auch gerne mit dem Fernrohr am Fenster. Felix, du warst mir der liebste Büropartner und ich freue mich an deinem Bewerbungsverfahren teilgenommen zu haben. Gabi, du bist wie eine liebevolle junge Tante für die Gruppe, welche uns jeden Tag versüßen kann, und mir beigebracht hat, noch ordentlicher zu arbeiten. Anja und Claudia, ihr wart stets ein Rückgrat für die Gruppe, eine Konstante, auch wenn der Rest der Besetzung stetem Wandel unterliegt.

Ein spezieller Dank gilt auch den drei Bachelorstudenten, die zu leiten ich die Ehre gehabt habe: Joshua Grabeck, Laura Buchwald und Rebekka Arnold. Durch euch habe ich die andere Seite der akademischen Arbeit kennengelernt und es war mir eine wahre Freude, euch zu lehren und in eurem eigenen universitären Werdegang zu unterstützen.

Auch den zahlreichen Kollaborationspartnern will ich danken, welche diese Promotion zu fruchtbaren Ergebnissen geführt haben: Denise Meinberger, Tom Cronenberg, Frank Nitsche, Eva Krakor, Michael Wilhelm, Pitter Huisgen, Pascal Engelhardt und noch einigen anderen, die sich an dieser Stelle gedankt fühlen sollen.

Nun will ich mich aber von der Universität weg und den restlichen Menschen in meinem Leben zuwenden, welche mich auf dem Weg hierhin begleitet, teils geführt und mit geformt haben. Daher danke ich meinen Freunden: Jonas Bongers, Jasmin Wagner, Lukas Münzer, Kai Lam, Simon Golenia, Can Senol, Tobias Marx und Patrick Greifzu. Ihr alle habt mich auf dem Weg meines Lebens begleitet und mich auf jeweils unterschiedliche Art und Weise wachsen lassen. Ich bin dankbar euch alle meine Freunde nennen zu dürfen.

Ich danke meiner Familie: Meiner Mutter Claudia, welche mich immer unterstützt hat und zu einem anständigen Menschen herangezogen hat, indem sie mich sowohl den Wert von harter Arbeit lehrte als auch, wie man sich um seine liebsten sorgt. Meinem Vater Rudolf, welcher mir viele praktische Lebenslektionen auf den Weg mitgegeben hat, an denen ich maßgeblich gewachsen bin, auch wenn wir nicht immer einer Meinung waren. Meiner Schwester Laura, welche immer gerne dafür sorgt, dass ich auf dem Boden der Tatsachen bleibe und mit der mich immer die längste Freundschaft meines Lebens verbinden wird. Ich wünsche besonders dir alles Gute auch für dein weiteres Studium und viel Glück im Leben!

Zuletzt möchte ich mich bei einem Menschen bedanken, welcher besonders in den letzten Jahren einen wichtigen Platz in meinem Leben eingenommen hat: Lars Prange. Mein Schatz, du hast mir gezeigt, was Liebe ist und mich in der Vergangenheit bei jeder Krise unterstützt, welche über mich kam. Ich bin übermäßig glücklich, dich gefunden zu haben und freue mich auf die weiteren Zeiten, die ich mit dir erleben darf.

Ich danke euch allen, vom ganzen Herzen.

12. Eidesstattliche Erklärung

Hiermit versichere ich an Eides statt, dass ich die vorliegende Dissertation selbstständig und ohne die Benutzung anderer als der angegebenen Hilfsmittel und Literatur angefertigt habe. Alle Stellen, die wörtlich oder sinngemäß aus veröffentlichten und nicht veröffentlichten Werken dem Wortlaut oder dem Sinn nach entnommen wurden, sind als solche kenntlich gemacht. Ich versichere an Eides statt, dass diese Dissertation noch keiner anderen Fakultät oder Universität zur Prüfung vorgelegen hat; dass sie - abgesehen von unten angegebenen Teilpublikationen und eingebundenen Artikeln und Manuskripten - noch nicht veröffentlicht worden ist sowie, dass ich eine Veröffentlichung der Dissertation vor Abschluss der Promotion nicht ohne Genehmigung des Promotionsausschusses vornehmen werde. Die Bestimmungen dieser Ordnung sind mir bekannt. Darüber hinaus erkläre ich hiermit, dass ich die Ordnung zur Sicherung guter wissenschaftlicher Praxis und zum Umgang mit wissenschaftlichem Fehlverhalten der Universität zu Köln gelesen und sie bei der Durchführung der Dissertation zugrundeliegenden Arbeiten und der schriftlich verfassten Dissertation beachtet habe und verpflichte mich hiermit, die dort genannten Vorgaben bei allen wissenschaftlichen Tätigkeiten zu beachten und umzusetzen. Ich versichere, dass die eingereichte elektronische Fassung der eingereichten Druckfassung vollständig entspricht.

Teilpublikationen:

- **“Multistep optimization of a cell-penetrating peptide towards its antimicrobial activity”**
M. Drexelius, A. Reinhardt, J. Grabeck, T. Cronenberg, F. Nitsche, P. F. Huesgen, B. Maier, I. Neundorf, *Biochem. J.* **2021**, 478, 63–78.
- **“Application of Antimicrobial Peptides on Biomedical Implants: Three Ways to Pursue Peptide Coatings”**
M. G. Drexelius, I. Neundorf, *Int. J. Mol. Sci.* **2021**, Vol. 22, Page 13212 2021, 22, 13212.
- **“Rational design of bifunctional chimeric peptides that combine antimicrobial and titanium binding activity”**

M. G. Drexelius, R. Arnolds, D. Meinberger, M. Wilhelm, S. Mathur, I. Neundorf,
J. Pept. Sci. **2023**, DOI 10.1002/PSC.3481.

Posterpräsentationen:

- **“Influence of fluorinated amino acids on the antimicrobial activity of a cell penetrating peptide.”**
M. Drexelius and I. Neundorf, (2019) 14th German Peptide Symposium,
Cologne, Germany

- **“Creating antimicrobial titanium surfaces by immobilization with chimeric peptide variants of sC18.”**
M. Drexelius, R. Arnold and I. Neundorf, (2022) 36rd European Peptide
Symposium, Sitges, Spain

Köln, 07.02.2023, Marco Gerry Drexelius

13. Lebenslauf

Persönliche Daten

Name: Marco Gerry Drexelius
Geburtsdatum: 15.11.1994
Geburtsort: Köln
Staatsangehörigkeit: Deutsch

Ausbildung

Seit 02 / 2019 Promotion am Institut für Biochemie
Universität zu Köln bei Frau Prof. Dr. Ines Neundorf

10 / 2016 – 01 / 2019 Masterstudium Chemistry (Master of Science)
Math-Nat Fakultät, Universität zu Köln
Masterarbeit bei Prof. Dr. Ines Neundorf

10 / 2013 – 10 / 2016 Bachelorstudium Chemie (Bachelor of Science)
Math-Nat Fakultät, Universität zu Köln
Bachelorarbeit bei Prof. Dr. Karsten Niefind

08 / 2005 – 06 / 2013 Europaschule – Gymnasium der Stadt Kerpen
Abschluss: Abitur
Leistungskurse Mathematik und Chemie

08 / 2001 – 06 / 2005 Grundschule St. Elisabeth, Kerpen Blatzheim